

Eötvös Loránd University  
Faculty of Science

Hungarian Academy of Sciences  
Centre for Energy Research



Doctoral School of Environmental Sciences  
Head of the doctoral school:  
Prof. Dr. Imre Jánosi

Environmental Physics Doctoral Programme  
Head of the doctoral programme: Prof. Dr. Imre Jánosi

## **Degradation of sulfonamides in aqueous solution by ionizing radiation**

Doctoral thesis

by Gyuri Sági

Supervisors

Prof. Dr. Erzsébet Takács  
Professor emerita  
Centre for Energy Research

and

Prof. Dr. Zoltán Homonnay  
Professor  
Eötvös Loránd University

Consultants

Prof. Dr. László Wojnárovits  
Professor emeritus  
Centre for Energy Research

and

Dr. Tamás Csay  
Head of research analytics  
Soneas Research Ltd.

Budapest  
2017



## Table of contents

---

<b>1 Introduction</b> .....	7
<b>2 Review of the literature</b> .....	8
2.1 Sulfonamide antibiotics .....	8
2.1.1 Mechanism of action, absorption and excretion.....	8
2.1.2 Application of sulfonamide antibiotics .....	9
2.1.3 Resistance development .....	11
2.2 Conventional treatment of municipal wastewater.....	12
2.3 Advanced Oxidation Processes .....	14
2.3.1 Fenton-type reactions .....	15
2.3.2 Photocatalysis.....	17
2.3.3 Ozone reactions .....	19
2.4 Ionizing radiation treatment.....	21
2.4.1 Energy deposition and product distribution .....	21
2.4.2 Primary intermediate and final products in water radiolysis.....	23
2.4.3 Pollutant removal by ionizing radiation in general .....	26
2.4.4 Ionizing radiation treatment of sulfonamide antibiotics .....	27
<b>3 Background summary</b> .....	29
<b>4 Objectives</b> .....	31
4.1 Degradation efficiency and product analysis; general degradation mechanism.....	31
4.2 Evaluation of changes in toxicity, biodegradability and antibacterial activity.....	31
4.3 Pollutant load dependence of biological responses and effects of H <sub>2</sub> O <sub>2</sub> .....	32
<b>5 Materials and methods</b> .....	33
5.1 Materials .....	33
5.2 Sample preparation and irradiation procedure.....	34
5.3 Pulse radiolysis .....	35
5.4 Product identification.....	36
5.4.1 Liquid chromatography – tandem mass spectrometry .....	36
5.4.2 Ion chromatography .....	36
5.4.3 Cu(II)/phenanthroline test for H <sub>2</sub> O <sub>2</sub> determination.....	37
5.5 Sum parameters for water quality characterization .....	37
5.5.1 Total sulfur content .....	37
5.5.2 Total nitrogen content .....	38
5.5.3 Total organic carbon content.....	38
5.5.4 Chemical oxygen demand.....	38
5.5.5 Biological oxygen demand.....	39
5.6 Toxicity assessment .....	42

5.6.1	Selection of test organisms .....	42
5.6.2	Sample preparation .....	42
5.6.3	<i>Vibrio fischeri</i> acute toxicity .....	43
5.6.4	<i>Pseudokirchneriella subcapitata</i> chronic toxicity.....	43
5.6.5	<i>Daphnia magna</i> acute toxicity.....	44
5.6.6	Activated sludge respiration inhibition.....	45
5.6.7	BOD <sub>5</sub> as toxicity indicator.....	47
5.7	Antibacterial susceptibility testing .....	47
5.7.1	Selection of test organisms and sample preparation.....	47
5.7.2	Agar diffusion test .....	48
5.7.3	Broth microdilution assay.....	49
5.8	Statistical methods.....	49
<b>6</b>	<b>Results and Discussion</b> .....	<b>50</b>
6.1	Separation and evaluation of radical reactions involved in degradation.....	50
6.2	Intermediate product analysis.....	52
6.3	Separation and identification of stable organic products .....	54
6.4	Determination of inorganic ions.....	60
6.4.1	Nitrogen content and related inorganic ions.....	60
6.4.2	Sulfur content and related inorganic ions .....	63
6.5	Mineralization rate .....	64
6.6	Oxidation rate .....	65
6.7	Biodegradability .....	67
6.7.1	Impact of different pollutant load exposure and H <sub>2</sub> O <sub>2</sub> .....	67
6.7.2	Biodegradation in activated sludge.....	70
6.7.3	Biodegradation in river water .....	71
6.7.4	General evaluation of biodegradability .....	72
6.8	Toxicity assay.....	73
6.8.1	Impact of different pollutant load exposure and H <sub>2</sub> O <sub>2</sub> .....	73
6.8.2	<i>Daphnia magna</i> acute mortality .....	76
6.8.3	<i>Pseudokirchneriella subcapitata</i> chronic growth inhibition .....	77
6.8.4	<i>Vibrio fischeri</i> acute luminescence inhibition .....	78
6.8.5	Activated sludge respiration inhibition.....	79
6.9	Antibacterial activity .....	84
<b>7</b>	<b>Summary</b> .....	<b>88</b>
<b>8</b>	<b>Theses</b> .....	<b>93</b>
<b>9</b>	<b>List of publications related to PhD theses</b> .....	<b>95</b>
<b>10</b>	<b>List of other publication</b> .....	<b>95</b>
<b>11</b>	<b>Acknowledgement</b> .....	<b>96</b>
<b>12</b>	<b>References</b> .....	<b>97</b>

## List of abbreviations, acronyms and symbols

---

AOP	advanced oxidation processes
ATCC	American type culture collection
BOD <sub>5</sub>	five-day biological oxygen demand
COD	chemical oxygen demand
<i>G</i>	radiation chemical yield
GC	gas chromatography
IC	ion chromatography
ICP-MS	inductively coupled plasma mass spectrometry
<i>k</i>	reaction rate constant
LC	liquid chromatography
LET	linear energy transfer
MS	mass spectrometry
MS/MS	tandem mass spectrometry
OD	optical density
OUR	oxygen uptake rate
<i>P</i>	probability, ranging in value from 0 to 1
<i>pK<sub>a</sub></i>	acid-base dissociation equilibrium
SAA	sulfanilamide
SCT	sulfacetamide
SDZ	sulfadiazine
SGD	sulfaguanidine
SMX	sulfamethoxazole
SMZ	sulfamethazine
SSZ	sulfisoxazole
STZ	sulfathiazole
SUM	sumetrolim
TMP	trimethoprim
TN	total nitrogen
TOC	total organic carbon
TOF-MS	time of flight mass spectrometry
TS	total sulfur
UV-Vis	ultraviolet-visible



## 1 Introduction

---

Demand for preserving natural resources has particularly increased in the last few decades due to continued growth of human population. Potable water supply and protection of water resources are among the most urgent environmental and development issues arising in the topic of sustainability. Freshwater is a finite resource that is vital to life, and thus, its safe provision in adequate capacity and quality is a global concern.

Recent studies have shown that water bodies all around the world are more or less polluted with chemicals, like pesticides, pharmaceuticals, personal care products or their metabolites. Occurrence of these substances – even at low concentrations – may have a large impact on natural systems. They may cause disorders in living organisms, hence, disrupt the integrity of the ecosystem. In addition to toxic effects, development and dissemination of antibacterial resistance poses serious threat to public health that makes the treatment of infectious diseases more and more challenging. Antibiotic resistance is a natural phenomenon predating the modern selective pressure of clinical antibiotic application. For this reason, it is difficult to imagine a complete suppression of resistance prevalence, but maintaining the background levels and preventing wide spreading seems to be a reasonable objective. In this context, it is important to recognize that the persistence of pollutants is not the only cause for concern, since the continual release of antibiotics to the environment induces the same effect.

Wastewater effluents contain considerable amounts of pharmaceuticals that largely contribute to appearance of resistant pathogenic bacterial strains. In this respect, wastewater treatment plants and the close proximity of effluent outlets are hot spot areas. To increase the removal rate of refractory substances and to reduce discharge of hazardous substances, new decomposition techniques are under development or testing. A group of these methods is the Advanced Oxidation Processes (AOP). Advanced oxidation induced by ionizing radiation is in the focus of interest because of its highly effective toxicant removal performance. Oxidation of organic molecules by this technique takes place mainly due to reactions of hydroxyl radicals ( $\bullet\text{OH}$ ), similarly to other AOP. Ionizing radiation treatment represents a promising complementary option to the conventional wastewater treatment. Application of this method for treatment of sulfonamide antibiotic solutions – a group of emerging pollutants – was detailed in this dissertation. In addition to the chemical characterization of the degradation process, special attention was paid to the behavior of decomposition products in biological assessments.

## 2 Review of the literature

---

### 2.1 Sulfonamide antibiotics

“Sulfonamides” is a generic term for derivatives of sulfanilamide, which carries the smallest structural unit required to induce antibacterial action. Sulfonamide antibiotics were the first agents regularly applied for treatment and prophylaxis of bacterial infections in humans [1]. Their discovery and subsequent widespread application was followed by a sharp reduction in the number of illnesses and deaths. Appearance of penicillin and other antibiotics greatly reduced their usage, so as the development of bacterial resistance against sulfonamides. Although their significance reduced over the years, sulfonamides are still present in diverse application fields. Furthermore, combination of sulfamethoxazole with trimethoprim gave a new impetus to their further usage in medication. Sulfonamides also play an important role in veterinary practice, animal husbandry and aquacultures. The widespread utilization is evidenced by their usage in apiary against *Paenibacillus larvae* ssp. *larvae*, and in agriculture against *Holcus lanatus*, *Echinochloa crus-galli*, *Avena fatua*, *Rumex obtusifolius*, etc. [2].

#### 2.1.1 Mechanism of action, absorption and excretion

Sulfonamide antibiotics are synthetic bacteriostatic antibiotics; they inhibit bacteria proliferation during therapy. Sulfonamides prevent synthesis of folic acid that is essential in cell growth. Folic acid diffuses or is transported into human cells following intake by food or drink, but folic acid cannot cross bacterial cell walls by diffusion or active transport. For this reason, bacteria must synthesize folic acid from *para*-aminobenzoic acid. This is the point where sulfonamides act, as these agents are competitive antagonists of *para*-aminobenzoic acid. Sulfonamides substitute *para*-aminobenzoic acid and in this way inhibit the action of dihydropteroate synthetase enzyme and the production of folic acid. In practice, sulfonamides are often combined with synergistically acting diaminopyrimidines (trimethoprim or pyrimethamine) that provides a wider possibility of application as separately used.

Absorption of sulfonamides takes place mainly in the small intestine, but a small fraction may be absorbed from the stomach and from the bowel in case of specially designed drugs. From 70% up to 100% of the administered dose is absorbed and distributed in the body. The active agent may undergo metabolic alterations and appear in the urine already in 30



minutes. The major metabolic product is the acetylated form of the parent compound, but oxidation and conjugation with glucuronic acid also takes place. During acetylation, the sulfonamides lose their antibacterial activity but retain their toxic potential. Nevertheless, retransformation to active substances may also occur [3, 4, 5]. The sulfonamides are usually eliminated by kidneys and only small amounts are released via feces, milk or bile [1, 6].

### 2.1.2 Application of sulfonamide antibiotics

Sulfonamides are applied against a wide range of both Gram-positive and Gram-negative bacteria in human therapy. They are often used in treatment of *P. jirovecii*, *T. gondii* and other *Toxoplasma* species, *Plasmodia*, *Coccidians*, *Chlamydia*, *Nocardia* and *Actinomyces* [6, 7]. In medication of gastrointestinal infections, succinylsulfathiazole and sulfaguanidine are mainly applied. Although they do not represent the first choice, sulfisoxazole or sulfamethopyrazine are often prescribed in case of urinary tract infections. *Meningitis* is treated by sulfamethazine or sulfadiazine, while respiratory tract infections by the combination of sulfamethoxazole and trimethoprim. The combination of pyrimethamine and sulfadiazine is an effective therapeutic against *toxoplasmosis*. *Nocardiosis* can be cured with sulfadiazine or sulfisoxazole, but for advanced cases, a second antibiotic is also recommended. The combination of sulfadoxine and pyrimethamine is used for treatment – and for prophylaxis – against malaria. Some sulfonamides are applied topically, as well. For instance, sulfacetamide is widely used for treatment of ophthalmic infections, while silver sulfadiazine for prevention of wound or burn infections. It provides reliable protection against all pathogenic bacteria and fungi. Sulfanilamide is effective in *vaginitis* treatment in form of cream or suppository [1, 6, 7].

According to the Food and Agriculture Organization (FAO) of the United Nations (UN), 800 million people, from the total 7.2 billion, suffer from chronic malnourishment [8]. Feeding this huge crowd is a serious task that heavily depends on the use of pharmaceutical compositions. As reported by the USA Animal Health Institute [9], there are 24 billion chickens, more than 1 billion cattle and sheep, 750 million pigs and goats in the world. Such large number of animals unavoidably couples with application of enormous veterinary medicine amounts. In animal applications, antibiotics are used for handling existing diseases, for prophylactic purposes and for production enhancement (e.g. growth promotion) [10]. Sulfonamides are worldwide commonly used in veterinary therapy for treatment of inter alia *actinobacillosis*, respiratory infections, *metritis*, *colibacillosis* and

*toxoplasmosis* [6]. Moreover, sulfonamides are one of the most frequently used chemicals in production of medicated feed and authorized medicated pre-mixes. Their share is around 70 – 80% in countries like Finland, Bulgaria, UK, Germany etc. [11]. Similarly to the human medication, sulfonamides are often combined with trimethoprim in preparations used in veterinary practice. Application of sulfonamides for growth promotion in the USA, China and Brazil highlights the utilization of these antibiotics in huge amounts, as these three countries are the largest poultry meat producers in the world [12, 13].

Considering the impact of veterinary pharmaceuticals on natural waters, aquacultures are attracting more and more attention. According to a recent publication of the Food and Agriculture Organization on the state of world fisheries and aquaculture [8], the world fishery capture was 91.3 million tons in 2012, while 66.6 million tons of fish were provided by aquacultures in the same year. The wild capture showed a constant rate in the last two decades, while the share of the aquacultures significantly increased during this period. For the continuous and stable production, sulfonamides are also utilized for disease treatment, prophylaxis and growth promotion [14]. The most important characteristic of the aquacultures is that pharmaceutical containing excrement and unconsumed medicated feed is in environmental aqueous media. Therefore, leaching into groundwater is relatively unhindered and the undercurrents may wash these substances to distant sites [15]. Pollution with sulfonamides may take place through agricultural activities, due to fertilization by slurry or manure, which may contain unmetabolized active agents in high concentrations. Sulfonamides were detected above  $\mu\text{g dm}^{-3}$  concentrations in fishponds and effluents of swine farms that are 1 – 2 orders of magnitude higher than those found in wastewater effluents [16, 17]. In this way, drug residues may significantly contribute to pollution of freshwater via runoff to surface waters [18] or the previously mentioned infiltration to groundwater at attenuated levels [19]. Sulfonamide concentrations up to few hundred  $\text{ng dm}^{-3}$  were usually published in studies investigating pharmaceutical occurrence in groundwater [20, 21, 22, 23, 24]. Moreover, ubiquitous occurrence of sulfonamides was evidenced in offshore waters at around 10 – 20  $\text{ng dm}^{-3}$  mean concentration [15, 25, 26]. The presence of these pollutants was linked with high density of human activities, including the large share of aquacultures or maricultures.

### 2.1.3 Resistance development

Development of antibacterial resistance means reduction in the effectiveness of antibacterial preparation. The sensitivity to a pharmaceutical is different among individual organisms of the bacteria population; therefore, a surviving fraction may occur following the medication. If the surviving organisms are capable of reproduction, the offspring will inherit this ability and result in a more resistant population. This is an evolutionary response of living organisms placed under pressure. A natural selection takes place among the differently sensitive microorganisms exposed to a pharmaceutical and the generation with high level of resistance survives. However, it was shown that this natural phenomenon is predated the modern selective pressure of clinical antibiotic application [27]. Furthermore, the extraordinary genetic capacities of microbes allow evolution of multiple resistance mechanisms to each antibiotic [28]. There are four general mechanisms of resistance emergence:

- Inactivation or modification of the antibiotic
- Alteration in the target site of the antibiotic
- Modification of metabolic pathways of the antibiotic
- Reduced antibiotic accumulation

The overproduction of *para*-aminobenzoic acid or modified dihydropteroate synthetase is the most common mechanism in emergence of resistance in case of sulfonamides [6].

Wastewater effluents contain considerable amounts of pharmaceuticals [29, 30], which exert selective pressure on bacteria and strongly accelerate resistance development in the recipient water bodies [31]. This process can be further facilitated by microbial strains with acquired resistance genes that are released into the lakes or rivers following the wastewater treatment [32]. Therefore, it is of special interest to completely remove both antibiotics and pathogens from the wastewater effluents.

## 2.2 Conventional treatment of municipal wastewater

To maintain the quality of effluent receiving water bodies, reduction of high organic content is the primary purpose during purification of municipal wastewater. However, discharge of large nitrogen or phosphorus amounts may also lead to eutrophication and finally result in excessive load of organic matter and oxygen depletion [33]. Therefore, removal of these nutrients is vital, as well. Due to diverse composition and wide pollutant size range in the raw influent, multistage operation system is needed for wastewater treatment. Purification process is strongly concentrated in time and space and it is performed under strictly controlled conditions.

The incoming raw wastewater passes through bar screens, which remove big objects, like plastic bottles, branches etc. In the next step, wastewater is introduced to a grit channel, where the flow rate is adjusted for separation of rapidly settling particles, like stones, sand or grit. The wastes from the screens and grit channel are usually taken to landfills. These operations are often labelled as the preliminary stage of wastewater treatment. Treatment at conventional plants consists of two further steps: primary and secondary purification. In the primary stage, wastewater enters primary clarifier tanks, where oil and grease are floated to the surface and skimmed off. Suspended solids are settled as much as possible and subsequently also removed. Organic matter and numerous inorganic compounds are eliminated in the secondary treatment by metabolic processes of microorganisms. Biological treatment is carried out by using microorganisms suspended in primarily treated wastewater or by densely positioned surface layers that are covered with biofilms. Organic pollutants are utilized as nutrients and they are transformed to carbon dioxide, water, non-degradable metabolic products or cellular materials. Ammonifying, nitrifying and denitrifying bacteria strains convert ammonia nitrogen to atmospheric nitrogen, while polyphosphate-accumulating organisms facilitate phosphorus removal by accumulation of polyphosphate within their cells. Phosphorus is often eliminated by addition of metal salts (e.g.  $\text{FeCl}_3$ ,  $\text{FeSO}_4$ ). Sulfur concentration in the wastewater is usually low – similarly to the concentration of dissolved salts and heavy metals –, but still high enough to cause issues with safety, corrosion and odor complaints [34]. Sulfur is removed by contribution of sulfur oxidizing and sulfate reducing bacteria. Following the biological treatment, microorganisms and solids are settled in the secondary clarifiers. A certain fraction of the sludge is fed back to the aeration basin in order to ensure a constant microorganism concentration.

Antibiotics enter the sewage through well-defined routes [35]. Administered drugs are usually not completely absorbed in the body; therefore, a substantial fraction of the parent medicine, its conjugates or bioactive metabolites are excreted and released to the sewage system. Outdated or unused drugs are often simply just flushed down the sink or toilet that also contributes to discharge from private households. Wastewater from hospitals are usually also released to the sewage. It was shown that higher antibiotic concentrations are present in hospital effluents than in the influents of municipal wastewater treatment plants [36]. The results indicated notable contribution to the total antibiotic amounts present in the municipal wastewater. Numerous studies investigated occurrence of xenobiotics in raw wastewater and evidenced presence of sulfonamides in ng –  $\mu\text{g}$  concentration range [37, 38, 39, 40, 41, 42, 43].

Metabolic processes of microorganisms intended to remove organic pollutants from wastewater are adapted to natural chemical compounds (biogenic materials). Chemically synthesized compounds that do not occur in nature (xenobiotics) possess structural features to which microorganisms have not been exposed to during evolution (e.g. compounds with  $-\text{CF}_3$ ,  $-\text{Cl}$ ,  $-\text{N}=\text{N}-$ ,  $-\text{NO}_2$  groups). Differences between the structures of xenobiotics and biogenic materials result in lack of compatible enzymes, which are responsible for activation of metabolic processes [44]. As the attack by microbial catabolic enzymes is blocked, degradation efficiency of numerous artificial compounds at conventional wastewater treatment plants is insufficient [45, 46, 47, 48]. Beside the “unphysiological” substituents, recalcitrant organic compounds have some other typical features. They have high molecular mass, low solubility in water, quaternary carbon atoms, three-fold substituted nitrogen atoms, condensed benzene and pyridine ring (especially polycyclic structures) [49]. Inefficient removal by biological treatment leads to deterioration of wastewater effluent quality and considerable discharge of persistent organic pollutants to surface waters [50, 51, 52, 53]. Poor removal of sulfonamides in the secondary treatment is evidenced by their presence in effluents up to several hundred  $\text{ng dm}^{-3}$  [4, 54, 55, 56]. Consequently, sulfonamides appear in surface waters in notable amounts. Concentration of sulfonamides present in natural water matrices is strongly dependent on the characteristics of the recipient and the pharmaceutical amount emitted from the treatment plant [57, 58, 59, 60].

The secondary treatment deficiencies can be counteracted in the next step of the purification process. Therefore, tertiary treatment is vital in order to achieve an appropriate quality level of treated wastewater prior to their release. There are some existing methods for removal of non-biodegradable compounds, like adsorption or filtration. However, the pollutants are not degraded with these methods, they are only transferred from a medium to another and their disposal remains unsolved. For this reason, there is an urgent need for an economically feasible solution for removal of these pollutants that is viable on industrial scale. Numerous methods, like photocatalysis, ionizing radiation and ferrate techniques have shown promising results in the development phase.

### **2.3 Advanced Oxidation Processes**

To improve the removal efficiency of non-biodegradable hazardous substances, numerous AOP are under development or testing. Complete mineralization of stable chemicals may result in a solution to the final pollutant disposal with no further purification steps required. However, degradation to less complex substances with higher biodegradability and/or lower toxicity may also be advantageous.

AOP are usually applied at – or near – ambient conditions, and they are considered to be clean technologies [61, 62]. The common feature of these methods is the oxidation of pollutants by reactions mainly attributed to  $\bullet\text{OH}$  and other oxygen containing reactive species.  $\bullet\text{OH}$  can be produced by numerous approaches that distinguish the various advanced oxidation methods. Important shortcoming of these techniques is that the presence of harmless organic matter (e.g. humic or amino acids) and inorganic ions (e.g. chloride, carbonate and bicarbonate) act as scavengers of hydroxyl radicals [62]. In this way, AOP intended to treat raw wastewater is not sustainable [63]. However, this can be overcome by integration of AOP into the conventional wastewater treatment as a post-treatment process, following the biological purification stage [63, 64]. AOP are regarded as a promising complementary option to the conventional wastewater treatment, as elimination of persistent organic compounds with these methods proved to be highly effective [65, 66, 67, 68, 69, 70].

The most notable techniques are briefly summarized in chapters 2.3.1 – 2.3.3, while AOP based on generation of  $\bullet\text{OH}$  by ionizing radiation is detailed in chapter 2.4.

### 2.3.1 Fenton-type reactions

Fenton reaction is a cyclic process, in which radicals formed during catalytic decomposition of  $\text{H}_2\text{O}_2$  in acidic medium oxidize the organic matter [71]. In course of reactions, ferrous ( $\text{Fe}^{2+}$ ) catalyst is applied in form of iron(II) sulfate ( $\text{FeSO}_4$ ). Reaction of  $\text{Fe}^{2+}$  with  $\text{H}_2\text{O}_2$  results in complexes, which decompose to, *inter alia*,  $\bullet\text{OH}$  (Reaction 1).  $\bullet\text{OH}$  oxidizes not only the organic substances, it also transforms ferric ( $\text{Fe}^{3+}$ ) to  $\text{Fe}^{2+}$ , in the presence of  $\text{H}_2\text{O}_2$  (Reaction 2). The acidic medium (pH optimum = 2.5 – 3) is important in order to prevent iron precipitation [62]. The iron(III) hydroxide ( $\text{Fe}(\text{OH})_3$ ) precipitate may bind pollutants; and thus, hinder their decomposition. In addition,  $\text{Fe}(\text{OH})_3$  consumes  $\text{H}_2\text{O}_2$  that leads to reduced  $\bullet\text{OH}$  yield.



The efficiency of the Fenton reaction can be enhanced by application of UV-Vis illumination that results in higher yield of  $\bullet\text{OH}$  (Reaction 3). This is the so-called photo-Fenton reaction, and it accelerates  $\text{Fe}^{3+}$  reduction to  $\text{Fe}^{2+}$  [72]. Another Fenton type technique is the electro-Fenton process. This method combines the classical Fenton reaction with electrocoagulation [71].

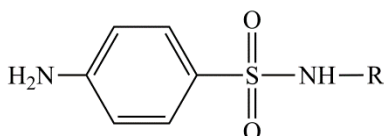


The advantage of Fenton-type reactions is the application of environmentally safe substances and that no special equipment is required [61]. Nevertheless, the amounts of acids and alkaline used may be quite high.

Fenton-type reactions – performed with application of different  $\text{H}_2\text{O}_2$  doses and various catalysts – was found to be able to remove sulfamethazine, sulfadiazine, sulfathiazole and sulfamethoxazole from aqueous solution [65, 73, 74, 75, 76, 77]. Degradation of pollutants was coupled with high reduction of the total organic carbon content (up to 100%).

Trovó et al. [74] proposed two initial transformation routes of sulfamethoxazole. Fragmentation patterns suggested that the initial  $\bullet\text{OH}$  attack takes place on the isoxazole

ring and yields two isobaric monohydroxylated products with  $m/z = 270$  (LC-TOF-MS; positive ionization mode). (See general structure of sulfonamide antibiotics in Scheme 1). Further oxidation of monohydroxylated products results in substitution of the amino group by a hydroxyl group in the aromatic ring, or  $\bullet\text{OH}$  attack on the double bond on the isoxazole ring. Consequently, appearance of double hydroxylated products with  $m/z = 271$  or 288 takes place, respectively. However, benzene ring was found to be more persistent than the other parts of the molecules, since the majority of intermediates contained benzene structure ( $m/z = 288, 270, 244, 216$  and 198). Wan et al. [77] proposed  $\bullet\text{OH}$  attack on the C – N bond of the sulfamethazine pyrimidine ring, leading to formation of product with  $m/z = 214$  (GC-MS). They also evidenced cleavage of the N – S bond that entails formation of products with  $m/z = 173$  and 123. Barhoumi et al. [76] also suggested that oxidation process is initiated at these two sites. In their work, similar products were identified with GC-MS ( $m/z = 214, 173, 123$ ), as in the study of Wan et al. [77], but they detected some other products, as well ( $m/z = 189, 109, 153$ ). However, a possible reaction pathway is likely to start with the desulfurization of sulfamethazine, according to Pérez-Moya et al. [65]. Towards the end of degradation procedure, carboxylic acids, such as acetic, formic, pyruvic, oxamic, fumaric, maleic and oxalic acids were detected [74, 76]. Formation of inorganic species, like  $\text{NH}_4^+$ ,  $\text{NO}_3^-$  and  $\text{SO}_4^{2-}$  have also been reported [74, 76, 77].



**Scheme 1.** General structure of sulfonamide antibiotics.

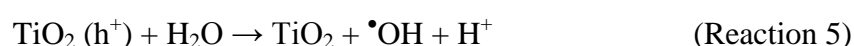
Regarding changes in the biological effects, experiments conducted on *Daphnia magna* and *Vibrio fischeri* test organisms indicated reduced toxicity of the solutions following the treatment [73, 74]. Gonzalez et al. [73] pointed out that biodegradability notably increased (from 0 to 0.3  $\text{BOD}_5 \text{ COD}^{-1}$ ) parallel with the toxicity reduction. However, in the case of sulfamethazine toxicity assessment performed on *V. fischeri*, *Escherichia coli* and *Staphylococcus aureus*, formation of some toxic intermediates was revealed [65, 76]. Nevertheless, there is a questionable issue regarding sample application in biological experiments. In the vast majority of experiments targeting quantification of changes in biodegradability or toxicity, conclusions are drawn by a simple comparison of solutions obtained at different stages of the oxidation. These results do not express properly the toxic potential or biodegradability of distinctive product groups, due to performing investigations



without taking into account the decrease of organic content caused by mineralization. Mineralization reduces the concentration of pollutants; and thus, relieves the pressure on test organism. In this way, reduced toxicity can be measured in treated solutions even if products with higher toxic potential than the parent compounds are formed, simply due to their presence in significantly lower concentration. This issue is well illustrated by the results obtained by Barhoumi et al. [76]. Increase of the 40% initial *Vibrio fischeri* luminescence inhibition to about 45% was reported in course of sulfamethazine degradation by electro-Fenton process. Such difference seems to be insignificant at first sight. However, if we complement this data with the fact that the organic content reduced by 60% at this point, the situation becomes quite different. In spite of the high decrease in organic pollutant content, the toxicity somewhat increased. This indicates that the products have notably higher toxic potential than the initial molecules, despite the negligible difference shown by the toxicity test. The authors correctly concluded higher toxicity of the resulting solution, but the extent is a more difficult issue. Pérez-Moya et al. [65] prepared reference solutions that contained the initial compound (sulfamethazine) in the same TOC amounts as the solutions treated by photo-Fenton. In this way, they achieved exposure of test organisms (*Escherichia coli* and *Staphylococcus aureus*) to equal pollutant loads; and therefore, direct and accurate comparison of the toxic potentials.

### 2.3.2 Photocatalysis

Photocatalysis is based on photo-excitation of valence band electrons of semiconductors, most often TiO<sub>2</sub>. Electron-hole pairs are usually generated with UV photons, which subsequently dissociate and migrate to the surface of the photocatalyst (Reaction 4) [62]. The holes transform to <sup>•</sup>OH in reaction with water (Reaction 5), contribute to formation of superoxide radical anion (O<sub>2</sub><sup>•-</sup>) in the presence of oxygen (Reaction 6) or recombine with electrons that reduces radical yield [78]. The natural light is badly utilized by catalysts, only a narrow wavelength range is useful.



Baran et al. [79] evidenced degradation of  $1 \times 10^{-4}$  mol dm<sup>-3</sup> sulfanilamide, sulfacetamide, sulfathiazole, sulfamethoxazole and sulfadiazine in photocatalytic processes involving

TiO<sub>2</sub>, and Fe salts. The degree of TOC removal reached values as high as 70%. Kaniou et al. [80] reported similarly high degree of sulfamethazine degradation (100%) and mineralization (80%) in experiments performed in presence of TiO<sub>2</sub> P-25 and ZnO photocatalysts. Experimental results of Hu et al. [81] and Abellán et al. [82] also demonstrated that mineralization of SMX can be achieved by UV irradiation of aqueous solutions containing TiO<sub>2</sub>. 80% mineralization was measured by Hu et al. and only 41% was detected by Abellán et al. due to different experimental conditions used.

The major photocatalytic degradation processes of sulfonamides involve hydroxylation of the aromatic ring, elimination of the amide group, elimination or substitution of the amide and the sulfonyl group, opening of the aromatic ring. Degradation mechanism proposed for sulfamethoxazole starts by <sup>•</sup>OH addition on the aromatic ring that generates hydroxycyclohexadienyl radical, from which another <sup>•</sup>OH can abstract a hydrogen to form hydroxyl-substituted product with  $m/z = 268$  or  $270$  (LC-MS/MS negative or positive ionization mode, respectively). In another pathway, <sup>•</sup>OH addition takes place on the isoxazole ring, resulting in tertiary carbon-centered radical that transforms to peroxy radical in the presence of dissolved oxygen. This peroxy radical can abstract a hydrogen atom from a donor to form the corresponding hydroperoxide, which cleaves homolytically to produce <sup>•</sup>OH and the corresponding alkoxy radical. Stable product forms through abstraction of another hydrogen atom by the previously formed radical moiety. This product was identified in LC-MS/MS experiments with  $m/z$  values of 286 or 288 (negative or positive ionization mode, respectively). In course of the third degradation pathway, <sup>•</sup>OH attack leads to cleavage of the S – N bond that results in formation of product with  $m/z = 97$  in negative ionization mode. Calza et al. [83] proposed similar degradation mechanism for sulfadiazine, sulfamerazine, sulfadimethoxine and sulfathiazole, as the one detailed above for sulfamethoxazole [81, 84]. The characteristic products determined by ion trap mass spectrometer in that study were hydroxylated derivatives. Hu et al. [81] evidenced similar degradation rates of different sulfonamide analogues from which they infer applicability of degradation mechanisms proposed for SMX to sulfonamide antibiotics in general. However, Huang et al. [85] concluded – in a work involving 10 sulfonamide antibiotics and nanophase TiO<sub>2</sub> plus UV and nTiO<sub>2</sub>/activated carbon fiber plus UV – that the substituent groups have a substantial impact on the degradation efficiency.

Investigation of inorganic ions revealed that nearly complete sulfur content is present in form of  $\text{SO}_4^{2-}$  following the photocatalysis [80, 81, 82, 83]. Formation of notable  $\text{NH}_4^+$  amounts was characteristic from the beginning of the treatment, while only low amounts of  $\text{NO}_3^-$  were detected following sufficient reaction times [80, 81]. No evidences were found about the presence of  $\text{NO}_2^-$  in treated sulfamethoxazole or sulfamethazine solutions [81, 82].

Photocatalytic degradation of sulfacetamide, sulfathiazole, sulfamethoxazole and sulfadiazine led to significantly reduced toxicity on *Chlorella vulgaris* and increased biodegradability [82, 86]. Cai and Hu [84] reported no acute toxicity of sulfamethoxazole on *Vibrio fischeri* when continuous LED/UVA/ $\text{TiO}_2$  process was used, but increased chronic toxicity was measured (13 – 20%). In the same study, antibacterial activity against *Escherichia coli* (ATCC 25922) was eliminated, as shown by broth microdilution assays.

### 2.3.3 Ozone reactions

Ozone is a strong oxidizing agent that can degrade organic pollutants directly or indirectly by hydroxyl radicals.  $\bullet\text{OH}$  reacts less selectively and faster than  $\text{O}_3$ .  $\bullet\text{OH}$  is generated with higher yields in alkaline medium during ozonation processes [87]. Formation of radical species starts with reaction of hydroxide ( $\text{OH}^-$ ) and  $\text{O}_3$ , that leads to formation of hydroperoxide ion ( $\text{HO}_2^-$ ) and  $\text{O}_2^{\bullet-}$  (Reaction 7). Both  $\text{HO}_2^-$  and  $\text{O}_2^{\bullet-}$  decompose  $\text{O}_3$  in the next step, while ozonide ions ( $\text{O}_3^{\bullet-}$ ), hydroperoxyl radical ( $\text{HO}_2^{\bullet}$ ) and dioxygen is generated (Reaction 8 and 9). In the further reactions, the ultimate decomposition of  $\text{O}_3^{\bullet-}$  takes place, and it is followed by formation of  $\bullet\text{OH}$  (Reaction 10 and 11), which induces  $\text{O}_3$  conversion to  $\text{HO}_2^{\bullet}$  after an intermediate reaction (Reaction 12 and 13) [88].



The rate of ozonation can be enhanced by the presence of H<sub>2</sub>O<sub>2</sub> (Reaction 14), by UV irradiation (Reaction 15) or by combined application UV irradiation and H<sub>2</sub>O<sub>2</sub> [89, 90, 91, 92]. Here, the UV radiation usually has an output maximum at 254 nm, whereby the molar absorption coefficients ( $\epsilon$ ) of O<sub>3</sub> and H<sub>2</sub>O<sub>2</sub> are 3300 and 18.6 mol<sup>-1</sup> dm<sup>3</sup> cm<sup>-1</sup>, respectively [93].



Ozonation proved to be effective for degradation of sulfonamide antibiotics, showing removal efficiencies higher than 90% in experiments involving sulfamethoxazole, sulfachloropyridazine, sulfadimethoxine, sulfamerazine, sulfamethazine, sulfathiazole, sulfadiazine, sulfapyridine, sulfamethizole [67, 94, 95, 96, 97, 98, 99, 100, 101]. In the work of Dantas et al. [97] complete degradation of sulfamethoxazole was achieved by reaching just 10% mineralization.

The reaction rate constant ( $k$ ) of O<sub>3</sub> with sulfamethoxazole was found to be  $\sim 2.5 \times 10^6 \text{ mol}^{-1} \text{ dm}^3 \text{ s}^{-1}$  (at pH 7 and 20°C) [67]. The reactivity reduced to  $k_{\text{O}_3} = 2 - 3 \times 10^4 \text{ mol}^{-1} \text{ dm}^3 \text{ s}^{-1}$  in acidic medium (pH = 2 and 22°C), according to results of Garoma et al. [99]. This phenomenon is due to the two acid-base dissociation equilibria ( $\text{p}K_{\text{a}}$ ) of sulfonamides. At pH lower than the  $\text{p}K_{\text{a}1}$  value, the nitrogen of the amino group is in a protonated form, which is less susceptible to ozone attack, while at pH values above  $\text{p}K_{\text{a}2}$ , the dissociation of the hydrogen present in the sulfonamide group promotes a slight increment in the reactivity [97]. Therefore, pH plays an important role in the efficiency of sulfonamide degradation by ozonation.

del Mar Gómez-Ramos et al. [100] described five pathways of sulfamethoxazole degradation by means of ozonation that involved reactions of both molecular ozone and  $\cdot\text{OH}$ . They proposed decomposition of initial molecules going through hydroxylation on the benzene ring that was evidenced by product identified with  $m/z = 270$  (LC-TOF-MS in positive ionization mode) or oxidation of the amine group at the benzene ring (evidenced by two products with  $m/z = 284$ ). In addition, oxidation of the methyl group at the isoxazole ring (evidenced by a third product with  $m/z = 284$ ); oxidation of the double bond C = C at the isoxazole ring (evidenced by product with  $m/z = 288$ ); and S – N bond cleavage (evidenced by product with  $m/z = 99$ ) was also described. The latter reaction, cleavage of

sulfonamide bond was found to be the main degradation pathway that led to formation of the most abundant intermediate ( $m/z = 99$ ). An interesting finding was the identification of three isobaric compounds ( $m/z = 284$ ). It was assumed that  $O_3$  attack takes place on the aniline moiety of sulfadiazine, sulfamethoxazole, sulfapyridine and sulfathiazole [96, 97, 101].

*Daphnia magna*, *Pseudokirchneriella subcapitata* and *Vibrio fischeri* assays revealed increasing toxic effects at the early stages of ozonation [97, 100]. del Mar Gómez-Ramos et al. [100] detected considerable toxicity even following complete removal of initial molecules. In contrast, reduced toxicity was reported by Kim et al. [101].

In addition to the previously discussed ones, there are many other procedures for hydroxyl radical generation, such as application of ultrasound, vacuum UV, photolysis of hydrogen peroxide etc. [102]. Utilization of ionizing radiation for radical generation is discussed in the following section.

## 2.4 Ionizing radiation treatment

### 2.4.1 Energy deposition and product distribution

The most commonly applied irradiation sources for radiolytic treatment of aqueous medium are  $^{60}\text{Co}$   $\gamma$ -sources and electron accelerators. During irradiation with  $^{60}\text{Co}$  gamma rays ( $E_1 = 1.33$  MeV and  $E_2 = 1.17$  MeV), the main physical interactions with matter are the photoelectric effect (mostly at  $E < 0.1$  MeV, in molecules with light atoms), Compton effect ( $E = 0.01 - 100$  MeV) and pair production ( $E > 3$  MeV). In case of irradiation of aqueous solution, Compton scattering takes place decisively. These randomly occurring events involve significant energy losses at each interaction and result in formation of secondary electrons. In this way,  $\gamma$ -irradiation can be interpreted as a fast electron producing method within the sample [103]. Application of particle accelerators provides a possibility of direct introduction of monoenergetic electrons. Both in  $\gamma$ -irradiation and accelerated electron irradiations, the fast secondary electrons trigger chemical changes predominantly, with energies ranging from few tenths of keV to few keV. Contrary to photons, electrons lose kinetic energy in sequence of small energy transfers. The main processes are ionization, excitation and emission of X-rays or Cherenkov radiation. The energy transfer can be characterized by the linear energy transfer (LET) defined as the

deposited energy per unit length ( $\text{eV nm}^{-1}$ ). This value heavily depends on the characteristics of the particle (e.g. mass, charge, velocity etc.). Gamma rays and accelerated high-energy electrons are both characterized by low LET. The probability of energy deposition to the electrons of the medium along a unit path is inversely proportional to the square of the particle velocity. Simply expressed, longer time spent in the vicinity of a molecule increases the probability of interaction with electron cloud. Therefore, a penetrating fast electron induces only very few ionization events at the beginning of its path. Nevertheless, as the velocity attenuates – during traversing Coulomb fields and collisions with the surrounding molecules – the number of ionization events increases. The consequence of variable energy transfer cross section is an inhomogeneous distribution of reactive intermediates and final products. As the energy is transferred in different sized packets at various points of the path, zones of excited and ionized species are formed in variant dimensions. Their spatial arrangement is not always unified. Spherical composition is prevailing up to ten ion pairs, while cylindrical composition is dominant above ten ion pairs. Based on the transferred energy, they are assigned to four groups: Spurs (6 – 100 eV), blobs (100 – 500 eV), short tracks (500 – 5000 eV) and branch tracks ( $> 5000$  eV). Spur usually refers to both spurs and blobs. The ratio of spurs, blobs and short track entities in case of 1 MeV electron irradiation in liquid water was found to be 0.75 : 0.12 : 0.13, respectively [104]. The line connecting spurs shows the route of the electron passing through the medium and it is simply called primary particle track. Fig. 1 taken from the work of Choppin et al. [105] shows tracks of a 200 keV electron and a 47 keV  $\gamma$ -photon in a cloud chamber.

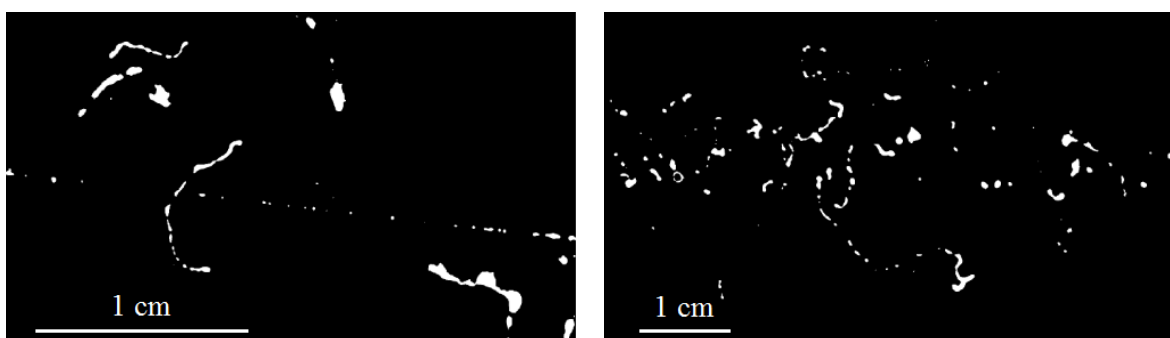


**Fig. 1.** 200 keV electron (left) and 47 keV  $\gamma$ -photon (right) cloud chamber tracks in air and methane, respectively, taken from the book of Choppin et al. [105].

The reactive zones initially contain one or more ion-electron pairs, ground-state and excited molecules. Freeman defined the reactive zones as “a grouping of reactive intermediates in

which there is a significant probability that some of the intermediates will react with each other before they can diffuse into the bulk” [106]. As the reaction rate constants ( $k$ ) of species formed in spurs are of the order of  $10^{10} \text{ mol}^{-1} \text{ dm}^3 \text{ s}^{-1}$ , their reaction kinetics is diffusion controlled [107]. In diffusion controlled kinetics, geminate recombination and/or bulk reactions may take place. This means that the initial species may react with each other or leave the spur. The fundamentals of spur reactions are provided by the time-dependent diffusion equation, with assumption of competitive reactions among:

- bimolecular reactions of the primary radicals formed
- pseudo-first order reactions of the primary radicals with scavengers
- and diffusion of the primary radicals to the bulk [108].

The reactions in spurs are complicated by their eventual overlapping, by solutes and by the differences between reaction rate constants. Low LET radiation leads to isolated spurs from which the majority of primary species can escape in high permittivity medium. Therefore, the spur reactions can be neglected in dilute aqueous solutions irradiated with electron or gamma radiation. Furthermore, distribution of the particles can be considered homogeneous after spur expansion that ends in  $10^{-7}$  seconds. The average distance between spurs in water is in the order of 100 nm and their average radius is  $\sim 2$  nm (Table. 1).

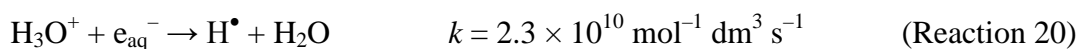
Radiation type	Energy (MeV)	Average LET value in water ( $\text{eV nm}^{-1}$ )	Average distance between reactive zones (nm)	Maximum range in water (mm)
Electron	1	0.24 <sup>a</sup>	400 <sup>a</sup>	4.37 <sup>b</sup>
Electron	10	0.19 <sup>a</sup>	500 <sup>a</sup>	53.8 <sup>b</sup>
<sup>60</sup> Co- $\gamma$ , average	1.25	0.26 <sup>c</sup>	1000 <sup>b</sup>	$X_{0.5} = 110^b$

**Table 1.** Average LET values, average distances between reactive zones and maximum ranges in course of irradiation of water by electrons or  $\gamma$ -rays emitted by <sup>60</sup>Co. The data were taken from <sup>a</sup>[106], <sup>b</sup>[109] and <sup>c</sup>[103].  $X_{0.5}$  is the half value range.

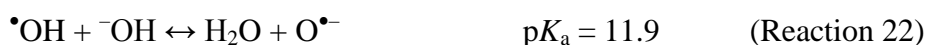
#### 2.4.2 Primary intermediate and final products in water radiolysis

Radiolytic decomposition of water by low LET irradiation leads to formation of dry electrons ( $e^-$ ) and water radical cations ( $\text{H}_2\text{O}^{+\bullet}$ ), according to Reaction 16. In high permittivity medium – such as water – most of the electrons have enough energy to overcome the attraction of positive ions. In this way, electrons escape geminate recombination as they leave the Coulomb field of  $\text{H}_2\text{O}^{+\bullet}$ . When these electrons lose a

substantial part of their energy (thermalize), they orient the surrounding water molecules with the positively charged parts toward themselves, and become solvated/hydrated (Reaction 17). As a result, the smallest anion, the hydrated electron ( $e_{\text{aq}}^-$ ) forms. On the other hand,  $\text{H}_2\text{O}^{+\bullet}$  may protonate the neighboring molecules; and thus, contributes to formation of  $\bullet\text{OH}$ , as shown in Reaction 18. The excess energy of excited water molecules ( $\text{H}_2\text{O}^*$ ) is dissipated by bond rupture and subsequent formation of  $\bullet\text{OH}$  and  $\text{H}^\bullet$  as shown in Reaction 19. However,  $\text{H}^\bullet$  may form in the reaction of  $\text{H}_3\text{O}^+$  and  $e_{\text{aq}}^-$ , as well (Reaction 20).



The reactions of intermediates are strongly influenced by the pH.  $e_{\text{aq}}^-$  is converted to  $\text{H}^\bullet$  in acidic medium, while  $\text{H}^\bullet$  forms  $e_{\text{aq}}^-$  in alkaline medium. These reactions are practically complete at  $\text{pH} < 2$  and  $\text{pH} > 10$ , respectively. The  $\text{p}K_{\text{a}}$  of the latter transformation is at  $\text{pH} = 9.6$ . Therefore,  $e_{\text{aq}}^-$  predominates under alkaline conditions, while  $\text{H}^\bullet$  is in the majority at low pH. At pH values higher than 11,  $\bullet\text{OH}$  and  $\text{H}_2\text{O}_2$  dissociate to  $\text{O}^{\bullet-}$  and  $\text{HO}_2^-$ , respectively (Reaction 22 and 23).



	pH	$G(e_{\text{aq}}^-)$	$G(\text{H}^\bullet)$	$G(\bullet\text{OH})$	$G(\text{HO}_2^\bullet)$
bulk	0.46	0 <sup>a</sup>	0.38 <sup>a</sup>	0.30 <sup>a</sup>	0.001 <sup>a</sup>
bulk	3 – 11	0.27 <sup>a</sup>	0.06 <sup>a</sup>	0.28 <sup>a</sup>	0.003 <sup>a</sup>
spur	neutral	0.49 <sup>b</sup>	0.14 <sup>b</sup>	0.63 <sup>b</sup>	

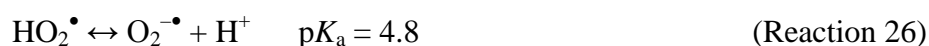
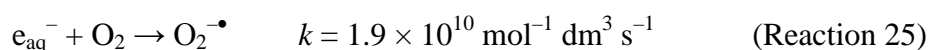
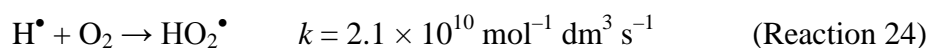
**Table 2.** Radiation chemical yields of reactive species during water radiolysis [ $\mu\text{mol J}^{-1}$ ] in the bulk <sup>a</sup>[109] and spur <sup>b</sup>[110].

The reactive intermediates form with well-known radiation chemical yields ( $G$ ). The yield of  $\bullet\text{OH}$  and  $e_{\text{aq}}^-$  is about the same in neutral or alkaline solutions,  $G = 0.28 \mu\text{mol J}^{-1}$  and

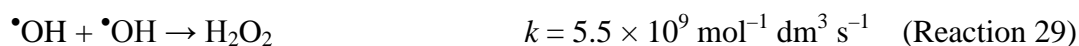
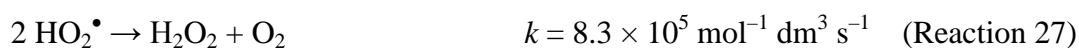


$G = 0.27 \mu\text{mol J}^{-1}$ , respectively, while  $\text{H}^\bullet$  forms with lower yield  $G = 0.06 \mu\text{mol J}^{-1}$ . The yields of intermediate and final products at different pH are summarized in Table 2.

Interactions of reactive intermediates generated during the radiolysis of water lead to formation of  $\text{H}_2$ ,  $\text{H}_2\text{O}_2$  and  $\text{O}_2$  as final products. In open systems,  $\text{H}_2$  is relatively inert and usually leaves the solution without any interaction. Oxygen molecules also escape continuously, but they are able to capture  $\text{H}^\bullet$  and  $\text{e}_{\text{aq}}^-$  that may result in formation of  $\text{HO}_2^\bullet$  and  $\text{O}_2^{\bullet-}$ . In air or oxygen saturated solutions, higher concentrations of  $\text{HO}_2^\bullet$  and  $\text{O}_2^{\bullet-}$  occur (Reaction 24 and 25). In such solutions, the contribution of these radicals to degradation of solutes should also be considered, in addition to  $\bullet\text{OH}$  induced degradation. Reaction 26 determines the balance between  $\text{HO}_2^\bullet$  and  $\text{O}_2^{\bullet-}$  ( $\text{p}K_{\text{a}} = 4.8$ ).



Formation of  $\text{H}_2\text{O}_2$  is of great significance due to its disruptive effects to numerous analytical methods and toxic potential measurements. In course of ionizing radiation treatment, the main sources of  $\text{H}_2\text{O}_2$  are the self-termination reactions (Reaction 27, 28 and 29).



In addition to notable  $\text{H}_2\text{O}_2$  concentrations ( $\sim 3 \times 10^{-4} \text{ mol dm}^{-3}$ ) detected in ionizing radiation treatment [111], application of other advanced oxidation methods also caused considerable residual  $\text{H}_2\text{O}_2$  content. These concentrations ranged from  $\sim 10^{-4} \text{ mol dm}^{-3}$  to  $\sim 10^{-3} \text{ mol dm}^{-3}$  [112, 113, 114, 115, 116]. However, photochemical  $\text{H}_2\text{O}_2$  formation rates of  $10^{-6} \text{ mol dm}^{-3} \text{ h}^{-1}$  [117] allow concentration levels up to a few times  $10^{-9} \text{ mol dm}^{-3}$  in natural freshwaters [118]. Therefore, aquatic organisms are evolutionarily adapted to low  $\text{H}_2\text{O}_2$  concentrations, but they are unable to eliminate high amounts of intracellular  $\text{H}_2\text{O}_2$  [118]. Consequently, presence of significant  $\text{H}_2\text{O}_2$  may distort experiments involving living organisms by the strong toxic effects. In addition,  $\text{H}_2\text{O}_2$  liberates  $\text{O}_2$  that distorts analytical

laboratory tests based on respirometry or manometry [119]. Considerable  $\text{H}_2\text{O}_2$  amounts interfere in chemical oxygen demand (COD) experiments, as well [120, 121, 122].

#### 2.4.3 Pollutant removal by ionizing radiation in general

Reactive intermediates generated by high-energy irradiation interact with a wide range of pollutants. These interactions include redox reactions, dye decoloration, organic material decomposition, biological sterilization, removal of antibacterial activity and so on [123, 124, 125, 126]. It was evidenced that  $\bullet\text{OH}$  is the main reactant under a variety of different experimental conditions [127, 128, 129].

$\bullet\text{OH}$  is an extremely reactive radical, with low selectivity that is advantageous in terms of pollutant removal. The reaction rate coefficients are predominantly diffusion limited up to supercritical temperature [130]. Compared to other oxygen radicals involved in the degradation processes,  $\bullet\text{OH}$  reacts faster. Depending on the organic substances, initial  $\bullet\text{OH}$  attack can take place by hydrogen abstraction (saturated organics) or by addition (aromatic and olefinic solutes) [131, 132].  $\bullet\text{OH}$  readily reacts with  $\text{C}=\text{C}$  and  $\text{C}=\text{N}$  (but not with  $\text{C}=\text{O}$ ) due to electrophilic character of double bonds. Hydrogen abstraction usually takes place on  $\text{C}-\text{H}$  bonds.

Aromatic hydrocarbons have low excitation and ionization energy levels coupled with relatively high bond energies that also make them extremely resistant to radiation. The excited states have long lifetimes (from ns to s) and may often relax through luminescence. Aromatic hydrocarbons have a conjugated  $\pi$ -electron system; therefore, the energy is taken up and distributed to the entire molecule. In this way, the energy is rarely confined to a single bond, which means that the probability of bond rupture is low. This interesting phenomenon is related to the special electron system, which exerts protecting effect. The energy absorbed directly by aliphatic fragment of the molecules is transferred to aromatic fraction, where it is mostly converted to thermal energy [133]. The effect also occurs in case of alkyl side chains.

Chemical phenomena caused by energy absorption during irradiation, like rupture or rearrangement of chemical bonds, are examined by radiation chemistry [134]. These processes can be considered to begin with formation of small clusters containing reactive species [106]. These clusters were discussed previously (section 2.4.1). From the point of

view of radiation chemistry, the most of the environmental bodies of water and municipal wastewater can be considered as dilute aqueous solution. During ionizing radiation treatment, water molecules absorb the transmitted energy predominantly and the vast majority of the resulting reactive intermediates interact with dissolved substances [109]. Therefore, great effects can be achieved with a relatively low absorbed dose that is extremely important in case of radiation processing [135]. Depending on the pollutant content and the level of infection, aqueous solutions can be separated into two groups. Natural water and polluted drinking water both possess considerably lower concentration of contaminants than industrial, municipal or agricultural wastewater.

Substantial degree of purification can be achieved with  $\sim 1$  kGy absorbed dose, in case of natural water and polluted drinking water [136]. Such absorbed dose ensures decoloration, deodorization, disinfection and dechlorination of organic chlorocompounds. Irradiation of municipal wastewater usually takes place in a dose range suitable for disinfection (2 – 3 kGy) [136]. Industrial wastewater requires high absorbed doses due to high concentrations and variety of contaminants that are often highly toxic, as well. Therefore, irradiation of such solutions is reasonable by combining it with other techniques [137]. Liquid animal wastes contain high amount of microbial cells and organic materials. The latter act as radical scavengers and in this way provide protection to bacteria, viruses and parasites. Therefore, absorbed doses above 25 kGy are needed for an appropriate disposal. Such high doses can be reduced by additives (e.g. ammonia) or by combined application with other methods.

The first studies applying ionizing radiation treatment were focusing on disinfection (1950s), but soon the attention turned to purification of wastewater and water. Numerous laboratory scale experiments led to realization of pilot scale plants or mobile electron beam facilities in Russia, Austria, Germany, USA, Italy, Brazil and Republic of Korea [138]. Industrial scale facilities were built in Russia and in the Republic of Korea [139, 140].

#### 2.4.4 Ionizing radiation treatment of sulfonamide antibiotics

In the literature, elimination of sulfamethoxazole, sulfadimethoxine, sulfanilamide, sulfadiazine or sulfamethazine from aqueous solution by application of e-beam or gamma irradiation was investigated under different conditions. Results referred to efficient degradation of the selected sulfonamides up to  $130 \text{ mg dm}^{-3}$  concentration and attainable

high degree of mineralization [101, 141, 142, 143]. Nevertheless, complete removal of initial molecules was reached even with mineralization lower than 10% [144, 145]. Nitrogen content remained in the solutions even if absorbed dose high as 5 kGy was used [146]. Irradiation improved the biodegradability and significantly reduced toxicity on *Pseudokirchneriella subcapitata* [101, 147, 148, 149]. However, no considerable changes in toxic effects towards *Daphnia magna* or *Vibrio fischeri* were evidenced [147].

Regarding degradation mechanism, several possible pathways were proposed. As main processes, hydroxylation, desulfonation and cleavage take place. Liu et al. [141] proposed  $\bullet\text{OH}$  reaction with the nitrogen atom bonded on the aromatic ring of sulfadiazine, as it can be easily attacked due to the strong negative charge. Consequently, the N – H bond cleaves. However, Guo et al. [142] suggested addition of an OH group to this amino group that was supported by the appearance of product with  $m/z = 264$  (LC-MS, negative ionization mode) and by the quantum chemical calculations. Cleavage of N – S or C – N bonds followed by formation of products with  $m/z = 92, 97, 106, 119, 172, 213$  and  $226$  were also proposed as possible radiation-induced degradation pathways [142, 144]. In addition to N – S or C – N bond rupture, cleavage of N – benzene bond or S – benzene bond was proposed in sulfamethazine sulfanilamide, sulfamethoxazole and sulfadimethoxine containing solutions, as well [145, 150]. Kim et al. published a detailed study concerning identification of sulfamethoxazole degradation products and analysis of possible degradation mechanisms [151]. They proposed hydroxylation, desulfonation, deamination and oxidation routes in addition to bond ruptures in the parent molecules. Formation of  $\text{SO}_4^{2-}$ , acetic and formic acids was evidenced following ring decomposition and fragmentation of complex structures, while  $\text{NO}_2^-$ ,  $\text{NO}_3^-$  and  $\text{NH}_4^+$  were not detected [141, 144, 145, 146].

### 3 Background summary

---

The presence of sulfonamides in the environment contributes to antibacterial resistance prevalence and poses serious environmental risk by toxic effects, as well. Discharge of these antibiotic agents in industrialized regions is mainly associated with their inadequate removal from wastewater.

Effective removal of sulfonamides by ionizing radiation treatment indicates that this method could be adequate for reducing or preventing sulfonamide emission from wastewater treatment plants. Although there is sufficient literature on the chemical analysis and treatment performance, no paper was published on comparing the degradation of a large number of sulfonamides and evaluating both the chemical reaction mechanisms and the toxicology of products.

Application of ionizing radiation generates considerable  $H_2O_2$  content that interferes with both chemical and biological analyses, as discussed in section 2.4.2. In addition to these interferences, the sample application approach (see the controversial issue in section 2.3.1) may significantly affect the outcome of biodegradation and toxicity tests. Mineralization taking place during irradiation reduces the concentration of pollutants and thus relieves the pressure on test organism [152]. In the literature, screening biodegradability or toxicity changes was generally carried out without considering these factors.

The review of the literature revealed serious shortcomings on comprehensive biodegradability assessment. Literature data on biodegradability originates from experiments performed predominantly on activated sludge. Such investigation is inadequate for prediction of biodegradation in the natural water environment: Activated sludge might be adapted to compounds tested, since it is exposed to these pollutants continuously [153]. For this reason, only analyses performed with natural water provide an adequate picture on the status of biological availability of the degradation products in environmental water bodies.

An overview of the literature data also pointed out a lack in thorough toxicity screening. The available information is provided by tests conducted usually on a single test organism, using one or few sulfonamide antibiotics. To get a better image on the potential hazard, test

organisms from three different trophic levels has to be involved in a battery of toxicity experiments, as recommended in the literature [154, 155].

Despite the huge amount of studies carried out on account of reducing the risk of antibacterial resistance emergence, to date, no paper has been published that aimed at investigating the changes in antimicrobial activity in solutions of irradiated sulfonamides and the impact of the synergistically acting trimethoprim.

## 4 Objectives

---

### 4.1 Degradation efficiency and product analysis; general degradation mechanism

The identification and evaluation of the general characteristics of radiolytic sulfonamide decomposition is missing from the literature. One of the objectives of this work was to fill this gap. In order to accomplish the task, the reactions of eight sulfonamides (Table 3) were studied in a complex approach by a variety of analytical techniques.

Pulse radiolysis experiments were conducted to investigate the elementary steps of oxidation. Stable organic products were separated and identified by LC-MS/MS. Mineralization was quantified by TOC, while the degree of oxidation by COD measurements. Having regard to concerns mentioned in connection with nitrogen and sulfur (section 2.2), total nitrogen and total sulfur contents were also followed up. Additionally, nitrogen and sulfur species important in wastewater treatment ( $\text{NO}_2^-$ ,  $\text{NO}_3^-$ ,  $\text{NH}_4^+$ ,  $\text{SO}_4^{2-}$  and  $\text{SO}_3^{2-}$ ) were monitored by ion chromatography.

### 4.2 Evaluation of changes in toxicity, biodegradability and antibacterial activity

The second part of the study aimed at comprehensive biodegradability assessment, toxicity screening and evaluation of antibacterial activity along the purification process. These were also missing from the literature published to date.

To measure the biodegradability, BOD experiments were performed by seeding test solutions with activated sludge or river water. Screening toxicity along the purification was carried out by using test organisms from three different trophic levels (producer *Pseudokirchneriella subcapitata*, consumer *Daphnia magna* and decomposer *Vibrio fischeri*), incorporated in a battery of experiments. These are the most common test organisms used in ecotoxicity testing. Toxicity of sulfonamide antibiotics to activated sludge was tested by respiration inhibition tests and by using BOD<sub>5</sub> as toxicity indicator.

Reduction of antibacterial activity was tested on the most commonly applied sulfonamide substance, sulfamethoxazole. Changes were followed up by agar diffusion and broth microdilution assays, using pathogens commonly treated by pharmaceuticals containing sulfamethoxazole (*Staphylococcus aureus*, *Escherichia coli* and *Pseudomonas aeruginosa*).

Such medicines usually contain trimethoprim in addition to sulfamethoxazole. Therefore, investigations were carried out by involving both substances and a commercially available medicine. In the series of these tests, individual and combined effects were examined.

### **4.3 Pollutant load dependence of biological responses and effects of H<sub>2</sub>O<sub>2</sub>**

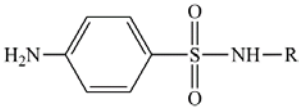
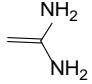
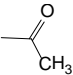
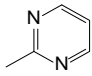
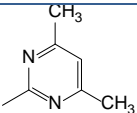
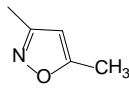
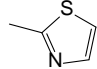
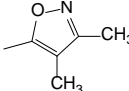
H<sub>2</sub>O<sub>2</sub> is always produced during radiolytic degradation of pollutants in water matrix. Despite the well-known toxic effects of H<sub>2</sub>O<sub>2</sub> to living organisms, its impact on test organisms in different toxicity assays is usually disregarded. To determine these effects, ecotoxicity and antibacterial activity measurements were performed using dilution series of H<sub>2</sub>O<sub>2</sub>. On the other hand, the organic content decreases during degradation of the pollutants. This leads to exposure of test organisms to different loads of pollutants when solutions from different stages of the treatment are examined. This effect was also investigated by setting the pollutant concentration to equal COD or TOC values.



## 5 Materials and methods

### 5.1 Materials

The selected sulfonamides (Table 3), sulfathiazole (STZ, 4-amino-N-(1,3-thiazol-2-yl)benzenesulfonamide), sulfanilamide (SAA, 4-aminobenzenesulfonamide), sulfisoxazole (SSZ, 4-amino-N-(3,4-dimethyl-1,2-oxazol-5-yl)benzenesulfonamide), sulfamethoxazole (SMX, 4-amino-N-(5-methylisoxazol-3-yl)benzenesulfonamide), sulfaguanidine (SGD, 4-amino-N-[amino(imino)methyl]benzenesulfonamide), sulfadiazine (SDZ, 4-amino-N-(pyrimidin-2-yl)benzenesulfonamide), sulfacetamide (SCT, N-[(4-aminophenyl) sulfonyl]-acetamide) and sulfamethazine (SMZ, 4-amino-N-(4,6-dimethylpyrimidin-2-yl)benzenesulfonamide) were provided by Sigma-Aldrich Ltd. (Hungary).

General structure			
Sulfonamide Abbreviation	Formula	R substituent	
Sulfanilamide SAA	C <sub>6</sub> H <sub>8</sub> N <sub>2</sub> O <sub>2</sub> S MM: 172.20 pK <sub>a1</sub> : 2.0, pK <sub>a2</sub> : 10.5	—H	
Sulfaguanidine SGD	C <sub>7</sub> H <sub>10</sub> N <sub>4</sub> O <sub>2</sub> S MM: 214.24 pK <sub>a1</sub> : 1.6, pK <sub>a2</sub> : 11.3		
Sulfacetamide SCT	C <sub>8</sub> H <sub>10</sub> N <sub>2</sub> O <sub>3</sub> S MM: 214.24 pK <sub>a1</sub> : 1.8, pK <sub>a2</sub> : 5.3		
Sulfadiazine SDZ	C <sub>10</sub> H <sub>10</sub> N <sub>4</sub> O <sub>2</sub> S MM: 250.28 pK <sub>a1</sub> : 2.1, pK <sub>a2</sub> : 6.4		
Sulfamethazine SMZ	C <sub>12</sub> H <sub>14</sub> N <sub>4</sub> O <sub>2</sub> S MM: 278.33 pK <sub>a1</sub> : 2.6, pK <sub>a2</sub> : 7.4		
Sulfamethoxazole SMX	C <sub>10</sub> H <sub>11</sub> N <sub>3</sub> O <sub>3</sub> S MM: 253.28 pK <sub>a1</sub> : 1.6, pK <sub>a2</sub> : 5.7		
Sulfathiazole STZ	C <sub>9</sub> H <sub>9</sub> N <sub>3</sub> O <sub>2</sub> S <sub>2</sub> MM: 255.32 pK <sub>a1</sub> : 2.2, pK <sub>a2</sub> : 7.2		
Sulfisoxazole SSZ	C <sub>11</sub> H <sub>13</sub> N <sub>3</sub> O <sub>3</sub> S MM: 267.30 pK <sub>a1</sub> : 1.5, pK <sub>a2</sub> : 5.0		

**Table 3.** Names, abbreviated names of sulfonamides used in the text, formulae, molecular masses (MM), acid-base dissociation equilibria (pK<sub>a</sub>) and the R substituents on —SO<sub>2</sub>—NHR.

Trimethoprim and the chemicals used for COD measurements were obtained from Molar Chemicals Ltd., Hungary, while Sumetrolim was purchased from Egis Pharmaceuticals PLC, Hungary. N<sub>2</sub>O and N<sub>2</sub> gases were purchased from Linde Gas Hungary Co. Ltd., and Messer Hungarogas Ltd., Hungary, respectively. H<sub>2</sub>O<sub>2</sub> test kit (Catalog Nr. 1.18789.0001) was bought from Merck Ltd., Hungary, while all other chemicals were obtained from VWR International Ltd., Hungary. The liquid-dried *Vibrio fischeri* Beijerinck (Vibrionales: Vibrionaceae) (ATCC 49387) was supplied by Hach Lange GmbH., Germany, while the standard laboratory colony of *Daphnia magna* Straus (Crustacea: Cladocera) originated from LAB Research Ltd., Hungary. *Pseudokirchneriella subcapitata* (Korshikov) (Chlorophyta: Selenastraceae) (ATCC 22662) was obtained from Agro-Environmental Research Institute, National Research and Innovation Centre, Budapest, Hungary. The National Collection of Agricultural and Industrial Microorganisms (NCAIM, Szent István University, Budapest, Hungary) supplied the Gram-positive *Staphylococcus aureus* (ATCC 6538), the Gram-negative *Escherichia coli* (ATCC 8739) and *Pseudomonas aeruginosa* (ATCC 9027) bacterial strains. Trypto-casein soy broth was supplied by Biokar Diagnostics, France. Municipal activated sludge was taken from the aeration basin of the South Pest Wastewater treatment Plant (Budapest Sewage Works Pte Ltd., Hungary), while river water was taken from the Danube River at 47° 25' 2.02" N, 19° 5' 52.79" E.

## 5.2 Sample preparation and irradiation procedure

Irradiation was performed with a <sup>60</sup>Co SSL-01 panoramic type facility, operated by the Institute of Isotopes Co. Ltd. Budapest, Hungary. The radiation source is located in the irradiation room during the treatment of the solutions, while after irradiation it is sank to its shielded storage room, a water pool under the irradiation room (Fig. 2). Doses absorbed in course of irradiation were determined by ethanol chlorobenzene dosimetry with oscillometric detection [156].

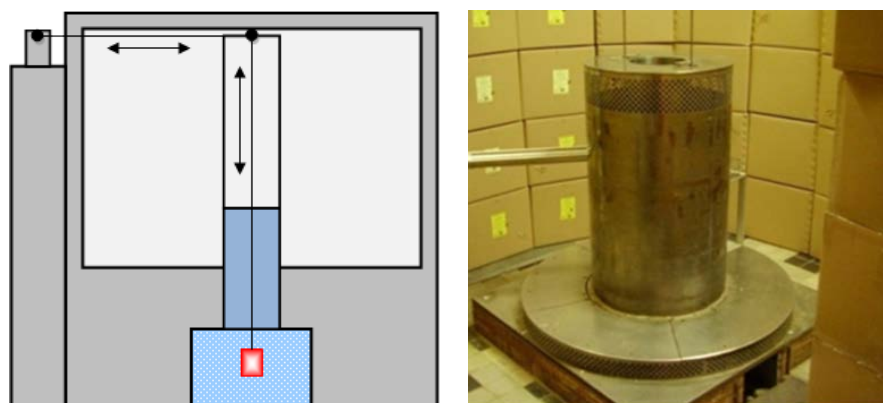


**Fig. 2.** SLL-01 type pilot scale  $\gamma$ -facility.

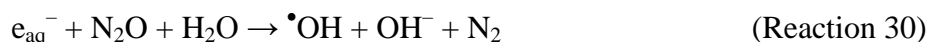
Irradiation was conducted using freshly prepared, unbuffered aqueous solutions, containing different sulfonamides in  $1 \times 10^{-4} \text{ mol dm}^{-3}$  concentration. The reason for the choice of such initial concentration was to obtain treated solutions containing products in well measurable range of the available devices. (The initial concentration selected is higher by a few orders of magnitude as compared to sulfonamide concentrations usually detected in the environment or wastewaters.) The treatment took place at room temperature with a dose rate of  $6.0 - 7.6 \text{ kGy h}^{-1}$ . The solutions in volume of  $1 \text{ dm}^3$  were saturated with air – in amber glass bottles – prior to irradiation, and they were constantly aerated during the procedure. Only the SMX solutions used for separation and evaluation of radical reactions were prepared in different way. These solutions were made by setting the pH to 4 and 8, in addition to the natural pH, and they were subsequently bubbled with appropriate gases for 4 minutes and immediately sealed airtight in  $5 \text{ cm}^3$  ampoules.

### 5.3 Pulse radiolysis

Fast reaction techniques, such as pulse methods, provide an opportunity to investigate transient species. In pulse radiolysis, the kinetics of radical intermediates generated by ionizing radiation can be followed up by direct observation of the transient product decay or growth [157]. In course of pulse radiolysis, the energy is subjected in a pulse that initiates fast chemical reactions on  $\mu\text{s}$  timescale. These reactions are followed up by kinetic spectrophotometric methods in the UV-Vis wavelength range.

The measurements were performed by using 800 ns pulse width of accelerated electrons (4 MeV), generated by a TESLA LINAC LPR-4 type electron accelerator. The dose/pulse was  $0.02 - 0.04 \text{ kGy}$  and the solutions continuously flowed through the optical cell. The optical detection took place in 1 cm cells with single-beam time-resolved spectrophotometry. The light passing through the non-irradiated system gave the reference intensity. Prior to experiments involving sulfonamides, dosimetry was carried out with potassium thiocyanate (KSCN) solutions, using  $7580 \text{ mol}^{-1} \text{ dm}^3 \text{ cm}^{-1}$  molar absorption coefficient for  $(\text{SCN})_2^{\bullet-}$  at 472 nm [158, 159]. For investigation of reactions attributed to  $\bullet\text{OH}$ , the solutions were bubbled with  $\text{N}_2\text{O}$  during the irradiation. The  $\text{N}_2\text{O}$  concentration was  $\sim 2 \times 10^{-2} \text{ mol dm}^{-3}$  in these experiments. Under these conditions,  $e_{\text{aq}}^-$  converts to  $\bullet\text{OH}$  according to Reaction 30. To observe the  $e_{\text{aq}}^-$  reactions in the absence of  $\bullet\text{OH}$ , *t*-BuOH was added to the samples prior to irradiation to capture the forming  $\bullet\text{OH}$  (Reaction 31). The reactivity of radicals formed in this

reaction is relatively low. In addition, N<sub>2</sub>-bubbling was used to remove the oxygen from the solutions.



## 5.4 Product identification

### 5.4.1 Liquid chromatography – tandem mass spectrometry

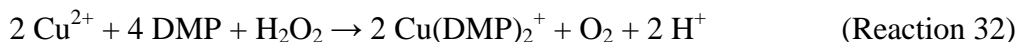
Liquid chromatography – tandem mass spectrometry (LC-MS/MS) is a highly specific technique that is a primary analytical tool for analysis of pharmaceuticals and their degradation products. The degradation products were separated with an Agilent 1200 liquid chromatograph (2.1 mm × 100 mm Phenomenex Kinetex XB-C18 column). Measurements were carried out with gradient elution with a flow rate of 0.2 cm<sup>3</sup> min<sup>-1</sup>, using 0.1% aqueous formic acid (A) and pure acetonitrile (B) eluents. The column temperature was set to 25 °C and the eluents were filtered with 0.2 μm regenerated cellulose filters. The eluent composition changed as follows: 3% B, 3% B, 50% B, 3% B, 3% B at 0 min, 2 min, 10 min, 15 min and 25 min, respectively. Product identification was performed by on-line tandem mass spectrometry, in both positive and negative ionization modes. An Agilent 6410 triple quadrupole tandem mass spectrometer was used for this purpose that was equipped with electrospray ionization system (ESI). Distinctive product ions were produced with collision induced dissociation by energies ranging from 0 V to 140 V, in order to perform degradation analyses.

### 5.4.2 Ion chromatography

Ion chromatography is one of the most often used methods for anion and cation determination that provides high selectivity and overcomes the drawbacks of the classical methods [160, 161]. NO<sub>2</sub><sup>-</sup>, NO<sub>3</sub><sup>-</sup>, NH<sub>4</sub><sup>+</sup>, SO<sub>4</sub><sup>2-</sup> and SO<sub>3</sub><sup>2-</sup> ions were identified and quantified with a Metrohm 861 Advanced Compact IC system. Measurements targeting anions were carried out at 30 °C, using a Metrosep A Supp 4-250/4.0 column with Metrosep A Supp 4/5 Guard precolumn. The elution with 1.8 × 10<sup>-3</sup> mol dm<sup>-3</sup> Na<sub>2</sub>CO<sub>3</sub> and 1.7 × 10<sup>-3</sup> mol dm<sup>-3</sup> NaHCO<sub>3</sub> buffer solutions took place at a flow rate of 1 cm<sup>3</sup> min<sup>-1</sup>. The loop volume was 20 μL. In NH<sub>4</sub><sup>+</sup> measurements, Metrosep C3 column and HNO<sub>3</sub> buffer solution eluent were applied. Guard column, flow rate and loop volumes were the same as in case of anion detection, whilst the column temperature was higher (40 °C). Calibrations were implemented with dilution series of analytical standard solutions.

### 5.4.3 Cu(II)/phenanthroline test for H<sub>2</sub>O<sub>2</sub> determination

H<sub>2</sub>O<sub>2</sub> concentration was measured with the Merck H<sub>2</sub>O<sub>2</sub> test kit. This Cu(II)/phenanthroline test is based on a redox reaction between H<sub>2</sub>O<sub>2</sub> and Cu(II) ions in the presence of 2,9-dimethyl-1,10-phenanthroline (DMP), as shown in Reaction 32 [162].



The absorbance of the yellow or orange complex formed in this reaction was determined spectrophotometrically at 454.5 nm. In course of the measurements, 250 – 250 μL of both reagents (Cu<sup>2+</sup> and phenanthroline) were added to the samples (4 cm<sup>3</sup>) and the absorbance was measured following 20 minutes reaction time, using a JASCO 550 spectrophotometer (1 cm cell). The method is applicable in the 4 – 10 pH range; therefore, the pH was set by HCl or NaOH when it was necessary. The H<sub>2</sub>O<sub>2</sub> concentration [mol dm<sup>-3</sup>] was determined as shown in Equation 1:

$$c[\text{H}_2\text{O}_2] = \frac{A}{\varepsilon} \quad (1)$$

Where *A* is the absorbance and  $\varepsilon$  is the molar absorption coefficient that was determined from the slope of the H<sub>2</sub>O<sub>2</sub> calibration curve (16300 ± 200 mol<sup>-1</sup> dm<sup>3</sup> cm<sup>-1</sup>).

## 5.5 Sum parameters for water quality characterization

### 5.5.1 Total sulfur content

Inductively coupled plasma mass spectrometry (ICP-MS) enables analysis of elements in wide atomic mass range. The method provides low detection limit (pg – fg) and high precision analysis. For determination of the sulfur (TS) content, ELEMENT2 type (Thermo Electron Corporation) high-resolution inductively coupled plasma sector field mass spectrometer (HR ICP-SF-MS) was applied. The experiments were carried out at the Nuclear Security Department of the Centre for Energy Research, Hungarian Academy of Sciences. The samples were introduced through a conical nebulizer system with an uptake rate of 1 cm<sup>3</sup> min<sup>-1</sup>. The flow rates of nebulizer, auxiliary and cooling gases were 0.95, 1.13 and 15.4 dm<sup>3</sup> min<sup>-1</sup>, respectively.

### 5.5.2 Total nitrogen content

Total nitrogen (TN) analyses were performed on a Shimadzu TOC-L CSH/CSN analyzer equipped with a TNM-L unit. The method is based on catalytic thermal decomposition at high temperature and chemiluminescent detection. The nitrogen content was decomposed to NO at 720 °C that was subsequently excited with O<sub>3</sub>. The light emitted upon returning to ground state, measured by the gas detector, is proportional to the total nitrogen content. A minimum of three measurements were made for each sample. Purified water was used as blank, while potassium nitrate (KNO<sub>3</sub>) standard solutions were used for calibration.

### 5.5.3 Total organic carbon content

Total organic carbon (TOC) content provides information on carbon content; therefore, it is a good indicator of the state of mineralization. TOC analyses were performed with a Shimadzu TOC-L CSH/CSN analyzer. TOC can be determined by subtraction of separately measured total carbon (TC) and total inorganic carbon (TIC) content or directly by measuring non-purgeable organic carbon (NPOC). The samples were continuously aerated during the irradiation procedure, which likely removes the possible purgeable organic compounds. Therefore, the NPOC and TOC was equal in our case. Since the differential method is much slower than the direct method – and the results obtained by the two methods agreed in preliminary experiments – the measurements were carried out by the NPOC technique. In the first step of the measuring procedure, the sample is acidified with small amounts of HCl to obtain pH less than 3, whereby all carbonates and bicarbonates convert to CO<sub>2</sub>. The CO<sub>2</sub> content is then volatilized by purging with the carrier gas (synthetic air). In this way, the resulting solution contains only organic materials and it is introduced to a furnace heated to 680 °C. The combustion takes place in a tube filled with platinum oxidation catalyst. After the organic carbon content is entirely transformed to CO<sub>2</sub>, it is introduced to the non-dispersive infrared detector (NDIR). At least three measurements were made for each sulfonamide sample. Purified water was used as blank and the calibration was made by using potassium hydrogen phthalate (C<sub>8</sub>H<sub>5</sub>KO<sub>4</sub>) reference solution.

### 5.5.4 Chemical oxygen demand

Digestion of 30 cm<sup>3</sup> samples was carried out with a Behrotest TRS 200 COD system, by using solutions prepared according to ISO 6060:1989 [163]. The 2-hour digestion procedure took place in sulfuric acid solution at high temperature (~ 150 °C). Potassium

dichromate ( $K_2Cr_2O_7$ ) was used as oxidizing agent and the reaction was catalyzed with silver sulfate ( $Ag_2SO_4$ ). Following digestion and the subsequent sample cooling to room temperature, the remaining oxidant was determined by titration with ammonium iron-(II)-sulfate, in the presence of ferroin indicator. Chemical oxygen demand (COD) was measured in solutions originating from at least three separate irradiation procedures. Three parallels were used for all samples and purified water was used as blank. The measured values were checked with data obtained in case of potassium hydrogen phthalate reference solution. Calculation of COD was carried out according to Equation 2.

$$COD = \frac{8000 \times c \times (V_b - V_s)}{V_v} \quad (2)$$

Where,  $c$  is the concentration of the ammonium iron-(II)-sulfate solution [ $mol\ dm^{-3}$ ],  $V_b$  and  $V_s$  are the volumes of ammonium iron-(II)-sulfate consumed by the blank and the samples investigated [ $cm^3$ ], respectively,  $V_v$  is the sample volume [ $30\ cm^3$ ] and 8000 is the molar mass of 0.5 mol  $O_2$  molecule [ $mg\ dm^3$ ].

### 5.5.5 Biological oxygen demand

#### *Selection of microbial communities*

In the concept of saprobity, the community structure of the aquatic environment is determined by the characteristics of pollution. In polysaprobic and  $\alpha$ -mesosaprobic water, the amount of dissolved oxygen is very low, high molecular mass organics are common, there are no algae present and the abundance of the bacteria is very high [164]. As the status of pollution is shifted towards  $\beta$ -mesosaprobic and oligosaprobic range, the bacteria abundance decreases, while the amount of dissolved oxygen increases, the molecular mass of the organic impurities is lower and the algae species become dominant. Based on these, an aeration basin of a municipal wastewater treatment plant can be roughly interpreted as a polysaprobic –  $\alpha$ -mesosaprobic habitat and the effluent recipient can be roughly classified as a  $\beta$ -mesosaprobic – oligosaprobic environment. In this way, biodegradability of sulfonamides and products can be traced along a purifying water quality gradient, if the wastewater treatment process is monitored and the path of the effluent is followed up in the recipient water body, as well. Two stages were selected from this route to examine the biodegradability in distinguished water quality media. These are aeration basin of a

conventional municipal wastewater treatment plant and river water in the vicinity of the plant outlet (Fig. 3).

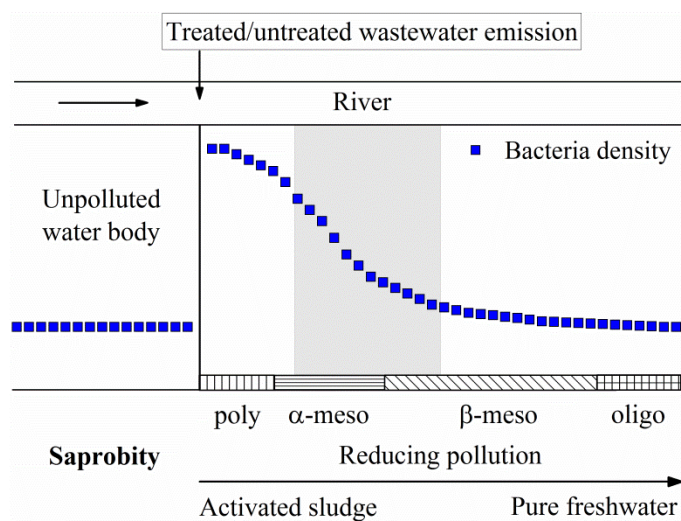


**Fig. 3.** Changes in bacteria density due to effluent discharge from wastewater treatment plant. Typical saprobity categories are indicated along purifying water quality gradient. The shaded zone refers to river water type used. The figure was composed based on [165].

#### Sample preparation

H<sub>2</sub>O<sub>2</sub> formed in course of ionizing radiation treatment showed strong inhibitory effects to inoculum communities (see later, section 6.7.1); therefore, H<sub>2</sub>O<sub>2</sub> was removed prior to BOD<sub>5</sub> experiments. Elimination of H<sub>2</sub>O<sub>2</sub> was performed by heterogeneous catalysis using 5 g dm<sup>-3</sup> MnO<sub>2</sub> (overnight stirred at 20 °C and pH = 10). Following the procedure, the catalyst was removed by 0.2 μm regenerated cellulose membrane filter. Although LC-MS/MS experiments showed that MnO<sub>2</sub> contributes to oxidation of some degradation products, H<sub>2</sub>O<sub>2</sub> removal by this method still represents a good compromise [166]. Preliminary experiments evidenced that this method is more efficient as compared to homogenous catalysis by Fe<sup>3+</sup> or enzymatic catalysis by catalase enzyme.

Experiments indicated significant pollutant concentration dependence of the BOD<sub>5</sub> results (see later, section 6.7.1), therefore microbial communities were exposed to equal pollutant concentration to obtain comparable results between samples irradiated by different doses. To achieve equal pollutant load exposure in case of all sulfonamide solutions, the samples were diluted with purified water to reach the lowest COD value (SAA, COD = 10 mg dm<sup>-3</sup>) measured at 2.5 kGy (that was the highest dose applied in these experiments). COD was selected as the measure of pollution on the grounds that COD and BOD<sub>5</sub> are strongly



related. Both express the amount of oxidizable organic matter, with the difference that BOD<sub>5</sub> shows the fraction of COD oxidizable solely by biological processes. However, BOD<sub>5</sub> was also evaluated by application of samples without H<sub>2</sub>O<sub>2</sub> removal or without pollutant load setting in case of SMX samples. These results were used to compare the different sample application approaches.

### *Measurement procedure*

BOD<sub>5</sub> experiments were performed by using OxiTop<sup>®</sup> Control BOD Respirometer System according to DIN EN 1899-1 [167]. Dilution water was prepared and conditioned as described in the OECD Test No. 301 [168]. 20 cm<sup>3</sup> supernatant of sedimented activated sludge was added to 1 dm<sup>3</sup> of this dilution water. Inoculated dilution water obtained in such way was used to seed the samples (pH set to 7 – 8 by NaOH or HCl) by a dilution factor of 2. Test mixtures contained allylthiourea nitrification inhibitor to ensure that oxygen consumption derives solely from the metabolism related to the carbon content. The resulting mixture was transferred to 500 cm<sup>3</sup> amber glass bottles with a 432 cm<sup>3</sup> overflow flask. Blank samples were prepared by addition of purified water to inoculated dilution water, instead of sulfonamide samples. The bottles were kept in dark during the incubation period, at 20 ± 1 °C. At least 3 parallels were used and the abiotic reactions were evaluated and separated from the biological processes by subtraction of results obtained with unseeded solutions. The results were corrected with those obtained with control solutions containing standards (D-glucose and L-glutamic acid) and nitrification inhibitor. Seeding with river water took place following the water filtration with 20 – 25 µm filter papers, without any other preparation steps. The mixtures seeded with river water were prepared and measured in the same way, as the ones seeded with activated sludge. Evaluation of O<sub>2</sub> consumed by the inoculum communities was determined from the pressure drop due to absorption of evolving CO<sub>2</sub>, as shown in Equation 3.

$$\text{BOD}_5 [\text{mg dm}^{-3}] = \frac{M(\text{O}_2)}{R \times T_m} \times \left( \frac{V_{\text{tot}} - V_i}{V_i} + \frac{T_m}{T_0} \right) \times \Delta p(\text{O}_2) \quad (3)$$

Where  $M(\text{O}_2)$  is the molecular mass of oxygen (32000 mg mol<sup>-1</sup>),  $R$  is the gas constant (83.144 dm<sup>3</sup> hPa mol<sup>-1</sup> K<sup>-1</sup>),  $T_0$  and  $T_m$  are the temperatures, 273.15 K and 293.15 K, respectively,  $V_{\text{tot}}$  is the bottle volume [cm<sup>3</sup>],  $V_i$  is the sample volume [cm<sup>3</sup>] and  $\Delta p(\text{O}_2)$  is the difference of the partial oxygen pressures [hPa].

## 5.6 Toxicity assessment

### 5.6.1 Selection of test organisms

Test organisms from three trophic levels were involved in the toxicity investigation. Green algae (*Pseudokirchneriella subcapitata*) and giant water flea (*Daphnia magna*) are commonly occurring freshwater species from two different trophic levels that adequately cover the entire spectrum that is eventually affected during the lifecycle of sulfonamides emitted to river water (Fig. 4). Both of them are widely used indicator species sensitive to the presence of toxic substances.

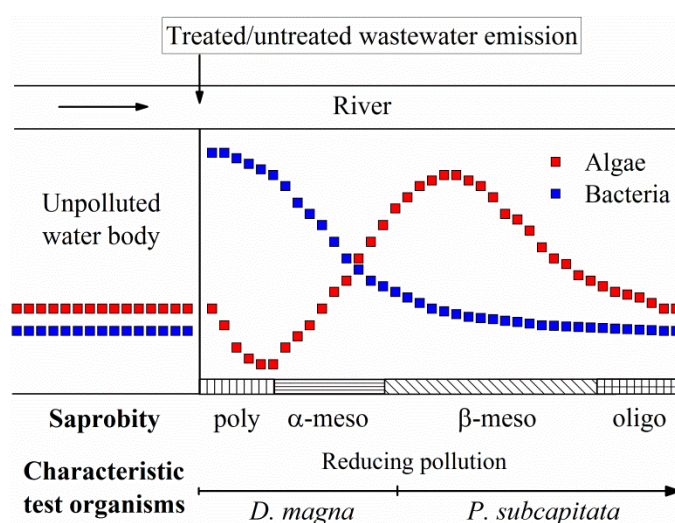


**Fig. 4.** Changes in bacteria and algae density caused by effluent discharge from wastewater treatment plant and the typical saprobity categories along purifying water quality gradient. Test organisms involved in toxicity assessment are indicated below the corresponding water quality type. The figure was composed based on [165, 169, 170].

Notwithstanding that *Vibrio fischeri* is not representative to the media of interest (wastewater or freshwater), it provides useful information on its trophic level. *V. fischeri* is a bioluminescent Gram-negative bacterium broadly used in ecotoxicity testing.

### 5.6.2 Sample preparation

H<sub>2</sub>O<sub>2</sub> was removed and the pollutant concentrations were set to equal values prior to toxicity experiments due to interferences mentioned in case of BOD experiments. The samples were prepared in the same way as for the BOD<sub>5</sub> measurements (section 5.5.5).

*V. fischeri* tests were also conducted by exposure of test organisms to pollutant concentration set to equal TOC, in addition to load setting to equal COD (as described previously). The

pollutant concentration adjustment based on TOC values took place by dilution with purified water to  $\text{TOC} = 10.4 \text{ mg dm}^{-3}$ . Such experiments were performed by using SMX solutions in order to compare the different sample application approaches. For the same reason, samples without  $\text{H}_2\text{O}_2$  removal or without pollutant load setting were also tested.

### 5.6.3 *Vibrio fischeri* acute toxicity

*V. fischeri* acute toxicity experiments performed according to DIN EN ISO 11348-2 employed liquid-dried luminescent bacterial strains [171]. The standard method is based on evaluation of light emission changes caused by the chemicals tested. Liquid-dried bacteria were reactivated by  $0.5 \text{ cm}^3$  ready-to-use glucose/sodium chloride reactivation solution at  $15 \pm 2 \text{ }^\circ\text{C}$ . Prior to exposure of test organisms to sulfonamide solutions, the pH of the samples was set to  $7 \pm 0.2$  by HCl or NaOH. The concentration of NaCl was set to 2% by addition of 0.3 g solid NaCl to  $15 \text{ cm}^3$  test solution. Luminescence intensity of the samples ( $0.5 \text{ cm}^3$ ) was determined by a LANGE LUMISTox 300 equipment, following 30 minutes of exposure to sulfonamide solutions at  $15 \pm 2 \text{ }^\circ\text{C}$ . Two parallels were used and the experiments were repeated three times. The inhibitory effects were calculated according to Equation 4.

$$\text{Luminescence inhibition [\%]} = \frac{I_0 - I_{30}}{I_0} \times 100 \quad (4)$$

Where  $I_0$  [relative unit] is the average luminescence intensity before addition of test solution, and  $I_{30}$  [relative unit] is the average luminescence intensity after 30 minutes contact time with test solution. The measurements satisfied the validity criteria of the protocol as the parallel determinations did not deviate from their mean by more than 3% for the control sample, and the potassium dichromate reference solution caused an inhibition in the acceptable range of 20 – 80%.

### 5.6.4 *Pseudokirchneriella subcapitata* chronic toxicity

*Pseudokirchneriella subcapitata* growth inhibition was determined according to OECD Test No. 201 [172] at the Agro-Environmental Research Institute, National Research and Innovation Centre. These measurements provide information on effects taking place over several generations, thus indicate chronic toxicity. The laboratory colony of *P. subcapitata* was cultured in Z8 growth medium, under continuous illumination at  $20 \pm 2 \text{ }^\circ\text{C}$ . The cell

growth was monitored by the changes in optical density (OD) measured at 750 nm. Test mixtures were prepared by addition of both Z8 growth medium and inoculum culture to sulfonamide solutions. The ratio of the samples and growth media in the test mixtures was 1 : 10. Nutrient providing growth media was prepared according to recommendations described in the Scandinavian Culture Collection for Algae & Protozoa [173]. The OD of the inoculum was set to 0.03 at the start of the measurement that corresponds to an initial biomass of  $10^4$  cells  $\text{cm}^{-3}$ , while the pH of the sulfonamide solutions was set to pH 7 – 8 by HCl or NaOH prior to analyses. 50  $\text{cm}^3$  of test mixtures were poured into 250  $\text{cm}^3$  conical flasks, which were subsequently capped with permeable gauze. The mixtures were constantly shaken by 100 rpm and illuminated with continuous, uniform “cool white” (8600 – 8800 lux) over the 72 h incubation period. Control samples did not contain sulfonamide solutions. Three replicates were used for each sample and the experiments were repeated three times. Following 72 hours, the OD was measured by a JASCO 550 UV/Vis spectrophotometer using 1 cm cell. Occasionally, dilution of samples with purified water was performed in order to avoid OD values higher than 1. The percentage inhibition of the cell growth was calculated according to Equation 5.

$$\text{Cell growth inhibition [\%]} = \frac{G_c - G_s}{G_c} \times 100 \quad (5)$$

Where  $G_c$  and  $G_s$  [%] are the average growths for control and test solutions, respectively. Validity criteria were satisfied as the biomass of the controls increased by a factor of at least 16, and the coefficient of variation of the replicates was below 7%. *P. subcapitata* sensitivity was tested using potassium dichromate.

#### 5.6.5 *Daphnia magna* acute toxicity

To assess the effects of sulfonamides and radiolytic products towards *Daphnia magna*, acute mortality tests were executed on the basis of OECD Test No. 202 [174] at the Agro-Environmental Research Institute, National Research and Innovation Centre. The laboratory colony of *D. magna* was cultured in reconstituted water and fed with *P. subcapitata* algal suspension, while maintained under 16/8 hours light/dark periods at  $20 \pm 2^\circ\text{C}$  temperature. Reconstituted water was prepared by addition of 25 – 25  $\text{cm}^3$  volumes of calcium chloride ( $11.76 \text{ g dm}^{-3}$ ), magnesium sulfate ( $4.93 \text{ g dm}^{-3}$ ), sodium bicarbonate ( $2.46 \text{ g dm}^{-3}$ ) and potassium chloride ( $0.23 \text{ g dm}^{-3}$ ) solutions to 1  $\text{dm}^3$  distilled water [174]. Test organisms were originating from the same stock, and they were aged less than 24 hours. *D magna* was

exposed to sulfonamide solutions (pH set to 7 – 8 by HCl or NaOH) for 48 hours. To ensure the appropriate conditions, test solutions were thoroughly aerated and nutrients were added in the form of stock solutions used for preparation of reconstituted water. The test organisms were not fed during the test. 20 test organisms were used for each experiment, by dividing them into four 15 cm<sup>3</sup> beakers (5 – 5 test organisms) with a solution volume of 10 cm<sup>3</sup> each. Temperature was kept between 18 – 22 °C and the light/dark periods were 16/8 hours. Mortality was recorded at 24 and 48 hours. The measurements were repeated three times. Correction was applied taking into account the mortality not associated with the chemicals tested according to Equation 6.

$$\text{corrected mortality [\%]} = \left(1 - \frac{n_s}{n_c}\right) \times 100 \quad (6)$$

Where  $n_s$  and  $n_c$  are the *D. magna* populations in the sample and in the control, respectively. The criteria of the test were verified. The acceptable 10% mortality in the control groups was not exceeded and the pH of the solutions remained between 6 and 9 during the analysis. The sensitivity of *D. magna* – determined by measuring the half maximal effective concentration (EC<sub>50</sub>) of potassium dichromate following 24 hours – was within the acceptable range of 0.6 – 2.1 mg dm<sup>-3</sup>.

#### 5.6.6 Activated sludge respiration inhibition

Toxicity tests typically measure the impact of chemical substances on individual members of the ecosystem. However, examination of individual species carries uncertainty, as the selected test organisms do not necessarily represent the entire community properly. Contrary to the previously described ecotoxicity experiments, for activated sludge respiration inhibition test a complex mixture of bacteria species is used. Effects of chemicals on this large number of different organisms present in activated sludge can be characterized by a single parameter, by the amount of oxygen consumed during their metabolism. Reducing oxygen uptake rate (OUR) in the presence of test substances refers to inhibited metabolic activity. Nevertheless, increased oxygen consumption indicates not only the harmfulness of chemicals tested, but also evidences rapid biodegradability.

In the respiration inhibition experiments, municipal activated sludge was used according to the ISO 8192:1986 standard method [175]. Test mixtures consisted of 3.3 – 9.3 cm<sup>3</sup> activated sludge (total suspended solids: 15 – 30 mg cm<sup>-3</sup>), 1.6 – 2.7 cm<sup>3</sup> sodium acetate

substrate (that corresponds to COD of 90 – 180 mg in 300 cm<sup>3</sup> Karlsruher flasks), 150 cm<sup>3</sup> sulfonamide solutions ( $1 \times 10^{-4}$  mol dm<sup>-3</sup>, pH = 7 – 8) and purified water in amounts to fill up to 300 cm<sup>3</sup>. The blank sample was prepared by using activated sludge, substrate and purified water. The control samples contained sulfonamide solutions, substrate and purified water. Test mixtures were stirred at  $20 \pm 2$  °C during the measurements. The changes in dissolved oxygen concentration were recorded in every 30 minutes – over 180 minutes – by a WTW inoLab® Multi 9310 IDS device, equipped with FDO 925 dissolved oxygen probe. The abiotic reactions were evaluated and subtracted from the results, just like the endogenous oxygen uptake rate. At least three parallel measurements were made. The respiration inhibition was calculated as shown in Equation 7.

$$\text{Respiration inhibition [\%]} = \frac{OUR_b - (OUR_t - OUR_c)}{OUR_b} \times 100 \quad (7)$$

Where,  $OUR_b$ ,  $OUR_t$  and  $OUR_c$  are the oxygen uptake rates [mg dm<sup>-3</sup> h<sup>-1</sup>] of the blank, test mixtures and the control, respectively. The OURs were obtained by applying Equation 8.

$$OUR \text{ [mg dm}^{-3} \text{ h}^{-1}] = \frac{c_1 - c_2}{\Delta t} \times 60 \quad (8)$$

Where  $c_1$  and  $c_2$  are the first and the last dissolved oxygen concentration values [mg dm<sup>-3</sup>] on the linear part of the time-concentration dependence curves.  $\Delta t$  is the time elapsed [min] between detecting  $c_1$  and  $c_2$ . The susceptibility of different activated sludge batches was checked by determining the EC<sub>50</sub> of 3,5-dichlorophenol (Cl<sub>2</sub>C<sub>6</sub>H<sub>3</sub>OH). These values were in the 3 – 7 mg dm<sup>-3</sup> range that satisfies the validity criteria (3 – 30 mg dm<sup>-3</sup>).

Formation of oxygen bubbles in solutions containing H<sub>2</sub>O<sub>2</sub> in  $\sim 10^{-4}$  mol dm<sup>-3</sup> concentration called attention to clarification of H<sub>2</sub>O<sub>2</sub> interference in respiration inhibition experiments. Toxic effects and the interference of oxygen were not separated, they were quantified together by using H<sub>2</sub>O<sub>2</sub> dilution series (up to  $10 \times 10^{-4}$  mol dm<sup>-3</sup>). However, O<sub>2</sub> formation due to H<sub>2</sub>O<sub>2</sub> decomposition was also investigated by application of  $5 \times 10^{-4}$  mol dm<sup>-3</sup> aqueous solution of H<sub>2</sub>O<sub>2</sub> and 5 cm<sup>3</sup> catalase enzyme solution in airtight sealed Karlsruher flasks. In these solutions, catalase decomposes H<sub>2</sub>O<sub>2</sub> and generates oxygen. The dissolved oxygen concentration was measured with a WTW inoLab® Multi 9310 IDS device, equipped with FDO 925 dissolved oxygen probe.

### 5.6.7 BOD<sub>5</sub> as toxicity indicator

As respiration inhibition analyses were performed in relatively short time (180 min) and with large amounts of activated sludge, the inhibitory effects on activated sludge were also evaluated by using BOD<sub>5</sub> data as a toxicity indicator. This approach provides data on long-term inhibitory effects (5 days). The BOD<sub>5</sub> value measured in case of the blank sample is regarded as a value where the organisms are not affected. Consequently, values higher than the blank imply that the contribution to metabolic activity is considerably higher than any eventual inhibitory effect, while lower values refer to notable inhibition. In this way, the dilution series of the sulfonamide solutions may provide information on toxic effects at the concentration range investigated. The measurements were performed as described previously (section 5.5.5), with the difference, that the test mixtures contained 50% inoculated dilution water or river water and 50% of H<sub>2</sub>O<sub>2</sub> solutions (+ nitrification inhibitor). The *I* inhibition was calculated according to Equation 9.

$$I [\%] = \frac{(BOD_{5b} - BOD_{5s})}{BOD_{5s}} \times 100 \quad (9)$$

Where  $BOD_{5b}$  and  $BOD_{5s}$  are the blank and the samples containing H<sub>2</sub>O<sub>2</sub>, respectively [mg dm<sup>-3</sup>]. These results show the effects of H<sub>2</sub>O<sub>2</sub> on the inoculum communities in the absence of a growth substrate. However, the measurements were also performed by addition of glucose and glutamic acid as growth substrates, in  $BOD_5 = 210 \pm 20$  mg dm<sup>-3</sup> amounts.

## 5.7 Antibacterial susceptibility testing

### 5.7.1 Selection of test organisms and sample preparation

Testing antibacterial activity following the ionizing radiation treatment is important since this attribute is responsible for one of the major environmental risks. The changes in biological activity were followed up by agar diffusion and broth microdilution assays, by using both Gram-positive (*Staphylococcus aureus*) and Gram-negative (*Escherichia coli* and *Pseudomonas aeruginosa*) bacterial strains. These pathogens have the ability to rapidly develop resistance to multiple classes of antibiotics that makes them excellent test subjects for susceptibility investigations [176, 177, 178, 179]. Nevertheless, sulfonamides are regularly applied for treatment of diseases caused by previously mentioned bacteria [1].

Antibacterial susceptibility was tested at the Department of Microbiology and Biotechnology, Szent István University of Budapest.

SMX is the most frequent sulfonamide antibiotic used in practice, therefore, bacterial growth inhibition assay was performed on the example of this substance. The investigation was carried out by involving trimethoprim (TMP), since the pharmaceuticals are usually prepared by combining SMX and TMP (in 5 : 1 molar ratio), as detailed in section 2.1. Therefore, experiments were carried out by mixing  $5 \times 10^{-4} \text{ mol dm}^{-3}$  SMX and  $1 \times 10^{-4} \text{ mol dm}^{-3}$  TMP solutions (SMX+TMP). Combined effects were also studied on a commercially available medicine (Sumetrolim, SUM) that contains SMX and TMP in previously mentioned ratio. The concentrations of the active ingredients in SUM measurements were also set to  $1 \times 10^{-4} \text{ mol dm}^{-3}$  TMP and  $5 \times 10^{-4} \text{ mol dm}^{-3}$  SMX. These samples may contain some stearin, glycerol, sodium carboxymethyl amylopectin, manganese stearate, gelatin, talc or potato starch residues in addition to SMX and TMP, despite the removal of insoluble fraction by  $0.2 \mu\text{m}$  regenerated cellulose membrane filter. In addition to the combined effects, impacts of SMX ( $5 \times 10^{-4} \text{ mol dm}^{-3}$ ) and TMP ( $1 \times 10^{-4} \text{ mol dm}^{-3}$ ) solutions were determined separately, as well.

### 5.7.2 Agar diffusion test

Agar diffusion test is a routinely applied method for evaluation of antibacterial susceptibility. The method is based on diffusion of antibacterial agents into the inoculated agar medium that inhibits germination and growth of microbial strains; and thus, a visible inhibition zone appears. Tryptocasein soy broth (TSB) agar plates containing suspended bacterial cells were used in these experiments. The concentration of the bacterial suspension prepared from an overnight culture was set to  $10^6 \text{ cells mL}^{-1}$  with a Grant bio DEN-1 suspension turbidity detector and 1 mL of this suspension was measured into each Petri dish. Thereafter, 20 mL molten agar was poured on the plates and the bacteria was distributed evenly. Following solidification, 100 – 100  $\mu\text{L}$  of antibiotic solution was added to wells punched aseptically with a sterile cork borer (diameter = 8 mm). The diameters of the inhibition zones were measured after 24 hours of incubation at  $37 \text{ }^\circ\text{C}$  in case of *S. aureus* and *E. coli*, while the temperature was set to  $30 \text{ }^\circ\text{C}$  in case of *P. aeruginosa* measurements. 4 parallels were measured for each sample in separate plates. Although the inhibition zones were not delimited by ideal circles in some cases, the measurement error did not exceed 1 mm. The results are presented by subtracted well diameters. Changes in



the antibacterial activity were determined based on tendencies of the average inhibition zone diameter changes.

### 5.7.3 Broth microdilution assay

Broth microdilution assay is a type of susceptibility test based on monitoring the bacterial growth during a certain incubation time in liquid medium. The bacterial growth was followed photometrically. In these experiments carried out on a Multiskan Ascent device (Thermo Electron Corporation), 135  $\mu$ L antibiotic solution, 135  $\mu$ L TSB and 30  $\mu$ L of cell suspension was pipetted into microplates (96 wells). To achieve the same TSB : cell suspension ratio – as the one used in agar diffusion test – concentrated TSB and microbe suspensions were prepared (2 $\times$  and 10 $\times$ , respectively, as compared to the ones used in the agar diffusion tests). Positive controls were prepared by addition of sterile water instead of antibiotic solution. Sterile water was used in place of bacterial suspension in negative controls to confirm the absence of contaminants in plates used. The measuring device was set to continuous kinetic reading mode at 37 °C in case of *S. aureus* and *E. coli* or at 30 °C in case of *P. aeruginosa*. The optical density was measured over 24 hours at 595 nm. Test mixtures were shaken in every 30 minutes (over 20 seconds) with 600 revolutions per minute. In this way, the sample mixtures were kept in solution over the whole experiment. The average of the OD was calculated from 3 parallel measurements, following the removal of significant outliers.

## 5.8 Statistical methods

Statistical analyses were performed on data from at least 3 independently repeated experiments (3 – 5 replicates for each) to obtain representative results. Iglewicz and Hoaglin's robust test for multiple outliers (two sided test) [180] was performed to determine significant outliers from the data sets at  $Z \geq 2$  criterion. In the study, mean values are presented and the data spread is expressed in form of standard deviation. To assess whether the mean values of two investigated groups are statistically different from each other, statistical significance tests (*t*-tests) were carried out by using GraphPad scientific statistics software.

## 6 Results and Discussion

### 6.1 Separation and evaluation of radical reactions involved in degradation

Ionizing radiation can induce oxidizing and reducing reactions. To evaluate degradation efficiencies related to different reactive species, experiments were performed under conditions allowing separate study of the radicals. The investigations were conducted on SMX solutions (pH = 5.8, called here natural pH) irradiated up to 5 kGy absorbed doses. One of the methods used to follow up the decomposition of initial molecules was UV-Vis spectrophotometry.

In air-saturated solutions, the dissolved  $O_2$  reacts with both  $e_{aq}^-$  and  $H^\bullet$  that entails formation of  $O_2^{\bullet-}$  and  $HO_2^\bullet$  as shown in Reactions 25 and 26. Consequently, degradation of pollutants in such solutions is due to  $^\bullet OH$  and  $O_2^{\bullet-}/HO_2^\bullet$  reactions. Under these conditions, the intensity of the 266.5 nm absorption band – belonging to the aromatic  $\pi - \pi^*$  transition – decreased as a function of the absorbed dose (Fig. 5/A). Spectral changes evidenced practically complete destruction of aromatic structure at 5 kGy absorbed dose.

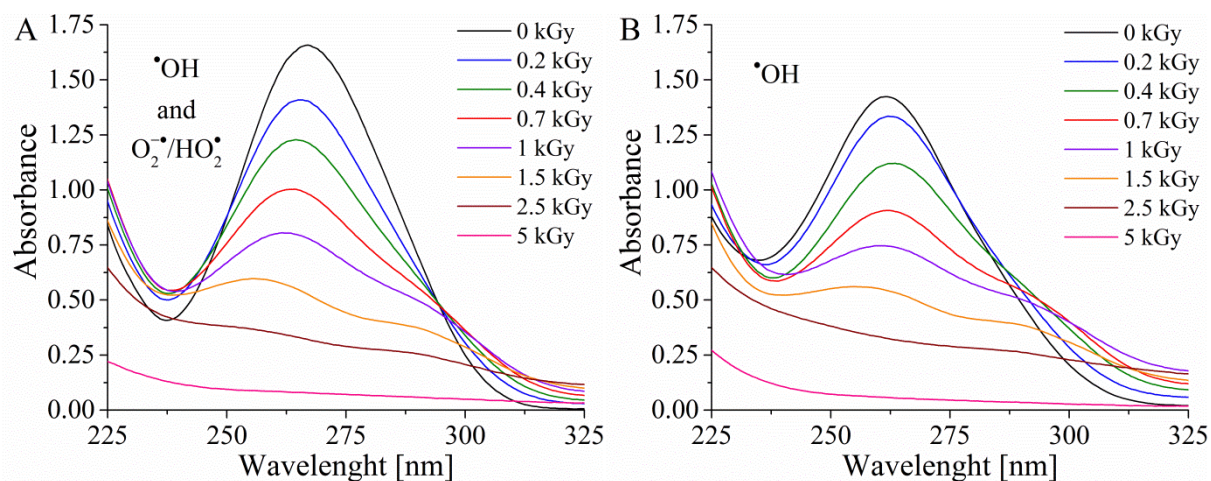


**Fig. 5.** Absorption spectra of air- (A) and  $N_2O$ - (B) saturated SMX solutions irradiated with doses indicated in the legend. The initial concentration and pH was  $1 \times 10^{-4} \text{ mol dm}^{-3}$  and 5.8 (natural pH), respectively.

Saturation of SMX solutions with  $N_2O$  induces conversion of  $e_{aq}^-$  to  $^\bullet OH$  and thus doubles the yield of  $^\bullet OH$  (as shown in Reaction 30). Spectra obtained in course of  $^\bullet OH$  reactions with SMX (Fig. 5/B) were very similar to those observed in joint reactions of  $^\bullet OH$  and  $O_2^{\bullet-}/HO_2^\bullet$  (Fig. 5/A).

Substantial spectral differences, compared to the previous ones, were seen in  $N_2$ -saturated solutions. Simultaneous reactions of  $\bullet\text{OH}$  and  $e_{\text{aq}}^-$  with target molecules led to a less intense decrease of the aromatic absorption band (Fig. 6/A). This refers to lower degradation efficiency of the  $e_{\text{aq}}^-$ .

Degradation related solely to  $e_{\text{aq}}^-$  was examined in  $N_2$ -saturated solutions containing *t*-BuOH (Reaction 31). The outcome of these experiments showed continuously decreasing absorbance, but the aromatic absorption band was seen even at 2.5 kGy and 5 kGy absorbed doses (Fig. 6/B). These results confirm that oxidizing species (mainly  $\bullet\text{OH}$ ) are primarily responsible for degradation of SMX. The same conclusion was drawn by Liu and Wang in case of radiolytic decomposition of SMZ [146].

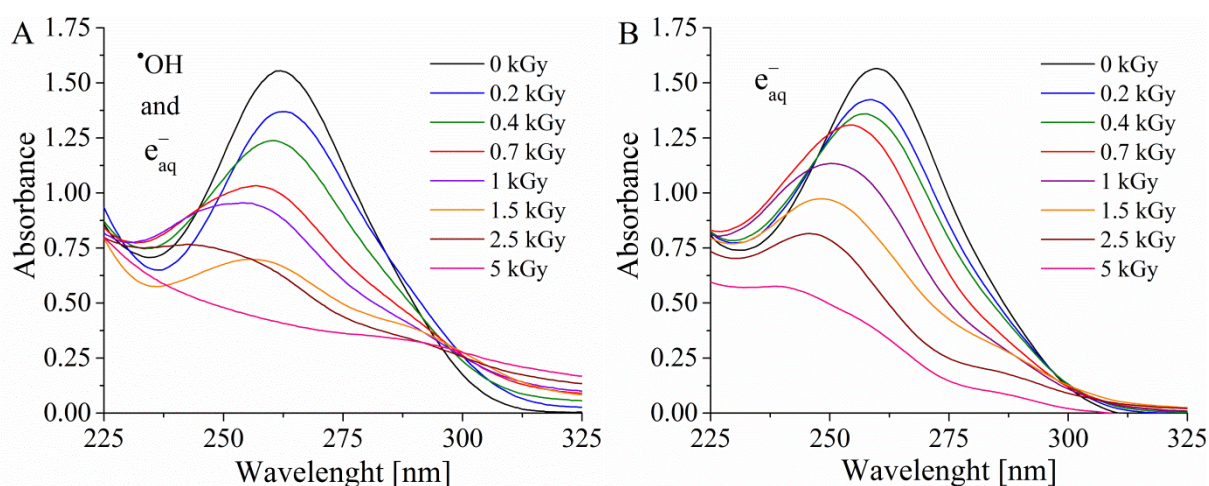


**Fig. 6.** Absorption spectra of  $N_2$ -saturated SMX solutions irradiated with absorbed doses indicated in the legend (A). The initial concentration and pH was  $1 \times 10^{-4} \text{ mol dm}^{-3}$  and 5.8, respectively. Part B of the figure shows the experiments performed under the same conditions but in the presence of 5% *t*-BuOH.

Changing the pH from 5.8 to 4.0 or 8.0 did not lead to notable changes in the absorbance decrease. Only a slight shift of the 266.5 nm absorption band was seen. This phenomenon is related to the protonation of SMX products, and it occurred under all experimental conditions. Sulfonamides generally have two acid-base dissociation equilibria. The  $\text{NH}_2$  group protonates/deprotonates at  $\text{pH} \sim 2$  ( $\text{p}K_{\text{a1}}$ ), while around  $\text{pH} 5 - 7$ , a second protolytic dissociation ( $\text{p}K_{\text{a2}}$ ) takes place at the  $\text{SO}_2 - \text{NH} - \text{R}$  group (Fig. 7) [181, 182, 183].

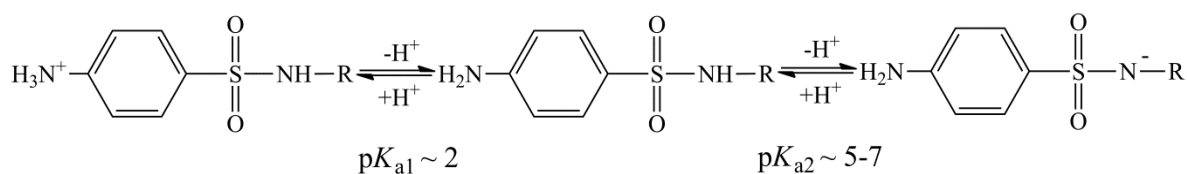


**Fig. 7.** General acid-base dissociation equilibria of sulfonamides.

Irradiation of sulfonamides for the further experiments was performed by constant aeration to avoid the O<sub>2</sub> depletion and without setting the pH. Such experimental conditions stand close to the practical implementation.

## 6.2 Intermediate product analysis

The initial steps of the degradation – related to the main reactant (<sup>•</sup>OH) – were investigated by transient intermediate kinetics, using pulse radiolysis technique on the example of SAA, SCT, SDZ, SSZ and SGD.

Absorption spectra of transient intermediates detected at 10 μs following the pulse in N<sub>2</sub>O-saturated SAA, SCT and SDZ solutions are shown in Fig. 8. The SAA spectrum peaked at 365 nm, while the maxima of SCT and SDZ spectra were slightly shifted to longer wavelengths (~ 410 nm). This value was 400 nm in experiments involving SSZ and SGD. The measured values are consistent with the ones published for SMZ (400 nm) and SMX (415 nm) [184]. In the experiment where <sup>•</sup>OH was scavenged by *t*-BuOH, this absorbance disappeared from the spectra, as shown on the example of SAA in Fig 8. The similarities in the absorption spectra and their intensities suggest that the preferred target of the <sup>•</sup>OH for all molecules is the benzene ring. The result of <sup>•</sup>OH addition to the aromatic ring is formation of hydroxy-cyclohexadienyl radicals. When the irradiation is carried out under aerated conditions, hydroxy-cyclohexadienyl radicals transform to peroxy radicals in reactions with dissolved O<sub>2</sub>. Peroxy radicals may transform to hydroxylated molecules by HO<sub>2</sub><sup>•</sup> elimination or they undergo ring opening to aliphatic compounds [185, 186]. The first products are expected to be mainly hydroxylated aromatic molecules.

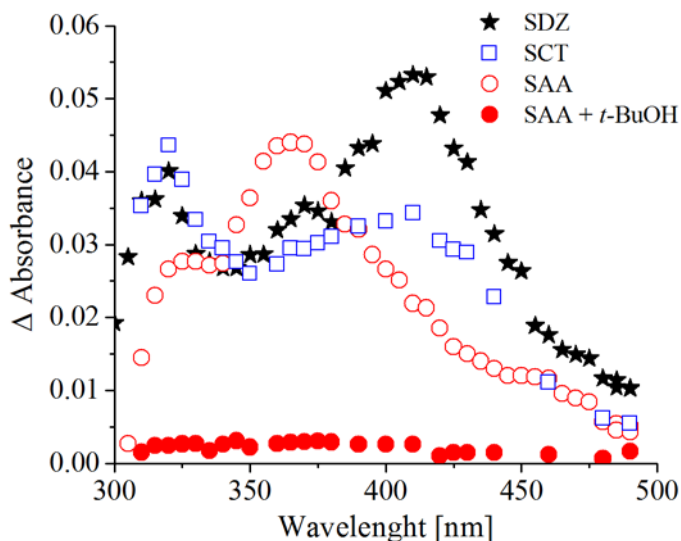


**Fig. 8.** Pulse radiolysis absorption spectra taken at  $10 \mu\text{s}$  following the pulse in  $\text{N}_2\text{O}$ -saturated  $1 \times 10^{-4} \text{ mol dm}^{-3}$  solutions of SDZ, SCT and SAA (without and with  $t\text{-BuOH}$ ).

The reaction rate constants of  $\bullet\text{OH}$  reactions with sulfonamides ( $k_{\text{OH}}$ ) were determined by the time dependence of the absorbance build-up, measuring the pseudo-first-order rate constants. The pseudo-first-order rate constants were determined in the  $2 \times 10^{-5} - 1 \times 10^{-4} \text{ mol dm}^{-3}$  concentration range. The slope of the pseudo-first-order rate constants plotted as a function of sulfonamide concentration provides the second-order rate constant.

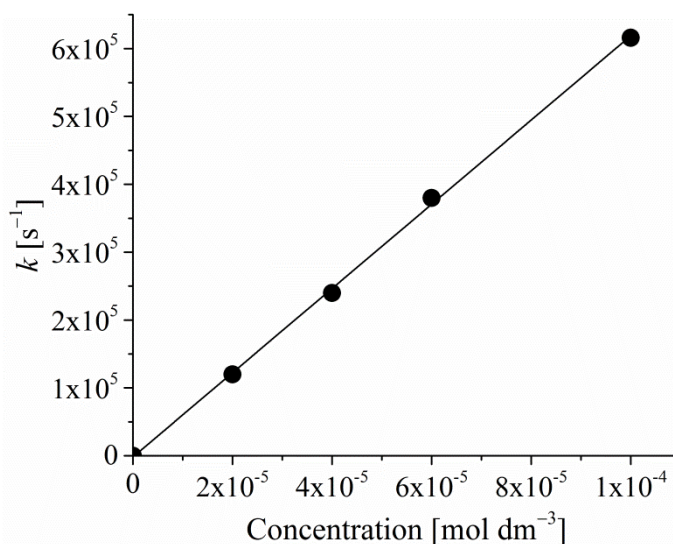


**Fig. 9.** Concentration dependence of the pseudo-first-order rate constant in SCT solutions, monitored by the absorbance build-up at 420 nm.

The second-order rate constant was  $5.3 \times 10^9 \text{ mol}^{-1} \text{ dm}^3 \text{ s}^{-1}$  in SCT experiments (Fig. 9), while  $4.5 \times 10^9$ ,  $9.5 \times 10^9$  and  $5.7 \times 10^9 \text{ mol}^{-1} \text{ dm}^3 \text{ s}^{-1}$  was obtained in SAA, SGD and SDZ

solutions, respectively. These values are similar to the  $6.6 - 8.5 \times 10^9 \text{ mol}^{-1} \text{ dm}^3 \text{ s}^{-1}$  range found in the literature [181, 182, 187].

The  $k_{\text{OH}}$  observed in sulfonamide solutions are close to the theoretical maximum, the diffusion controlled rate constant ( $1.1 \times 10^{10} \text{ mol}^{-1} \text{ dm}^3 \text{ s}^{-1}$ ). Such high  $k_{\text{OH}}$  values are typical for benzene derivatives [187, 188]. The rate constants with the free pyrimidine ( $1.6 \times 10^8 \text{ mol}^{-1} \text{ dm}^3 \text{ s}^{-1}$ ) and the isoxazole rings ( $3.5 \times 10^9 \text{ mol}^{-1} \text{ dm}^3 \text{ s}^{-1}$ ) are lower [189, 190]. The reaction rate constants determined – and the ones found in the literature – support the mechanism suggested by the absorption spectra, in which the  $\bullet\text{OH}$  attack mainly occurs on the benzene ring.

However, the transient absorption spectrum seen in SGD solution was different from all the others (not shown). In addition to the peak at 400 nm, two more absorption bands appeared in the 300 – 400 nm wavelength range. Moreover, the highest  $k_{\text{OH}}$  was also measured in SGD samples ( $9.5 \times 10^9 \text{ mol}^{-1} \text{ dm}^3 \text{ s}^{-1}$ ). This may indicate that the  $\bullet\text{OH}$  reaction with the guanidine part also considerably contributes to the degradation, beside the reaction with the benzene ring.

### 6.3 Separation and identification of stable organic products

Stable organic products formed in course of irradiation were identified by LC-MS/MS. As the highest product concentrations were found in the 0.2 – 0.8 kGy range, these samples were mainly used for the investigations. Although measurements were performed by both positive and negative ionization in the MS, more informative results were obtained by application of the positive mode. For this reason, results obtained by using positive ionization mode are presented below.

At the early stages of the decomposition, all products detected in high concentrations were hydroxylated derivatives, as foreshadowed by the results of pulse radiolysis experiments (section 6.2). In addition to formation of monohydroxylated products, double hydroxylation also took place in most cases, albeit with low yields. Products other than hydroxylated ones appeared in remarkably lower relative abundance, in approximately 5 – 10 times lower amounts. Concentration of hydroxylated products peaked at around 0.6 kGy, but these products quickly disappeared by increasing the absorbed dose to 1 kGy.

The presence of the aromatic ring of sulfonamide molecules in positive ionization mode is indicated by the simultaneous appearance of 156 and 108  $m/z$  fragments [191]. If both of these ions are present among the monohydroxylated molecules, the hydroxylation takes place on the R side chain (Table 3), and not on the ring. Similar is the case with the doubly hydroxylated products. In mono and double hydroxylated precursor and fragment ions, the  $m/z$  values are higher by 16 and 32 mass numbers, respectively, as compared to the not hydroxylated analogues. This is demonstrated on the example of STZ degradation in Fig. 10. The 256  $m/z$  value of the  $[\text{STZ}+\text{H}]^+$  precursor ion changes to 272 and 288 in course of mono and double hydroxylation, respectively. These changes were also observed in the two main fragments ( $156 \rightarrow 172 \rightarrow 188$ , and  $108 \rightarrow 124 \rightarrow 140$ ). These shifts indicate that hydroxylation occurs on the benzene ring.

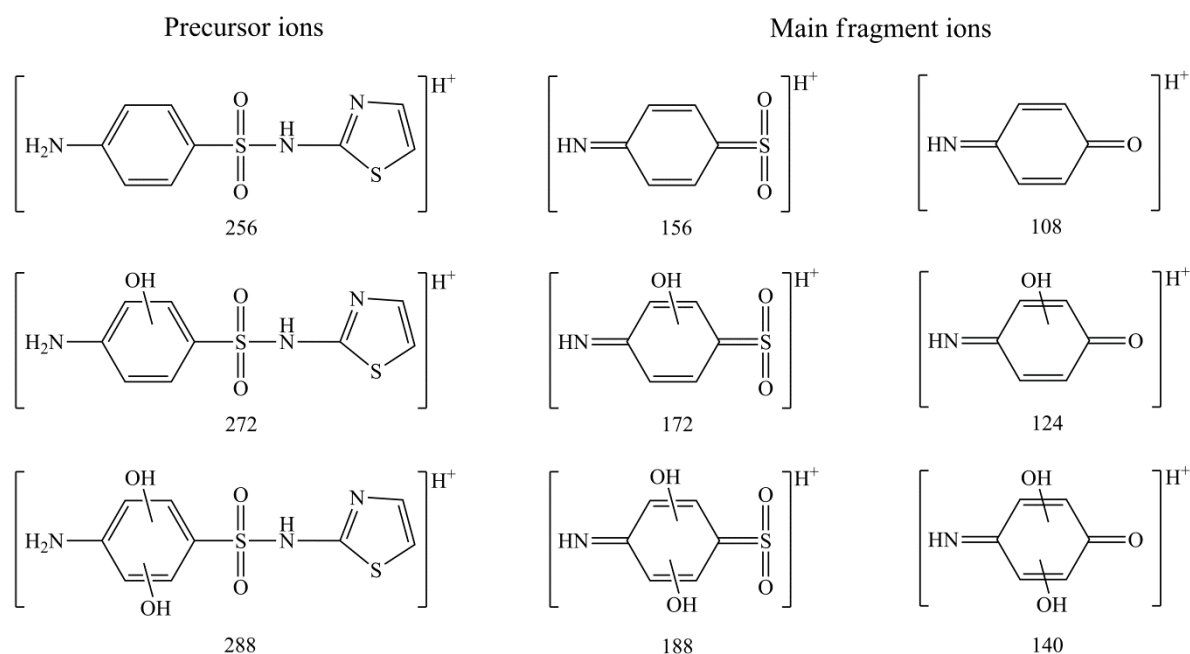


**Fig. 10.** Precursor and main fragment ions in hydroxylation of STZ.

The molecular ion of SSZ ( $m/z = 268$ ) shifts to 284 and then to 300. The 156  $m/z$  fragment ion transforms to an ion with  $m/z$  of 172, in both single and double hydroxylated molecules. It can be assumed that in the latter case, one of the OH-groups is attached to the benzene, the other to the oxazole ring. Nevertheless, only single hydroxylation was detected in case of SAA. The hydroxylated products probably decay very quickly in reactions other than second hydroxylation. In double hydroxylation of SMX, both hydroxyl groups were added to the benzene ring, similarly to STZ. This was shown by an ion with 99  $m/z$ , identified as  $[\text{NH}_2\text{-methoxazole} + \text{H}]^+$  that appeared in fragmentation of  $[\text{SMX} + \text{H}]^+$ ,  $[\text{SMX}(\text{OH}) + \text{H}]^+$

and  $[\text{SMX}(\text{OH})_2 + \text{H}]^+$ , as well. The precursor ions of both SGD and SCT have  $m/z$  of 215. Due to their mono and double hydroxylation, the  $m/z$  increased to 231, and then to 247  $m/z$ . The same trends were observed in cases of their 156 and 108  $m/z$  ions, as well. However, the second most intense SGD fragment was not the 108  $m/z$ , but the one with 60  $m/z$ , due to the guanidine fragment  $[(\text{NH}_2\text{C}(\text{NH}_2)\text{NH}) + \text{H}]^+$ .

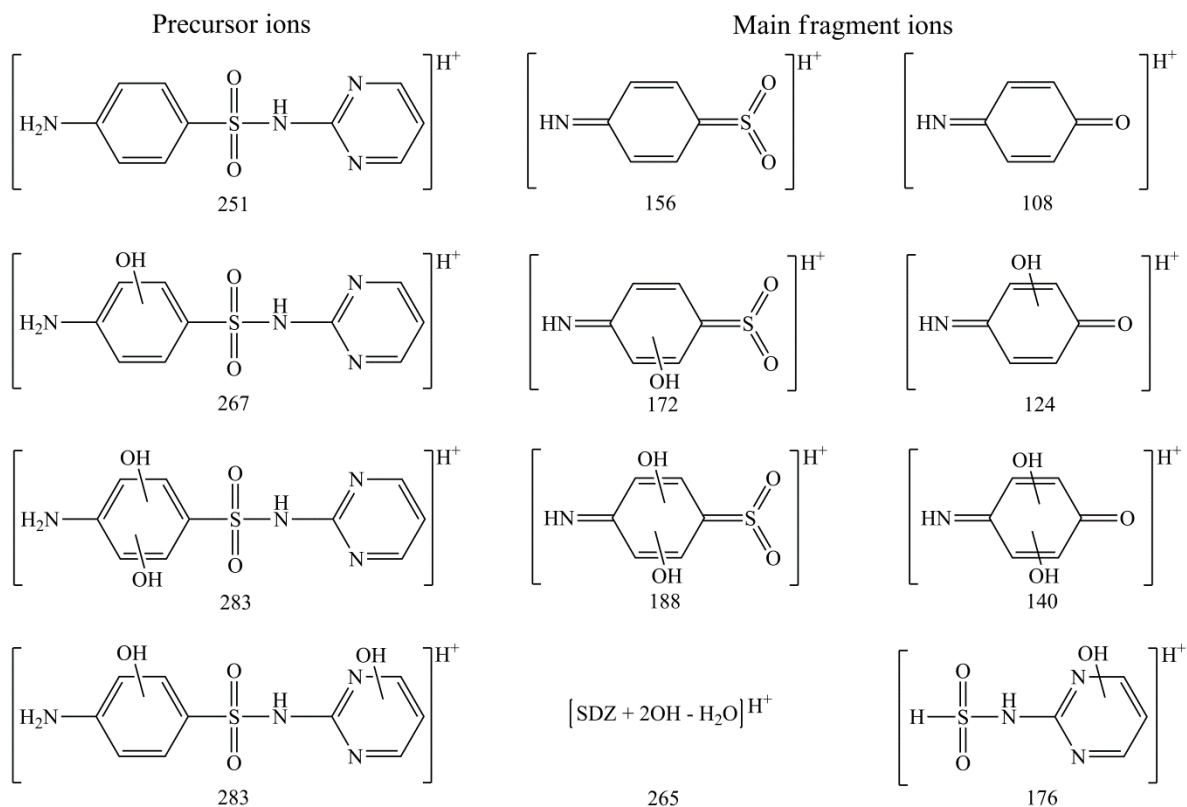


**Fig. 11.** Precursor and main fragment ions in hydroxylation of SDZ.

In SDZ solutions, the single and one of the double hydroxylation were found on the benzene ring. However, reactions on the benzene and on the pyrimidine rings were also observed (Fig. 11). This is supported by the appearance of fragment ion 176  $m/z$ . The main fragment ion had an  $m/z$  of 265  $[\text{SDZ}(\text{OH})_2\text{-H}_2\text{O} + \text{H}]^+$ . Appearance of product with  $m/z = 187$  refers to desulfonation. Formation of mono and double hydroxylated molecules was also reported in photo-Fenton, photocatalytic, ozonation and radiolytic degradation of SMX [74, 81, 100, 151].

The degradation pattern of the precursor ion and the reactions of the SMZ molecule with hydroxyl radical both represent a complicated case in SMZ samples. The precursor ion with 279  $m/z$  results in main ions with 186 and 124  $m/z$  in the collision chamber. These fragments contain the heterocyclic ring (Fig. 12). When the benzene ring is hydroxylated,



the  $[\text{SMZ}(\text{OH}) + \text{H}]^+$  ion gives ions with 186 and 124  $m/z$  as main fragments. When the heterocyclic ring is hydroxylated, the 124  $m/z$  increases to 140  $m/z$ . However, instead of the 186 + 16 ion, an ion with  $m/z$  of 229 was observed as the main fragment ion. Formation of this ion involves degradation of the heterocyclic ring in the MS. Rong et al. observed the same ion in the degradation of SDZ [192]. In the double hydroxylation, both rings are substituted with one OH-group.

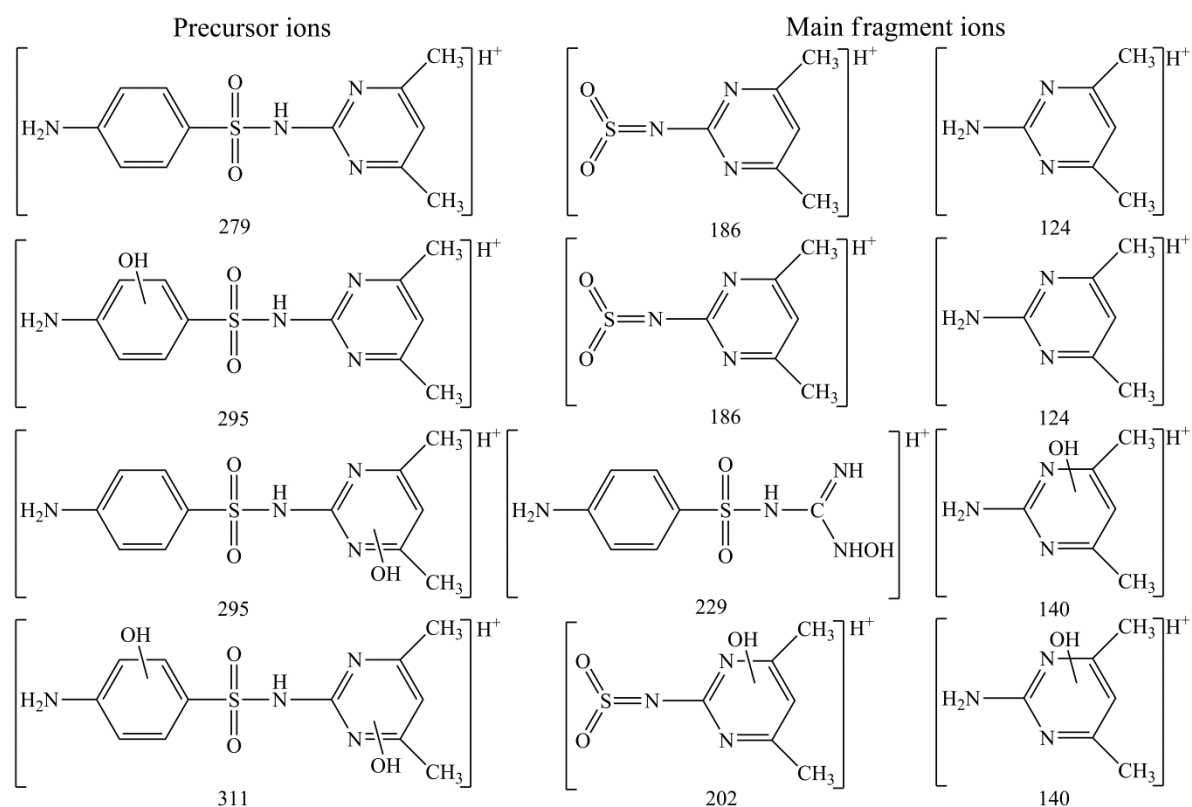


**Fig. 12.** Precursor and main fragment ions in hydroxylation of SMZ.

Results of multiple reaction monitoring performed on initial sulfonamide antibiotics and their degradation products are summarized in Table 4.

Compound	Fragmentor voltage [V]	Collision energy [V]	Parent ion [ $m/z$ ]	Fragment No. 1	Fragment No. 2
SAA	110	10	173	156	108
P1	110	20	189	172	108
SCT	60	10	215	156	108
P1	60	10	231	172	108
P2	80	5	247	188	124

**Table 4.** Molecules detected in multiple reaction monitoring.

Compound	Fragmentor voltage [V]	Collision energy [V]	Parent ion [ <i>m/z</i> ]	Fragment No. 1	Fragment No. 2
STZ	100	10	256	156	108
P1	100	10	272	172	108
P2	100	10	288	124	101
P3	60	10	101	74	59
P4	60	0	156	108	92
P5	60	20	168	124	93
P6	100	5	184	167	142
P7	100	10	246	204	140
P8	100	5	246	204	140
P9	60	5	264	156	92
P10	60	10	280	172	93
SSZ	80	10	268	156	113
P1	80	10	284	172	113
P2	80	10	300	129	108
P3	60	10	113	68	44
SDZ	100	10	251	156	108
P1	100	20	267	124	108
P2	100	20	283	124	96
P3	100	10	283	265	176
P4	100	30	187	145	65
P5	100	20	203	161	133
P6	100	20	203	161	133
P7	100	10	273	156	118
SMZ	120	10	279	186	156
P1	120	10	295	186	124
P2	120	10	295	202	156
P3	120	10	311	202	140
P4	120	20	124	107	67
P5	120	10	257	215	156
P6	120	10	273	172	102

**Table 4. Continued.** *Molecules detected in multiple reaction monitoring.*

Compound	Fragmentor voltage [V]	Collision energy [V]	Parent ion [m/z]	Fragment No. 1	Fragment No. 2
SGD	100	10	215	156	108
P1	100	10	231	172	60
P2	100	10	247	188	140
P3	100	10	190	172	80
P4	100	20	230	170	124
SP5	100	10	232	172	108
SMX	60	30	254	108	92
P1	60	20	270	124	108
P2	60	10	286	124	99
P3	60	10	272	254	147
P4	60	10	99	72	44

**Table 4. Continued.** Molecules detected in multiple reaction monitoring.

Formation of low molecular mass compounds is usually the last step prior to complete mineralization [73]. These final products are substances like aldehydes, alcohols, ketones and carboxylic acids [97, 193]. Their identification was not possible by LC-MS/MS. However, the strong decrease of the initial 4.9 – 5.9 pH seen in all sulfonamide solutions refers to appearance of acids in high concentration.

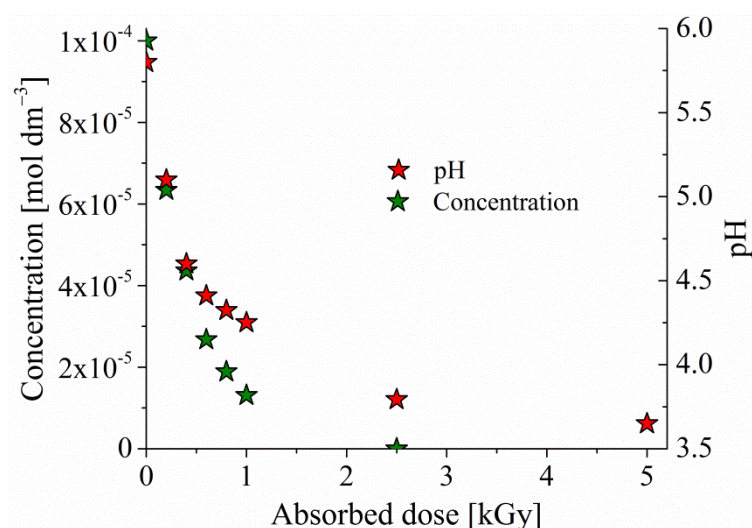


**Fig. 13.** Changes of SMX concentration and pH in function of absorbed dose.

The slope of the pH – dose dependence was very steep up to 1.5 kGy, in the phase where the ring disintegration was the most intense. Following the disappearance of the initial

molecules at around 2.5 kGy, the pH levelled off at constant values in the range of pH = 3.6 – 3.8. The reduction of the initial molecules and the parallel decrease in pH are shown in Fig. 13, on the example of SMX. Formation of oxamic-, maleic-, acetic-, formic-, pyruvic- and oxalic acids toward the end of mineralization was reported in the literature [74, 145, 146, 194].

## 6.4 Determination of inorganic ions

### 6.4.1 Nitrogen content and related inorganic ions

Formation of  $\text{NH}_4^+$ ,  $\text{NO}_3^-$  and  $\text{NO}_2^-$  ions was monitored with ion chromatography, while the changes in the total nitrogen content were determined by TN measurements. In this way, evaluation of the nitrogen mass balance during degradation of sulfonamides was enabled. Since very similar trends were seen in the investigated parameters for all sulfonamides, only the most informative (general, highest or lowest values, exceptions) dose dependences have been depicted.

The molecules investigated, SGD, SDZ and SMZ contain 4, SMX, STZ and SSZ 3, while SAA and SCT contain 2 nitrogen atoms in their structure. Irradiation of these sulfonamides yielded very low  $\text{NO}_3^-$  concentrations below 1 kGy absorbed dose. Up to this dose,  $\text{NO}_3^-$  concentrations higher than  $0.1 \text{ mg dm}^{-3}$  were observed only in SAA solutions (up to  $0.6 \text{ mg dm}^{-3}$ ) (Fig. 14).

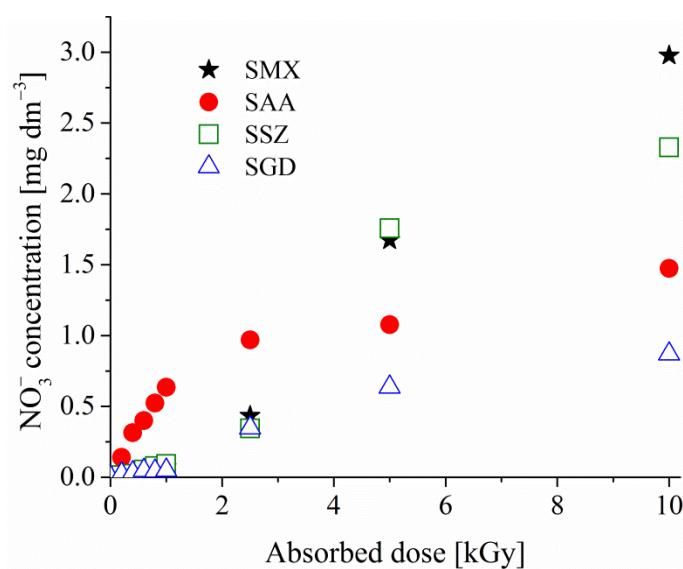


**Fig. 14.** Dose dependences of  $\text{NO}_3^-$  formation during irradiation of air saturated sulfonamide solutions.

$\text{NO}_3^-$  amount considerably increased with prolonged irradiation, and showed values high as  $3.0 \text{ mg dm}^{-3}$  (in SMX solutions at 10 kGy, Fig. 14). However, in cases of SMZ, SDZ, STZ, SCT and SGD, the  $\text{NO}_3^-$  concentration remained in the  $0.5 - 1.0 \text{ mg dm}^{-3}$  range. Results evidenced that generally 5 – 20% of the initial nitrogen content transforms to  $\text{NO}_3^-$ . Steeper slopes of  $\text{NO}_3^-$  formation curves above 1 kGy suggest that  $\text{NO}_3^-$  formation mainly occurs after the aromatic rings have been destructed to smaller fragments.

The kinetics of  $\text{NH}_4^+$  formation was completely different from that of the  $\text{NO}_3^-$  production. The  $\text{NH}_4^+$  concentration increased as a function of absorbed dose and leveled off at 2.5 kGy.  $\text{NH}_4^+$  concentrations were mostly higher than the concentrations of  $\text{NO}_3^-$  over the whole range investigated. Although even  $2.5 \text{ mg dm}^{-3}$   $\text{NH}_4^+$  was measured in SAA at 10 kGy absorbed dose, the  $\text{NH}_4^+$  amount was usually in the  $1.5 - 1.8 \text{ mg dm}^{-3}$  range (Fig. 15). These concentrations are notably higher than the  $\text{NO}_3^-$  amounts regularly detected at this stage ( $0.5 - 1.0 \text{ mg dm}^{-3}$ ). However, the increase of the  $\text{NH}_4^+$  formation curve was slower than the degradation curve of the starting sulfonamide molecules. This implies a complex  $\text{NH}_4^+$  formation process that takes place through several steps. Only 1 nitrogen atom of the molecules transforms to  $\text{NH}_4^+$  in solutions irradiated with 2.5 kGy and higher absorbed doses, as the  $\text{NH}_4^+$  concentrations were mostly in the  $1.5 - 1.8 \text{ mg dm}^{-3}$  range. It is obvious to assume that this nitrogen atom is in the  $\text{NH}_2$  group attached to the ring.  $\text{NH}_4^+$  concentration as high as  $2.5 \text{ mg dm}^{-3}$  in SAA solution (Fig. 15) suggests that  $\text{NH}_2$  group attached to  $\text{SO}_2$  also has a tendency to transform to  $\text{NH}_4^+$  during radiolytic degradation of this molecule.

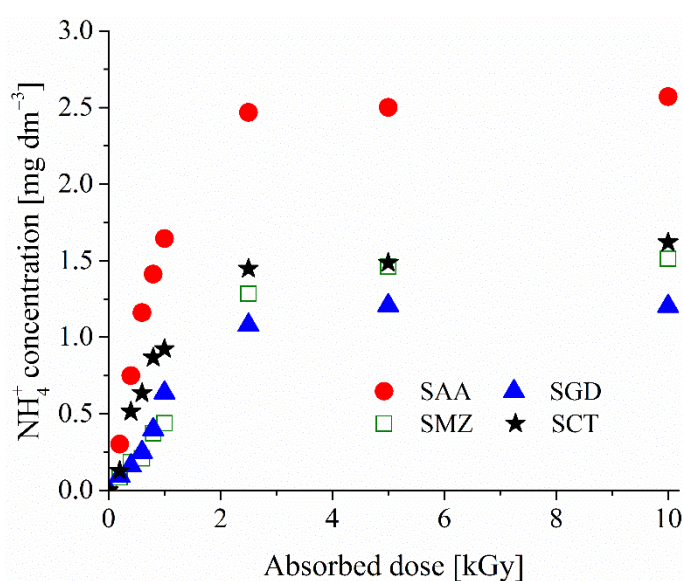


**Fig. 15.** Dose dependence of  $\text{NH}_4^+$  formation during irradiation of air saturated sulfonamide solutions.

Formation of  $\text{NO}_2^-$  was not observed in course of ionizing radiation treatment of the selected antibiotics that is consistent with the literature [151, 194].

TN measurements conducted on untreated samples showed a generally 15 – 20% lower nitrogen content than the expected theoretical values. The theoretical values were calculated on the basis of molar concentration and the molecular formula. Due to different number of nitrogen atoms in the structures, 3 different groups were distinguished. In the group of SGD, SDZ and SMZ, TN values were around  $4.6 \text{ mg dm}^{-3}$ ; in the group of SMX, STZ and SSZ, TN values were around  $3.6 \text{ mg dm}^{-3}$  and in the group of SAA and SCT, TN values were around  $2.2 \text{ mg dm}^{-3}$ . These results are shown in Fig. 16 on the example of SMZ, SSZ and SCT solutions. The decrease in nitrogen content following irradiation was significant up to 2.5 kGy, and no notable changes were detected thereafter. 30 – 40% reduction in nitrogen content was detected at 10 kGy, as compared to the initial nitrogen amount (Fig. 16).

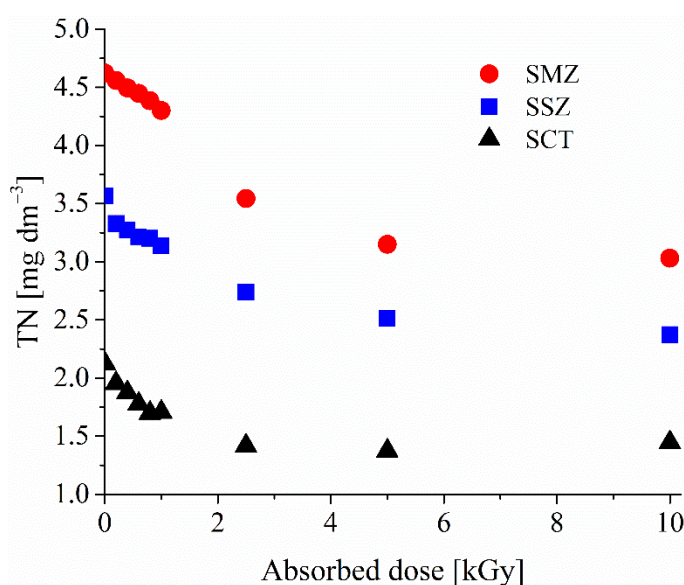


**Fig. 16.** Dose dependence of total nitrogen content during irradiation of air saturated sulfonamide solutions.

Taking into account  $\text{NH}_4^+$ ,  $\text{NO}_3^-$ ,  $\text{NO}_2^-$  concentrations and TN content, a perfect mass-balance was obtained only for SAA, while all other compounds showed 10 – 30% deficit. These results refer to incomplete mineralization of inter-chain nitrogen. The residue is probably in form of simple nitrogen containing organic acids. For instance, formation of oxamic acid was shown in catalytic ozonation of SMX [194]. The deficit seen in nitrogen

mass balances are probably due to volatile, nitrogen-containing products that are likely purged by aeration during the irradiation.

#### 6.4.2 Sulfur content and related inorganic ions

Formation of  $\text{SO}_4^{2-}$  and  $\text{SO}_3^{2-}$  were monitored with IC and only the most informative dose dependences have been depicted. All sulfonamide molecules selected contain only one sulfur atom in their structure, except STZ that contains two. Linear dose dependence of  $\text{SO}_4^{2-}$  formation was measured up to 2.5 kGy absorbed dose (Fig. 17). In most solutions,  $\text{SO}_4^{2-}$  concentration ranged from 6.2 to 8.8  $\text{mg dm}^{-3}$  at this dose. Higher amount (11.8  $\text{mg dm}^{-3}$ ) was detected only in STZ samples that is due to the double amount of sulfur in its chemical structure. By prolonged irradiation, notable  $\text{SO}_4^{2-}$  formation did not take place, the curves generally levelled off to constant values in the range of 8.9 – 9.8  $\text{mg dm}^{-3}$ . Nevertheless, STZ yielded 19.8  $\text{mg dm}^{-3}$   $\text{SO}_4^{2-}$  at this point. These values are in good agreement with the theoretical sulfur content in the solutions (based on the amounts calculated in untreated samples). Correspondingly,  $\text{SO}_3^{2-}$  was not present in measurable quantities.

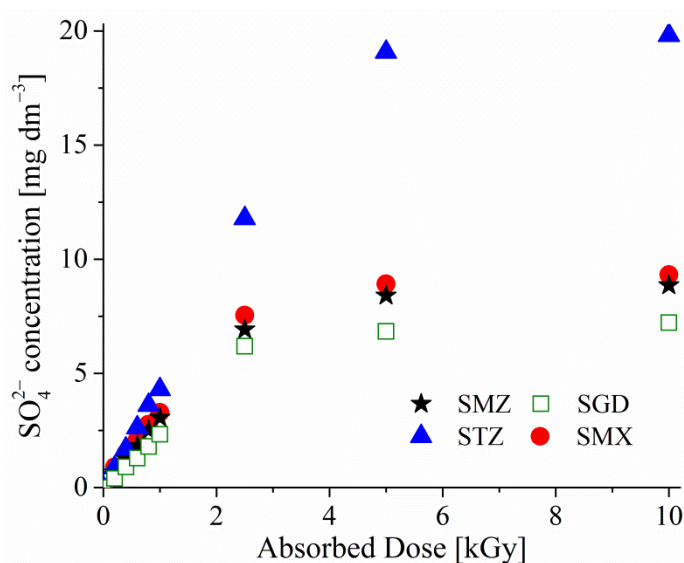


**Fig. 17.** Dose dependence of  $\text{SO}_4^{2-}$  formation during irradiation of air-saturated sulfonamide solutions.

The total sulfur content followed up by ICP-MS measurements, on the example of SMX solutions, also demonstrated that the amount of sulfur is practically not changing during irradiation. This shows that irradiation does not generate volatile sulfur containing

compounds. Similar results were reported in case of SMZ and SDZ solutions [145, 146, 192].

### 6.5 Mineralization rate

Total organic carbon (TOC) measurements conducted on initial samples showed results very close to the theoretical values, which were calculated on the basis of molar concentration and the molecular formula. Only a slight reduction of the starting values was observed up to 1 kGy absorbed dose (Fig. 18). 5% of the initial carbon content was mineralized up to this dose, except in SAA solutions (10%). Low mineralization at early stages of oxidation is related to hydroxylated derivatives. These are the major products forming up to 1 kGy, as it was anticipated by pulse radiolysis experiments and evidenced by LC-MS/MS product identification (section 6.2 and 6.3). Hydroxylated products contain the same number of carbon atoms as the initial molecules, and this is why TOC values similar to those of the starting solutions were measured at this stage of oxidative decomposition.

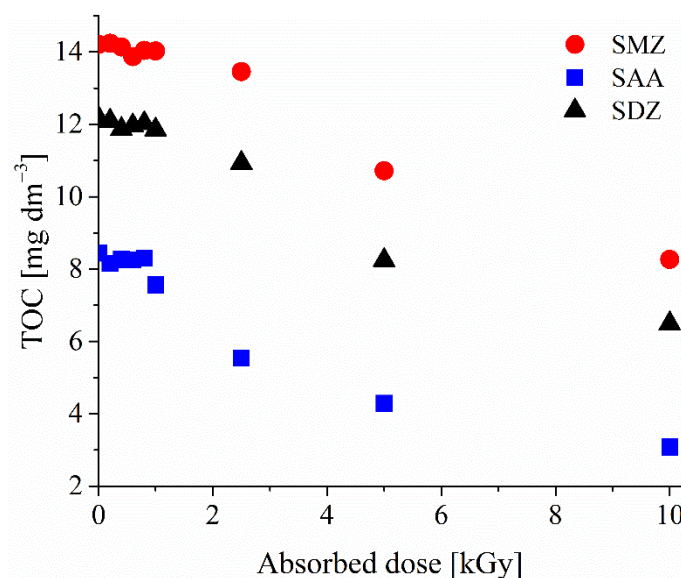


**Fig. 18.** Changes in total organic carbon content during irradiation of air-saturated sulfonamide solutions.

Prolonged irradiation led to accelerated organic carbon content reduction. Considerable drop in TOC occurred parallel with the ring opening reactions from around 1 kGy that were accompanied by CO<sub>2</sub> formation. Although the concentration of organically bound carbon was further reduced by increasing the absorbed dose, the intensity of the reduction was notably lower. The initial molecules disintegrated to smaller fragments (e.g. low molecular



mass acids) at this stage, which are known to degrade very slowly in oxidative decomposition [195]. The reaction of such compounds with  $\bullet\text{OH}$  is characterized by low reaction rate constants at around  $10^8 \text{ mol}^{-1} \text{ dm}^3 \text{ s}^{-1}$  [196]. Correspondingly, the lowest mineralization rate occurred toward the end of irradiation. The average degree of mineralization reached 40 – 60% at 10 kGy.

## 6.6 Oxidation rate

Chemical oxygen demand (COD) values measured in untreated solutions were in good agreement with the theoretical ones. The majority of the test substances showed an almost linear dependence on the dose, up to 1 kGy absorbed dose. However, in case of SAA and SGD, the compact chemical structure hinders high degree of oxidation of the starting molecules that leads to lower values, compared to the other samples treated with absorbed doses in the 0.2 – 0.6 kGy range (Fig. 19).

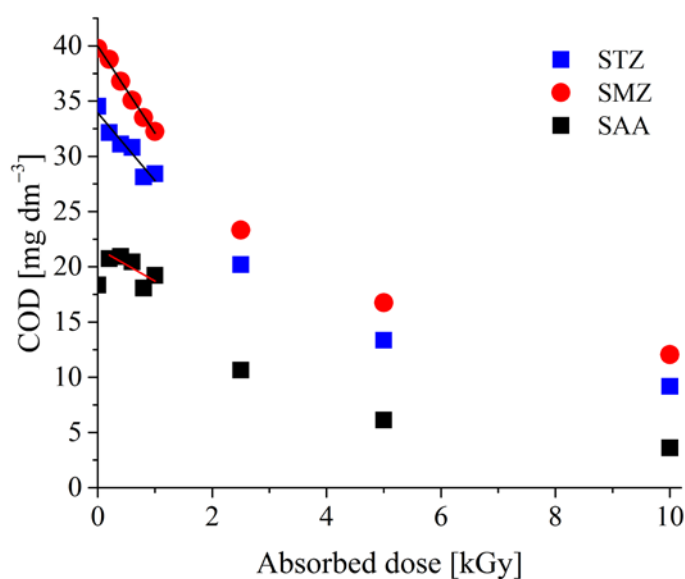


**Fig. 19.** Dose dependence of the chemical oxygen demand. The slopes of the straights fitted on the initial part of the data sets are shown in Table 5.

The initial slopes (0 – 1 kGy) of the COD – dose relations were in the range of  $4.5 - 7.6 \times 10^{-3} \text{ mg dm}^{-3} \text{ Gy}^{-1}$  ( $1.4 - 2.4 \times 10^{-7} \text{ mol dm}^{-3} \text{ Gy}^{-1}$ ) (Table 5). These data show that at the beginning of the process, the number of oxygen atoms in the products is on average higher by 1.5 than in the starting molecules. The value higher than 1 indicates that even at low doses, in addition to phenols (1 oxygen atom building in), some products with higher oxidized state also form. The high incorporation is attributed to organic radical reactions with dissolved  $\text{O}_2$  and subsequent oxidation reactions [196]. These results are in accordance

with LC-MS/MS results, that evidenced incorporation of 1 or 2 OH groups into the structure of initial molecules in the 0.2 – 0.8 kGy absorbed dose range (section 6.3). The almost linear trend of COD decrease up to 1 kGy implies that the reaction rate constant of the  $\bullet$ OH reaction is about the same in case of the products and the parent molecules. COD results also evidence that the initial products are easily oxidizable in course of ionizing radiation treatment, similarly to the majority of initial molecules, except SGD and SAA. The decrease of COD in SGD solutions was similar to that of SAA shown in Fig. 19 or Fig. 20.

Test substance	SAA	SMX	SSZ	SGD	SDZ	SMZ	STZ	SCT
COD/absorbed dose slope [ $\times 10^{-3} \text{ mg dm}^{-3} \text{ Gy}^{-1}$ ]	4.5	5.3	5.6	5.6	6.4	6.7	7.4	7.6

**Table 5.** The slopes of the COD – dose relation in the 0 – 1 kGy range.

The slope of the COD decrease considerably reduced by prolonged irradiation (above 1 kGy). This means that products formed at – and above – 1 kGy are not so easily oxidizable, as it was seen in case of products appearing up to 1 kGy. Such behavior is consistent with the idea of aromatic ring disintegration under oxidative conditions. Products formed before complete mineralization are known for being refractory to oxidation, as it was mentioned in section 6.5, and this causes the changes in COD decrease tendency. This fact may also provide explanation to similar results for the COD and TOC removals at high doses (Fig. 20) [73].

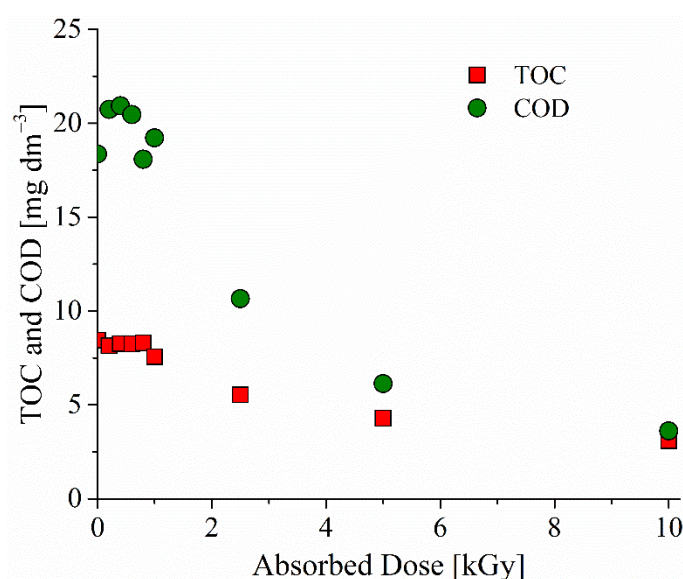


**Fig. 20.** Changes in COD and TOC as a function of absorbed dose in SAA solutions.

## 6.7 Biodegradability

To investigate the biodegradability of sulfonamides and their transformation products in natural water bodies and at the biological step of wastewater purification, BOD<sub>5</sub> was determined by inoculation with river water or activated sludge. The biodegradability was expressed in form of BOD<sub>5</sub> COD<sup>-1</sup> ratio. Nevertheless, factors strongly influencing the BOD<sub>5</sub> experiments were evaluated before measuring and discussing the biodegradation of target molecules. These factors are the pollutant concentration dilution – taking place along the treatment process due to mineralization – and the presence of H<sub>2</sub>O<sub>2</sub> formed in radical reactions.

### 6.7.1 Impact of different pollutant load exposure and H<sub>2</sub>O<sub>2</sub>

H<sub>2</sub>O<sub>2</sub> formation up to  $3 \times 10^{-4} \text{ mol dm}^{-3}$  was detected in course of ionizing radiation treatment up to 2.5 kGy, as shown in Fig. 21/A. To evaluate the impact of such concentrations on activated sludge, toxicity was tested by BOD<sub>5</sub> experiments in solutions containing H<sub>2</sub>O<sub>2</sub> up to  $5 \times 10^{-4} \text{ mol dm}^{-3}$  concentrations.

BOD<sub>5</sub> measurements carried out by using H<sub>2</sub>O<sub>2</sub> dilution series can be interpreted as a toxicity indicator. In such consideration, the blank sample reflects the maximal achievable BOD<sub>5</sub> and thus, the 0% inhibition. Increased inhibitory effects are indicated by BOD<sub>5</sub> values lower than the ones measured in the blank. Shifted adaptation periods and low inhibitory effects seen in BOD<sub>5</sub> results evidenced minor impact of H<sub>2</sub>O<sub>2</sub> present in trace amounts ( $0.1 \times 10^{-4} \text{ mol dm}^{-3}$ ). However, results displayed serious inhibition at concentrations higher than  $0.5 \times 10^{-4} \text{ mol dm}^{-3}$  (Fig. 21/B). Inhibitory effects higher than 50% were detected in solutions containing at least  $1 \times 10^{-4} \text{ mol dm}^{-3}$  of H<sub>2</sub>O<sub>2</sub> and complete inhibition was observed above  $2.5 \times 10^{-4} \text{ mol dm}^{-3}$ . Similar results were obtained in river water experiments.

Simultaneous effects of toxicity and O<sub>2</sub> formation (both stemming from H<sub>2</sub>O<sub>2</sub>) were investigated by measurements carried out on standard solutions (BOD<sub>5</sub> =  $210 \pm 20 \text{ mg dm}^{-3}$ ) in the presence of known H<sub>2</sub>O<sub>2</sub> concentrations. According to these results, negligible impact of H<sub>2</sub>O<sub>2</sub> ( $\Delta\text{BOD}_5 < 6\%$ ) was seen up to  $\sim 0.3 \times 10^{-4} \text{ mol dm}^{-3}$  H<sub>2</sub>O<sub>2</sub>, while significant effects were observed above  $\sim 4 \times 10^{-4} \text{ mol dm}^{-3}$ . The biological oxygen demand in solutions containing H<sub>2</sub>O<sub>2</sub> concentrations above  $4 \times 10^{-4} \text{ mol dm}^{-3}$  remained at around 50% lower than the expected value ( $225 \pm 20 \text{ mg dm}^{-3}$ ) even when the measurement

was prolonged to 7 days. Shift in lag periods from ~ 1 day to more than 5 days was also noticed in these solutions (not shown). The lengthened lag period also means that the biodegradation of sulfonamide test solutions would be suppressed at the beginning of the measurement, if H<sub>2</sub>O<sub>2</sub> remained in the solutions.

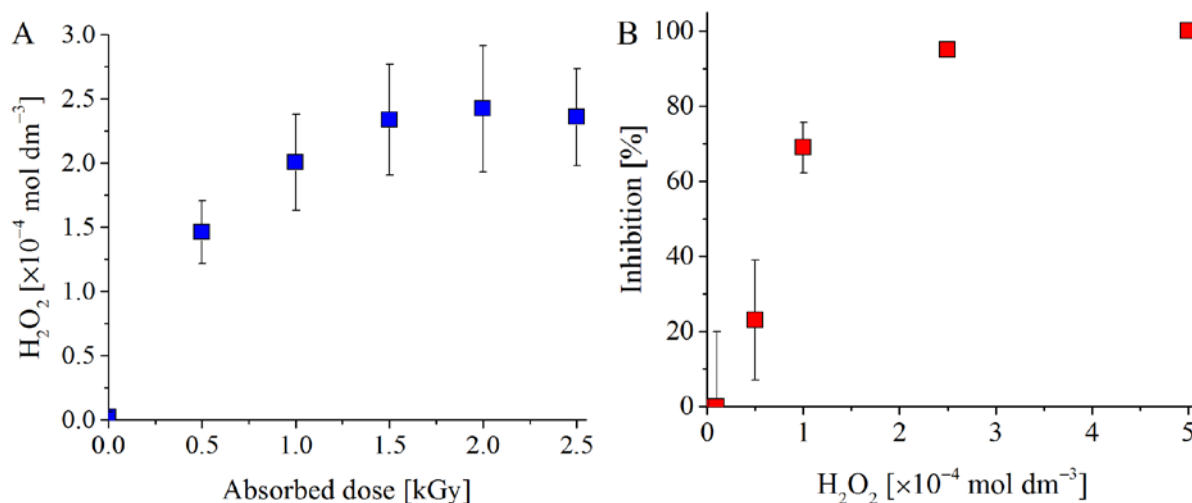


**Fig. 21.** Dose dependence of H<sub>2</sub>O<sub>2</sub> formation (A), and the inhibitory effects of H<sub>2</sub>O<sub>2</sub> on activated sludge in BOD<sub>5</sub> experiments (B).

To highlight the difference between different sample application approaches in biodegradation experiments, analyses were performed on the example of SMX. The evaluation was carried out by exposure of activated sludge microbial communities to equal pollutant concentration, by using untreated samples, and samples irradiated by 1 and 2.5 kGy. The H<sub>2</sub>O<sub>2</sub> content was removed prior to these experiments, as described in section 5.5.5. To achieve the same load exposure, the samples were adjusted to equal COD values, by dilution with purified water. 2.5 kGy was the highest dose applied in these experiments; therefore, the load was set to COD measured at this dose (10 mg dm<sup>-3</sup>). This sample application approach, referred to as biological, was compared to the one neglecting the pollutant concentrations and the presence of H<sub>2</sub>O<sub>2</sub> (technological approach).

Statistically significant differences were seen between the two sample application approaches (Fig. 22). The two-tailed *P* value equaled 0.0363, when the untreated samples were compared, while *P* was 0.0012 in comparison of oxidized solutions at both doses. The difference observed in solutions treated by 2.5 kGy is assigned solely to H<sub>2</sub>O<sub>2</sub>, as the pollutant load was equal at this dose between the two approaches. However, there was no H<sub>2</sub>O<sub>2</sub> in untreated solutions and still significant differences were seen.

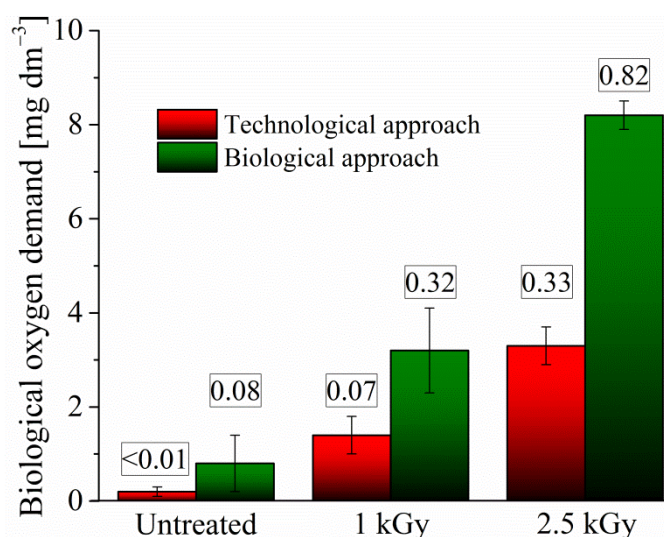


**Fig. 22.** *BOD<sub>5</sub> measured in SMX solutions inoculated by activated sludge. The samples were applied based on technological or biological approaches. BOD<sub>5</sub> COD<sup>-1</sup> ratios are indicated above the columns.*

Fundamental conclusions drawn from the biological and technological approaches regarding biodegradation trend changes are actually the same, since the biodegradation increased in both cases. The relevance of different approaches manifested in the extent of changes. Biological approach referred to readily biodegradable solutions (0.82), while only moderate (0.33) transformation to bioavailable substances was demonstrated by the technological approach (Fig. 22).

Generally, H<sub>2</sub>O<sub>2</sub> in concentrations detected following the irradiation of sulfonamides showed major impact on microorganism communities of activated sludge and river water. For this reason, H<sub>2</sub>O<sub>2</sub> concentration should be reduced to  $0.3 - 0.5 \times 10^{-4} \text{ mol dm}^{-3}$  to avoid notable toxic effects and interferences in manometric BOD evaluation. Similarly high impact was observed when the pollutant load was altered in the experiments. All these emphasize how decisive H<sub>2</sub>O<sub>2</sub> and different pollutant load exposure are in biodegradation experiments. Neglecting any of them may strongly distort the investigation and cause underestimated biodegradability. However, in experiments carried out by the biological approach, all these effects have been avoided by H<sub>2</sub>O<sub>2</sub> removal and by exposure of test communities to equal pollutant concentrations. The results presented in the following sections were obtained by such approach.

### 6.7.2 Biodegradation in activated sludge

Biodegradation experiments performed by application of activated sludge reflect the fate sulfonamides during biological wastewater treatment. Untreated sulfonamide solutions showed a  $BOD_5 COD^{-1}$  ratio in the range of 0.14 – 0.21 (Fig. 23). These results evidence limited biological availability of compounds tested. At the same time, oxidation of the initial molecules indicates presence of microorganisms with compatible set of enzymes; and thus, a certain extent of adaptation to sulfonamides investigated. Yang et al. reported sulfonamide utilization by *Acinetobacter* and *Pseudomonas* species that may contribute to the biodegradation observed, as they commonly occur in the sludge used [197].

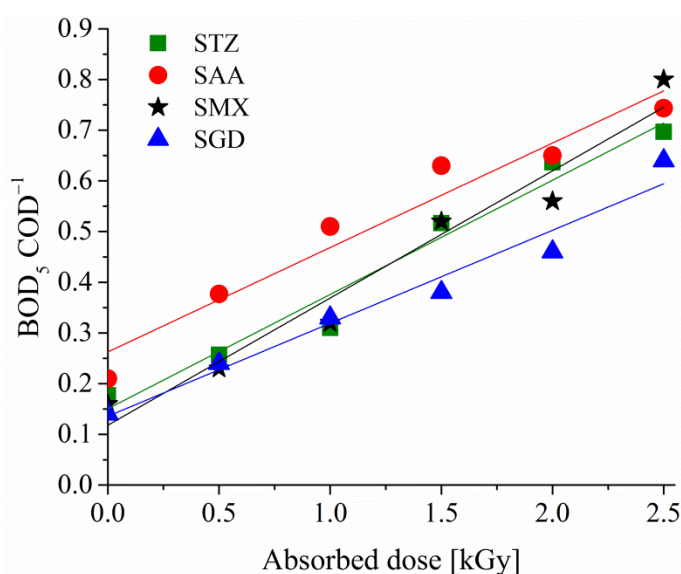


**Fig. 23.** Changes of the  $BOD_5 COD^{-1}$  ratio in function of absorbed dose in STZ, SAA, SGD and SMX solutions (with activated sludge inoculum).

Radiolytic degradation improved the biodegradability in all experiments (Fig. 23). The  $BOD_5 COD^{-1}$  ratio increased up to 0.31 – 0.51 at 1 kGy. The vast majority of molecules present in the solutions were hydroxylated derivatives, but intact initial molecules were also present in low amounts at this stage of treatment (section 6.3). Further oxidation demolished both initial and hydroxylated substances and entailed appearance of low molecular mass acids (section 6.3), which are known to degrade readily in biological processes [198]. Correspondingly,  $BOD_5 COD^{-1}$  ratios reached values as high as 0.64 – 0.80 at 2.5 kGy (Fig. 23). Generally, ionizing radiation treatment of sulfonamides by few tenths of kGy already enhanced the biodegradation in activated sludge and ready biodegradability was achieved by application of 1.5 – 2.5 kGy.

### 6.7.3 Biodegradation in river water

Biodegradation experiments with river water inoculum evaluate the fate of substances discharged to natural water bodies. Complete resistance to biodegradation of initial molecules was observed in these tests (Fig. 24). To investigate eventual changes taking place on longer time scale, the incubation period was prolonged to 10 days in experiments with SAA. However, the  $BOD_5 COD^{-1}$  ratio remained 0 even after 7 days and it remained low even at 10 days (0.18). This value is similar to those obtained using activated sludge inoculum following 5 days (0.14 – 0.21).

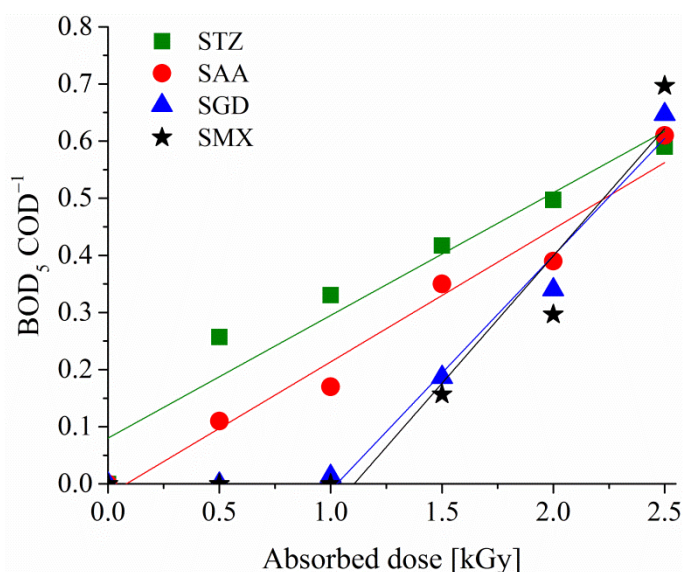


**Fig. 24.** Changes of the  $BOD_5 COD^{-1}$  ratio in function of absorbed dose in case of STZ, SAA, SGD and SMX solution (with river water inoculum).

Ionizing radiation treatment led to conversion of non-biodegradable sulfonamides to substances accessible for metabolic processes of microorganisms in river water. Fig. 24 shows the dose dependence of these biodegradability changes. The  $BOD_5 COD^{-1}$  ratios in SAA and STZ solutions reached 0.17 and 0.33 at 1 kGy, respectively. However, persistence up to 1 kGy absorbed dose was seen in cases of SMX and SGD that evidences resistance to biological degradation in solutions containing mainly hydroxylated derivatives of SMX or SGD. High level of biodegradation took place only when both initial and hydroxylated molecules were decomposed. Above 1 kGy, the increase in  $BOD_5 COD^{-1}$  ratio was higher by a factor of 2 in these solutions. This ultimately led to similar biodegradability as the ones seen in SAA and STZ solutions. 0.59 – 0.70  $BOD_5 COD^{-1}$  ratios were seen at 2.5 kGy in all solutions, these values are similar to those observed in activated sludge experiments.

#### 6.7.4 General evaluation of biodegradability

Practically identical slope parameters were observed in most of the cases, when the  $BOD_5 COD^{-1}$  ratio was plotted as a function of absorbed dose (Fig. 23 and 24). This refers to similar characteristics of sulfonamide conversion to biodegradable substances in both river water and activated sludge. The  $BOD_5 COD^{-1}$  ratios of initial solutions in activated sludge experiments displayed a shift to higher values as compared to results obtained in river water. This shift was also seen in analyses evaluating oxidized samples.

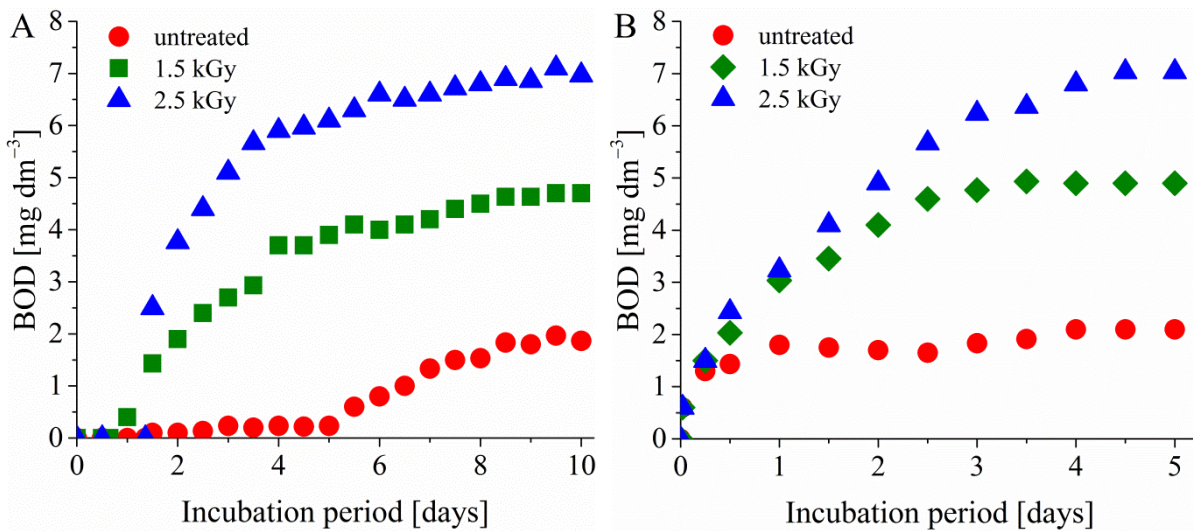


**Fig. 25.** Dose dependence of  $BOD$  in SAA solutions inoculated with river water (A) or activated sludge (B).

Considerably lower biodegradability in river water is due to significantly lower amount of bacteria species present and lower abundance of them, as compared to activated sludge. In this way, low incidence of compatible enzyme producers prolongs the adaptation/acclimatization of the microbes. Fig. 25 shows this phenomenon on typical  $BOD_5$  curves obtained in activated sludge and river water, on the example of SAA. Several days of adaptation/acclimatization period were needed prior to  $BOD_5$  increase in river water (Fig 25/A), while an immediate increase was observed in activated sludge (Fig 25/B). Incubation periods longer by  $\sim 2 - 5$  days led to the same level of biodegradation in river water (Fig. 25) as in activated sludge.

It has to be noted that in SMX and SGD river water experiments only the complete disappearance of both initial and oxidized products led to increased  $BOD_5 COD^{-1}$  ratio (Fig. 24). Different behavior was observed in all other cases, including measurements done with activated sludge. Nevertheless, ready biodegradability was reached in all solutions at



high dose (including SMX and SGD in river water), whilst the degree of mineralization remained relatively low (15 – 25%, section 6.5).

## 6.8 Toxicity assay

Negative effects of initial substances will not necessarily decrease during their decomposition, as pointed out in the literature [199, 200]. For this reason, toxicity was followed up along the irradiation treatment of sulfonamides. As previously evidenced in case of biodegradation,  $\text{H}_2\text{O}_2$  and exposure of test organisms to different pollutant loads may strongly modify the outcome of the biological experiments. These effects had been determined prior to toxicity testing of sulfonamide solutions.

### 6.8.1 Impact of different pollutant load exposure and $\text{H}_2\text{O}_2$

$5 \times 10^{-4} \text{ mol dm}^{-3} \text{ H}_2\text{O}_2$  showed remarkably high inhibition/mortality on all individual test organisms (Fig. 26). Such concentration led to  $100 \pm 0\%$ ,  $96 \pm 1\%$  and  $72 \pm 5\%$  inhibition on *D. magna*, *P. subcapitata* and *V. fischeri*, respectively. Hence, such high  $\text{H}_2\text{O}_2$  concentration hinders interpretation of results targeting toxicity of products formed in course of the treatment.

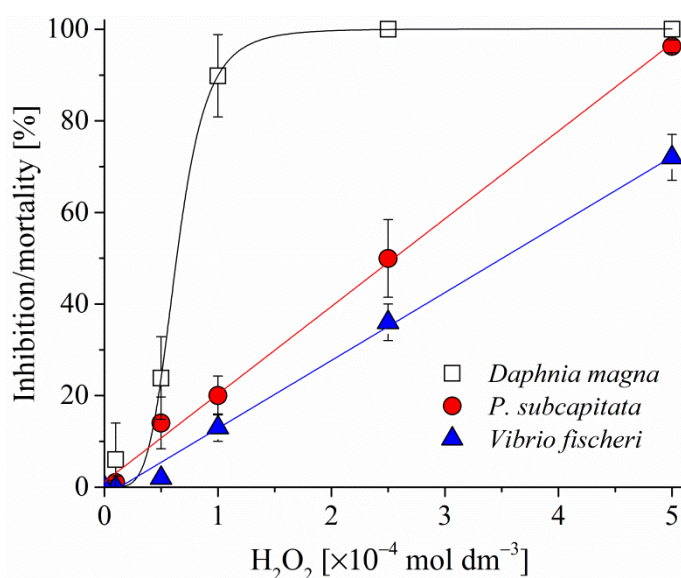


**Fig. 26.**  $\text{H}_2\text{O}_2$  concentration dependence of inhibition/mortality in *Daphnia magna*, *Pseudokirchneriella subcapitata* and *Vibrio fischeri* ecotoxicity experiments.

By lowering the  $\text{H}_2\text{O}_2$  concentrations, reducing inhibition was detected in *V. fischeri* and *P. subcapitata* experiments. Their responses to  $\text{H}_2\text{O}_2$  exposure showed a linear correlation in the range investigated (Fig. 26). Below  $0.5 \times 10^{-4} \text{ mol dm}^{-3}$ , the inhibitory effects of  $\text{H}_2\text{O}_2$  towards *V. fischeri* and *P. subcapitata* can be regarded as acceptable:  $2 \pm 0\%$  and

$14 \pm 6\%$ , respectively. However, *D. magna* showed a different behavior. The concentration – response curve was sigmoidal. No changes were observed in toxicity when reducing the  $\text{H}_2\text{O}_2$  concentration from  $5 \times 10^{-4} \text{ mol dm}^{-3}$  to  $1 \times 10^{-4} \text{ mol dm}^{-3}$ . Changing the  $\text{H}_2\text{O}_2$  concentration from  $1 \times 10^{-4} \text{ mol dm}^{-3}$  to  $0.5 \times 10^{-4} \text{ mol dm}^{-3}$  was coupled with mortality reduction from  $90 \pm 9\%$  to  $24 \pm 9\%$  (Fig. 26). Acceptable susceptibility of these test organisms was observed when the concentration of  $\text{H}_2\text{O}_2$  was reduced to  $0.1 \times 10^{-4} \text{ mol dm}^{-3}$  ( $6 \pm 8\%$  mortality). The half-maximal effective concentrations ( $\text{EC}_{50}$ ) were  $3.49 \times 10^{-4}$ ,  $2.51 \times 10^{-4}$  and  $0.64 \times 10^{-4} \text{ mol dm}^{-3}$  for *V. fischeri*, *P. subcapitata* and *D. magna*, respectively.

Effects stemming from exposure of test organisms to different pollutant concentrations and presence of  $\text{H}_2\text{O}_2$  are shown in Fig. 27. The investigation was performed by biological and technological approaches on the example of *P. subcapitata* growth inhibition experiments, using SGD solutions. The pollutant concentration was set to equal COD values ( $10 \text{ mg dm}^{-3}$ ) by dilution with purified water. Analyses conducted based on the technological approach revealed statistically significant reduction of inhibitory effects as a function of absorbed dose (Fig. 27). However, the  $(3.1 \pm 0.6) \times 10^5 \text{ cm}^{-3}$  *P. subcapitata* cell concentrations measured at 2.5 kGy still remained below the  $(4.6 \pm 0.7) \times 10^5 \text{ cm}^{-3}$  cell concentration measured in the blank sample. In contrast, biological approach evidenced statistically no significant differences between the blank sample and the solutions containing SGD (Fig. 27). Therefore, gradual formation of less harmful products was indicated by the technological approach, while presence of harmless molecules was shown by the biological approach.

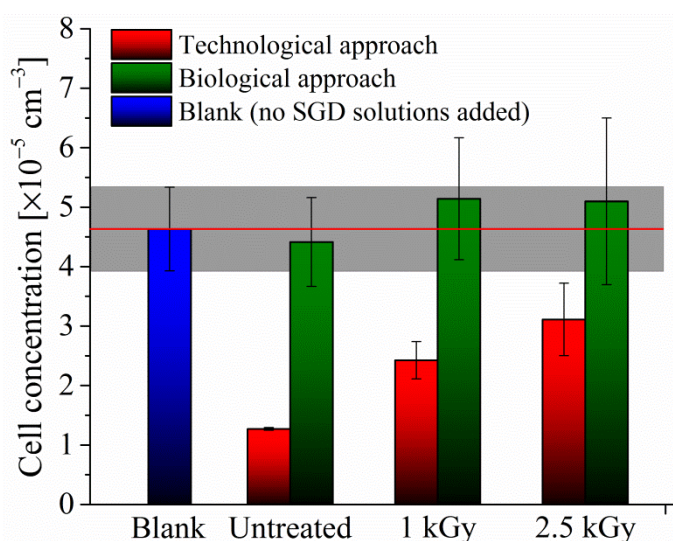


**Fig. 27.** *Pseudokirchneriella subcapitata* cell concentration measured in growth inhibition experiments by technological or biological approaches in SGD solutions.

Pollutant load setting to equal COD seems to be a more appropriate choice when evaluation of biodegradability is the primary goal, as both COD and BOD measure oxygen demands. However, exposure of test organism to equal pollutant amounts set by TOC may have more sense in analyses primarily aiming at ecotoxicity investigation, as inhibitory effect can be caused by any substance, not only by the oxidizable ones. *V. fischeri* inhibition tests were implemented on the example of SMX to investigate differences between load setting by TOC and COD in the biological sample application approach. The pollutant concentration was adjusted by dilution with purified water to TOC = 10.4 mg dm<sup>-3</sup> or COD = 10 mg dm<sup>-3</sup> and the H<sub>2</sub>O<sub>2</sub> was removed. In the technological approach H<sub>2</sub>O<sub>2</sub> was not removed and pollutant load was not set to equal values.

Measurements performed by technological approach showed 5% inhibition that increased to over 75% in oxidized samples (Fig. 28). This enormous change was partly due to H<sub>2</sub>O<sub>2</sub>, since toxic effects were considerably lower when H<sub>2</sub>O<sub>2</sub> was removed in the experiments conducted by the biological approach (30%) (Fig. 28). However, in measurements where the pollutant concentration was set to equal COD values, significantly lower results were seen as compared to experiments set by TOC content. The *P* value was < 0.0001 in the comparison of both untreated samples and the ones treated by 1 kGy. Such results are associated with high degrees of oxidation and low mineralization during initial stages of irradiation. Results in biological approach implemented by pollutant loading based on COD or TOC did not show differences in samples treated by 2.5 kGy, as these samples were used as obtained (the other samples were diluted to COD values measured at 2.5 kGy) (Fig. 28).

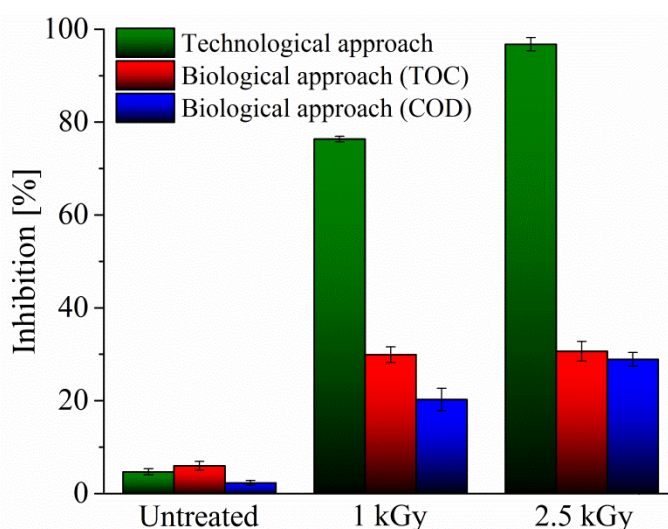


**Fig. 28.** Dose dependence of *Vibrio fischeri* luminescence inhibition in experiments carried out by technological or biological approaches in SMX solutions.

Generally, H<sub>2</sub>O<sub>2</sub> showed remarkably strong inhibitory effects on the individual test organisms at concentrations forming during ionizing radiation treatment. As pointed out in section 2.4.2, H<sub>2</sub>O<sub>2</sub> concentrations even notably higher than found in the present work are often detected in AOP. These effects may even completely hide the eventual impact stemming from the molecules investigated. In this way, the results become imperceptible regarding the target substances. Such results can easily be a source for misinterpretation of degradation product effects. According to the results shown in Fig. 26, elimination of H<sub>2</sub>O<sub>2</sub> concentrations above  $0.5 \times 10^{-4} \text{ mol dm}^{-3}$  is required in *V. fischeri* and *P. subcapitata* measurements prior to toxicity assays evaluating effects of decomposition products. In case of *D. magna*, practically complete H<sub>2</sub>O<sub>2</sub> removal is needed. Similarly to H<sub>2</sub>O<sub>2</sub> effects, mineralization caused pollutant dilution also modifies the results targeting toxicity characterization of product molecules. Therefore, it hinders proper comparison of toxic potentials attributed to different product groups. To overcome these interferences, biological approach was followed in the toxicity experiments presented below.

### 6.8.2 *Daphnia magna* acute mortality

*D. magna* cultures showed 97% mortality when they were exposed to untreated SGD (Fig. 29). In function of increasing absorbed dose – parallel with the disappearance of initial SGD compounds and formation of hydroxylated products (section 6.3) – the mortality reduced to 48% at 1 kGy. Removal of both initial and oxidized compounds further reduced the negative impact, indicated by mortality reduction to 11% at 2.5 kGy. Although mortality was significantly lower, toxic effects were detected even when SGD and hydroxylated products were all demolished.

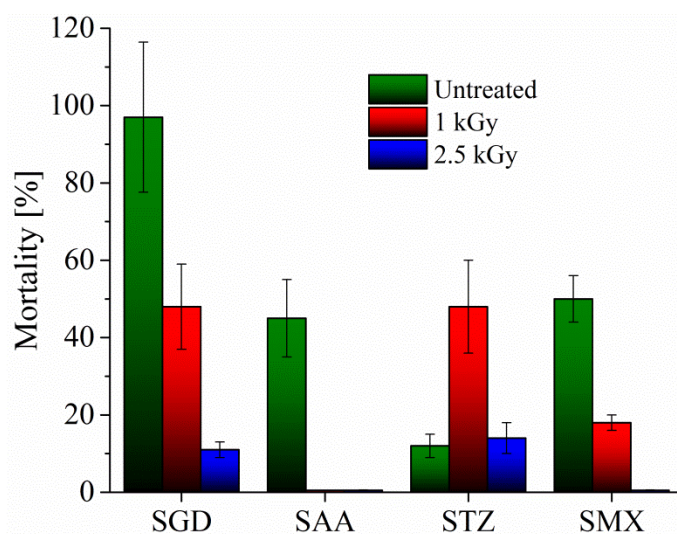


**Fig. 29.** Dose dependence of *Daphnia magna* mortality in solutions containing SGD, SAA, STZ or SMX.

Mortality of test organisms was notably lower when they were exposed to untreated SAA (45%) or SMX (50%) solutions, as compared to the one seen in SGD tests (97%). SAA solutions lost all harmful effects at 1 kGy that evidences no impact of hydroxylated products on *D. magna*. Toxic effects of irradiated SMX solutions reduced as a function of absorbed dose, as well, but complete termination was seen only at 2.5 kGy. In this way, the high noxious effects of initial SAA and SMX solutions were entirely eliminated by increasing the absorbed dose up to 2.5 kGy. In contrast, low *D. magna* mortality was determined in initial STZ solution (12%) that increased to 48% at 1 kGy. Increased negative effects cannot be clearly related to oxidation products formed in course of irradiation, as notably higher H<sub>2</sub>O<sub>2</sub> amounts remained in the samples after the H<sub>2</sub>O<sub>2</sub> removal procedure ( $0.7 \times 10^{-4} \text{ mol dm}^{-3}$ ) as in all other solutions investigated ( $\sim 0.3 \times 10^{-4} \text{ mol dm}^{-3}$ ). Such difference leads to approximately five times higher mortality on *D. magna* (40 – 60% mortality). Nevertheless, the mortality reduced by application of 2.5 kGy, but it did not reduce below the initial value.

### 6.8.3 *Pseudokirchneriella subcapitata* chronic growth inhibition

The chronic effects were investigated on the exponentially growing primary producer, *P. subcapitata*. Among the untreated sulfonamides involved in the experiments, the highest growth inhibition (92%) was measured in SMX solution (Fig. 30).

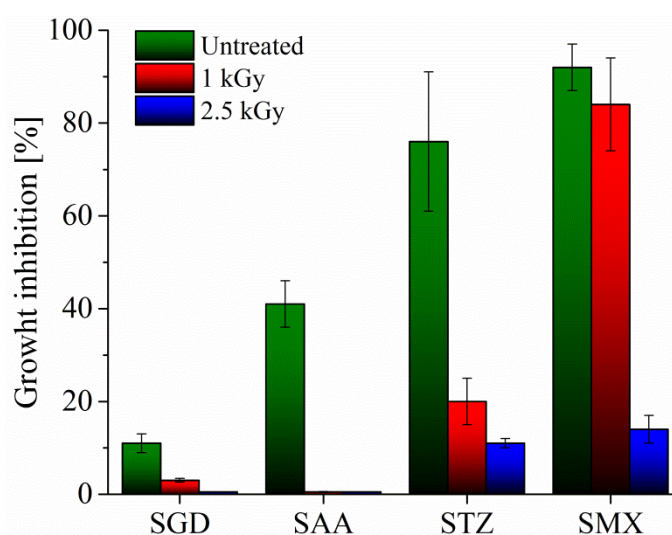


**Fig. 30.** Dose dependence of *Pseudokirchneriella subcapitata* growth inhibition in solutions containing SGD, SAA, STZ and SMX.

At 1 kGy absorbed dose, when SMX molecules were transformed to hydroxylated products no statistically significant differences were observed in toxicity as compared to untreated

samples. Growth inhibition reduced to 14% only at 2.5 kGy dose, where low molecular mass products are present. Similarly to untreated SMX solutions, strong adverse effects of initial molecules were found in initial STZ solutions (Fig. 30). However, this 76% growth inhibition considerably reduced at 1 kGy (20%), but even 2.5 kGy dose was not sufficient for complete elimination of the detrimental impacts (11%). Residual H<sub>2</sub>O<sub>2</sub> in STZ solutions does not play any role in *P. subcapitata* experiments, as it did in *D. magna* tests. *P. subcapitata* was not as sensitive to H<sub>2</sub>O<sub>2</sub> exposure as *D. magna*, as shown in section 6.8.1. Inhibitory effects of SGD (11%) and SAA (41%) were practically terminated at 1 kGy (Fig. 30). Prolonged treatment of these solutions led to higher cell growth than the ones measured in the control samples. A higher cell concentration in the sulfonamide samples refers not only to disappearance of unfavorable effects but also to contribution of oxidized molecules to biomass production.

#### 6.8.4 *Vibrio fischeri* acute luminescence inhibition

Negligible toxic effects were detected in solutions containing untreated SMX and STZ (~ 3% for both), while SGD had no influence on the luminescence of *V. fischeri* (Fig. 31). Similarly to the initial solutions, no inhibitory effects were observed when test organisms were exposed to irradiated SGD solutions. In contrast, the negligibly low impact of both SMX and STZ increased to 25% and 15%, respectively, at 1 kGy absorbed dose (Fig. 31). Prolonged treatment of SMX resulted in further increase in luminescence inhibition (34%), evidencing formation of progressively toxic SMX degradation products as a function of absorbed dose. Formation of products possessing higher toxic potential than in the initial STZ solution was observed, as well, since the inhibition remained higher in the treated samples than in the initial solution. Nevertheless, untreated SAA solution was much more toxic (49%), compared to other sulfonamides, but the toxic effects significantly reduced (12%) and ultimately disappeared by increasing the absorbed dose. Pintar et al. [201] suggested that carboxylic and dicarboxylic acids exert toxic effects on *V. fischeri*. Although such compounds dominate among the products at 2.5 kGy, increase in luminescence inhibition was not seen in SGD or SAA solutions. This may refer to presence of toxic products other than carboxylic or dicarboxylic acids.

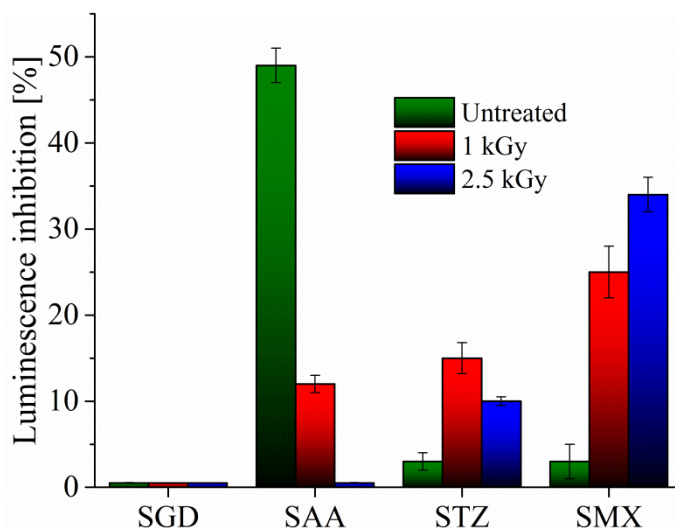


**Fig. 31.** Dose dependence of *Vibrio fischeri* light emission inhibition in solutions containing SGD, SAA, STZ or SMX.

### 6.8.5 Activated sludge respiration inhibition

Activated sludge respiration inhibition experiments provide data on inhibitory effects of sulfonamides and also give information on formation of rapidly biodegradable substances in course of irradiation procedure. Nevertheless, formation of oxygen bubbles in solutions containing  $\sim 10^{-4} \text{ mol dm}^{-3} \text{ H}_2\text{O}_2$  called attention to the interfering effects of  $\text{H}_2\text{O}_2$  in these experiments. Toxic effect of  $\text{H}_2\text{O}_2$  and the interference of oxygen formed during  $\text{H}_2\text{O}_2$  decomposition were not separated; they were quantified together by using  $\text{H}_2\text{O}_2$  dilution series.

#### *Impact of different pollutant load exposure and $\text{H}_2\text{O}_2$*

Formation of oxygen bubbles was observed in airtight sealed Karlsruher flask that contained  $5 \times 10^{-4} \text{ mol dm}^{-3}$  aqueous solution of  $\text{H}_2\text{O}_2$  and  $5 \text{ cm}^3$  catalase enzyme. In course of  $\text{H}_2\text{O}_2$  disintegration, dissolved oxygen concentration increased from the initial  $8.1 \text{ mg dm}^{-3}$  and reached equilibrium at  $15.6 \text{ mg dm}^{-3}$  after 15 – 20 min reaction time at  $20^\circ\text{C}$ . This increment ( $7.5 \text{ mg dm}^{-3}$ ) is close to the maximal oxygen amount forming in decomposition of  $5 \times 10^{-4} \text{ mol dm}^{-3} \text{ H}_2\text{O}_2$  ( $8.5 \text{ mg dm}^{-3}$ ). Similarly to these experiments, bubble formation in the first 30 minutes was observed in the respiration inhibition tests conducted on sulfonamide samples. The changes in dissolved oxygen concentration were consistent with the ones measured following the catalase addition to  $\text{H}_2\text{O}_2$  samples. All these evidence that the major part of  $\text{H}_2\text{O}_2$  transforms to oxygen in microbial decomposition. The transformation probably takes place due to the effect of catalase, superoxide dismutase or peroxidase produced by microbial strains [118]. Because of

oxygen formation, linear oxygen depletion dependence on time was found only between 30 and 180 minutes.

Results showed that the usual  $\text{H}_2\text{O}_2$  concentration ( $1.5 - 2.5 \times 10^{-4} \text{ mol dm}^{-3}$ ) measured in the solutions treated by 0.5 – 2.5 kGy absorbed doses exert strong inhibitory effects in respiration inhibition experiments (Fig. 32). An average inhibition of 40 – 60% was measured in this range that necessitates removal of  $\text{H}_2\text{O}_2$  from the treated samples prior to performing the respiration inhibition tests. Inhibitory effects were reduced to 10 – 20%, following the catalytic decomposition by  $\text{MnO}_2$ , although low amounts of  $\text{H}_2\text{O}_2$  remained in the solutions ( $2 - 7 \times 10^{-5} \text{ mol dm}^{-3}$ ). In case of respiration inhibition experiments, such impact can be regarded as an acceptable interference.

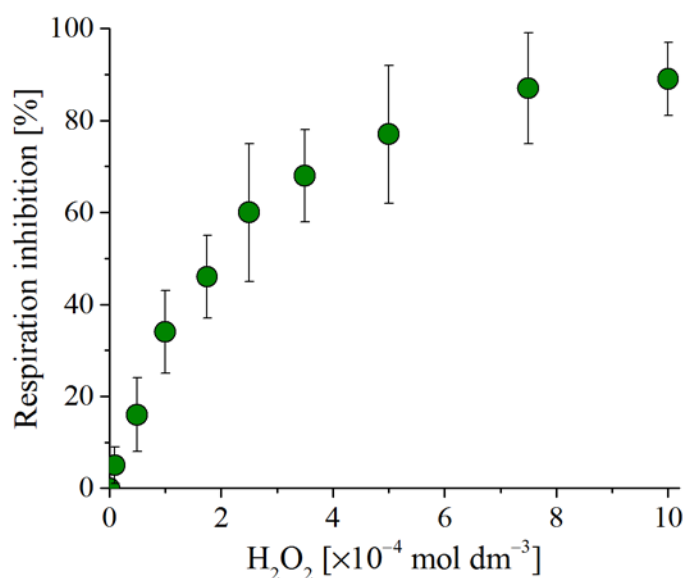


**Fig. 32.** Concentration dependence of respiration inhibition up to  $10 \times 10^{-4} \text{ mol dm}^{-3} \text{ H}_2\text{O}_2$  concentration.

Effect of different pollutant load exposure is shown on the example SMX solution treated by 0.6 kGy absorbed dose (Fig. 33). Samples for this experiment were prepared by dilution with purified water to COD values of 5, 10, 15, 20 and 25  $\text{mg dm}^{-3}$ . Pollutant concentration dependence of respiration inhibition clearly revealed growing toxic effect as a function of exposure to higher pollutant amounts. Inhibition was 5% when activated sludge was exposed to  $\text{COD} = 5 \text{ mg dm}^{-3}$  concentration of SMX solution treated by 0.6 kGy. This value increased to 35% in case of using  $25 \text{ mg dm}^{-3}$  concentration. Such difference in inhibitory effects in this narrow range of dilution ( $5 - 25 \text{ mg dm}^{-3}$ ) highlights a strong impact of mineralization caused pollutant dilution in toxicity screening (Fig. 33).



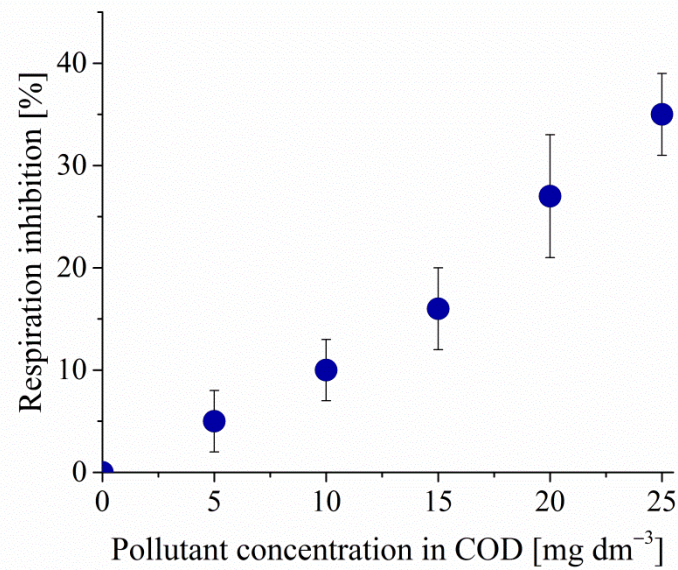


**Fig. 33.** Pollutant concentration dependence of inhibitory effects in respiration inhibition experiments in SMX solutions treated by 0.6 kGy.

Respiration inhibition experiments performed on SMX solutions following removal of H<sub>2</sub>O<sub>2</sub> and setting the concentration to COD = 10 mg dm<sup>-3</sup> (biological approach) showed significant differences as compared to samples applied without any modification (technological approach) (Fig. 34). The initial solution did not cause inhibitory effects; notably increased oxygen consumption was observed (-241% respiration inhibition). This finding indicates the presence of adapted microorganisms that are able to utilize SMX as substrate. This is in accordance with the results observed in evaluation of biodegradation (section 6.7.2).

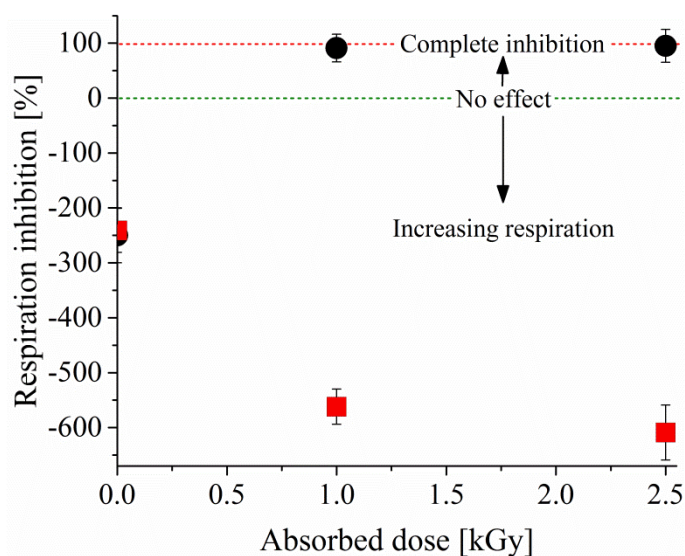


**Fig. 34.** Activated sludge respiration inhibition experiments performed by technological (●) or biological (■) approaches using SMX solutions.

In experiments conducted by the technological approach, inhibition of respiration was measured by increasing the absorbed dose. Values as high as 91% and 95% were detected at 1 kGy and 2.5 kGy, respectively. In contrast, measurements done by the biological approach showed increased oxygen uptake rate and thus increased availability of SMX radiolytic products to activated sludge. Respiration inhibition was  $-562\%$  and  $-609\%$  at 1 kGy and 2.5 kGy, respectively. Differences seen between the two approaches are stemming from the previously demonstrated toxic effects of  $\text{H}_2\text{O}_2$  formed during the irradiation procedure (Fig. 32) and the pollutant concentration dependence of activated sludge responses (Fig. 33).

### *Respiration inhibition of sulfonamides*

To avoid the interferences detailed in the previous subsection,  $\text{H}_2\text{O}_2$  was removed and the pollutant concentration was set to equal quantity prior to respiration inhibition tests. The pollutant concentration of all solutions tested were set to  $\text{COD} = 10 \text{ mg dm}^{-3}$ . Since no inhibitory effects were observed in respiration inhibition measurements, the result are presented in oxygen uptake rates (OUR) in order to get a clearer summarizing figure and to make the interpretation easier.

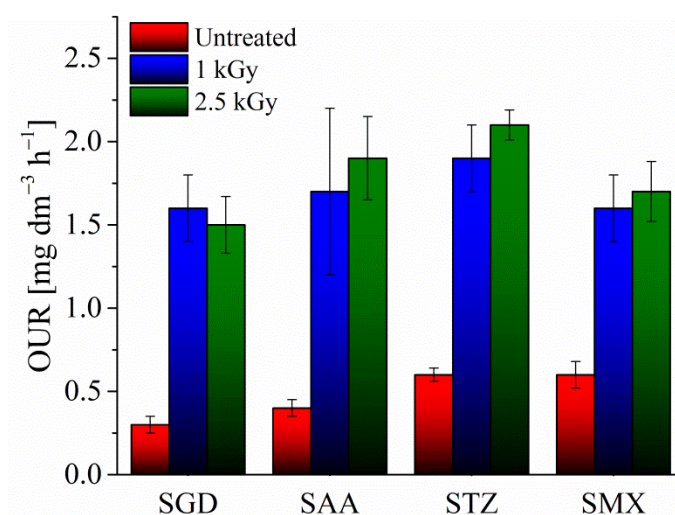


**Fig. 35.** Oxygen uptake rates calculated in activated sludge respiration inhibition experiments performed by using STZ, SAA, SGD and SMX solutions. Data were depicted following subtraction of the blank value ( $0.3 \text{ mg dm}^{-3} \text{ h}^{-1}$ ).

The OUR of the blank sample was  $0.3 \text{ mg dm}^{-3} \text{ h}^{-1}$  that notably increased in presence of untreated sulfonamide antibiotics. Initial SAA and SGD solutions showed  $0.6$  and  $0.7 \text{ mg dm}^{-3} \text{ h}^{-1}$  OUR, respectively, while  $0.9 \text{ mg dm}^{-3} \text{ h}^{-1}$  was obtained for both SMX and STZ (Fig. 35). This increment indicates that the molecules tested did not affect adversely

the metabolic activity of activated sludge. On the other hand, OUR values significantly higher than those for the blank also evidence presence of microorganisms that are able to utilize sulfonamides as nutrient source in their metabolic processes.

Although the biodegradation of test solutions in activated sludge respiration inhibition test is in agreement with the findings of biodegradation assessment displayed previously in section 6.7.2, the extent of OUR on a such time scale (180 minutes) is notably higher than expected. This may imply other processes taking place simultaneously with interactions of activated sludge with the samples. To get results that provide more obvious evidences, respiration inhibition tests were repeated with application of  $9.3 \text{ cm}^3$  activated sludge ( $180 \text{ mg COD in } 300 \text{ cm}^3$ ) on the example of SMX. The outcome of these experiments showed that OUR in test solutions containing SMX and growth substrate were significantly higher than the sum of OUR in any other possible processes that contributes to oxygen consumption (Fig. 36). This shows cooxidation/cometabolism in test mixtures. In these processes, the biological oxidation is dependent on the obligate presence of a growth substrate or a transformable substance [202]. In  $\text{BOD}_5$  measurements, only traces of organic residues were unintentionally added to the test mixtures during inoculation, while sufficient amount of readily biodegradable substrate (sodium acetate) was supplied in respiration inhibition tests. This is the reason why cooxidation/cometabolism took place only in course of respiration inhibition tests, which ultimately led to significantly higher consumption of oxygen.

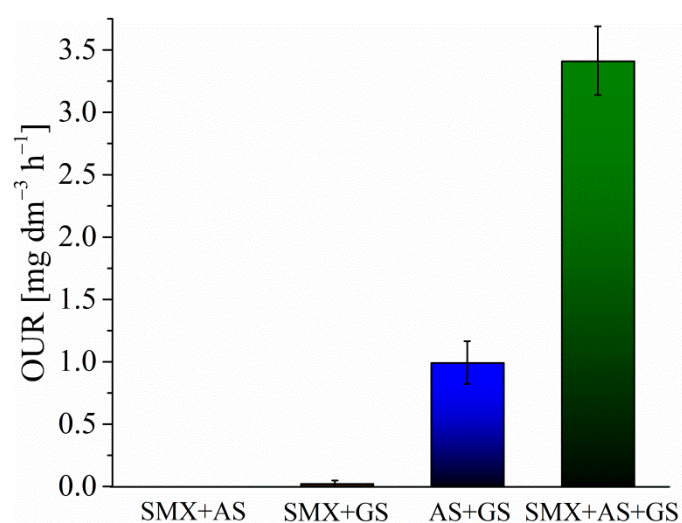


**Fig. 36.** Oxygen uptake rates of test mixtures containing activated sludge (AS), growth substrate (GS) and SMX ( $10^{-4} \text{ mol dm}^{-3}$ ). Endogenous oxygen uptake rate ( $0.82 \text{ mg dm}^{-3} \text{ h}^{-1}$ ) was subtracted from the results.

Similarly to experiments done on untreated samples, no toxic effects of oxidation products was seen. The OUR of all treated samples was higher than the OUR of the blank test mixture. The OUR of sulfonamides irradiated by 1 kGy were in the 1.9 – 2.2 mg dm<sup>-3</sup> h<sup>-1</sup> range (Fig. 35). Practically the same results were obtained (1.8 – 2.4 mg dm<sup>-3</sup> h<sup>-1</sup>) when 2.5 kGy absorbed dose was applied (Fig. 35). Treated samples resulted in significantly higher values as compared to tests conducted on initial solutions, referring to intensive metabolic activity, and thus a high degree of radiolytic degradation product utilization. However, difference between OUR in samples irradiated with 1 kGy or 2.5 kGy is considered to be statistically not significant. This character is different from the one observed in evaluation of ecotoxicity, since the effects of distinctive product groups formed at 1 kGy and 2.5 kGy firmly separated in the vast majority of those experiments (Fig. 29, 30 and 31). Increased OUR on such short time-scale shows appearance of rapidly biodegradable products, not just the absence of notable inhibitory effects. This is not surprising in case of samples treated by 2.5 kGy, since formation of readily biodegradable substances was evidenced in biodegradation experiments (section 6.7.2) and the literature provides data on appearance of readily biodegradable substances, as well [141, 146]. However, similarly high OUR values seen in solutions treated by 1 kGy was not expected as the biodegradation experiments showed notably lower biodegradability in these samples (section 6.7.2), as compared to the ones measured at 2.5 kGy. Such high OUR at this dose is probably due to cooxidation/cometabolism that was previously illustrated on the example of untreated SMX solution.

## 6.9 Antibacterial activity

Antibacterial activity of the most frequently used sulfonamide antibiotic (SMX) was investigated in broth microdilution and agar diffusion assays. As SMX is most commonly applied together with trimethoprim (TMP), the combined impact of these substances was also determined by mixing the active agents and by using a pharmaceutical preparation Sumetrolim (SUM). Prior to antibacterial activity testing, the effects of H<sub>2</sub>O<sub>2</sub> forming during ionizing radiation treatment were assessed on the bacterial growth. Results demonstrated no impact up to 3 × 10<sup>-4</sup> mol dm<sup>-3</sup> H<sub>2</sub>O<sub>2</sub> concentrations formed under conditions used (Fig. 21/A). This is in agreement with the literature that indicates negligible impact of even higher H<sub>2</sub>O<sub>2</sub> amounts [65]. Therefore, H<sub>2</sub>O<sub>2</sub> was not removed from the solutions used in antibacterial activity testing.

Exposure of *Staphylococcus aureus*, *Pseudomonas aeruginosa* or *Escherichia coli* to SMX solutions did not lead to formation of inhibition zones in agar diffusion experiments even when investigating untreated samples that contained SMX in  $5 \times 10^{-4} \text{ mol dm}^{-3}$  concentration (Fig. 37). Such outcome implies resistance to antibacterial action of SMX in amounts used. Simultaneous presence of SMX and TMP resulted in a more than twofold increase in *S. aureus* inhibition zone diameter (19 mm), compared to application of TMP itself (8 mm). Such behavior demonstrates synergistic antibacterial activity of SMX and TMP even when SMX is present in concentration that causes practically no detectable impact. Nevertheless, inhibition zones reduced by increasing absorbed doses, but absence of antibacterial activity was evidenced only in samples treated with 10 kGy. The outcome of experiments involving SMX+TMP or SUM was similar, notable differences were not observed.

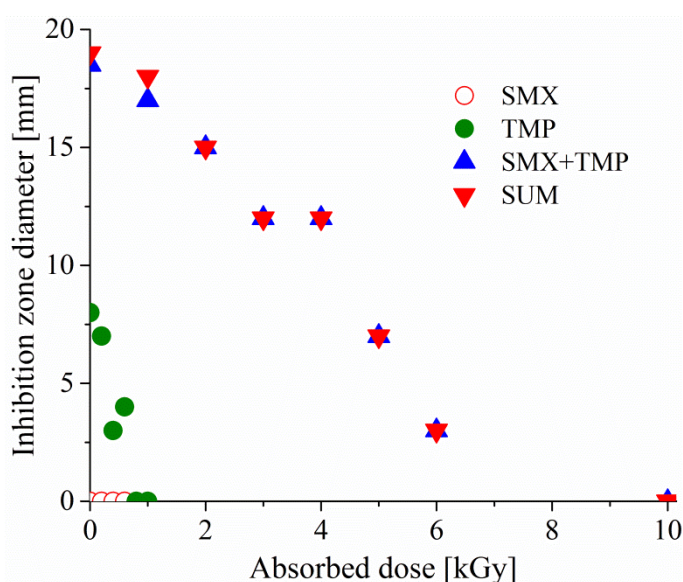


**Fig. 37.** Agar diffusion assay for testing SMX, TMP, SMX+TMP and SUM antibacterial activity against *Staphylococcus aureus* at different stages of radiolytic decomposition.

Results obtained in broth microdilution assays (Fig. 38) were similar to those in agar diffusion experiments. In both experiments, bacterial growth was observed in all SMX solutions. Therefore, both methods indicate notable resistance of *S. aureus* to SMX. Adamek et al. [203] reported similar results, as the most of test microorganisms used in their study did not exhibit any susceptibility against SMX at concentrations of  $\leq 0.5 \mu\text{mol dm}^{-3}$ . However, the reproductive capacity was somewhat hindered as indicated by the stationary phases leveling off at different values. Such growth curves are shown on the example of *S. aureus* in Fig. 38/A. The slopes of the bacterial growth curves obtained by

using the initial sample or the samples treated with 1 or 2 kGy were not as steep as the ones measured in solutions treated with higher doses. The differences between the *S. aureus* bacterial growth in solutions irradiated with doses  $\geq 3$  kGy were negligible. All these evidence low antibacterial activity that only slightly inhibits the bacterial growth up to 2 kGy. (This low antibacterial activity was not detectable by agar diffusion test.) Based on the broth microdilution experiments performed on SMX dilution series, the minimum inhibitory concentration (MIC) of SMX towards *S. aureus* bacteria was found to be around  $32 \mu\text{mol dm}^{-3}$  (Fig. 38/B). This MIC value is in a good agreement with the active agent concentrations measured in the irradiated solution, since the inhibitory effects completely disappear following the reduction of SMX below MIC at  $> 2$  kGy. Experiments also revealed a possible chronic toxicity of solutions irradiated with 8 or 10 kGy. The growth curves in these samples declined after reaching the stationary phase (Fig. 38/A). Similar antibacterial behavior of irradiated SMX solutions was seen when using *P. aeruginosa* or *E. coli* test organism. Difference was observed only in the sensitivity. The MIC was  $\sim 4$  and  $\sim 16 \mu\text{mol dm}^{-3}$  in case of *P. aeruginosa* and *E. coli*, respectively.

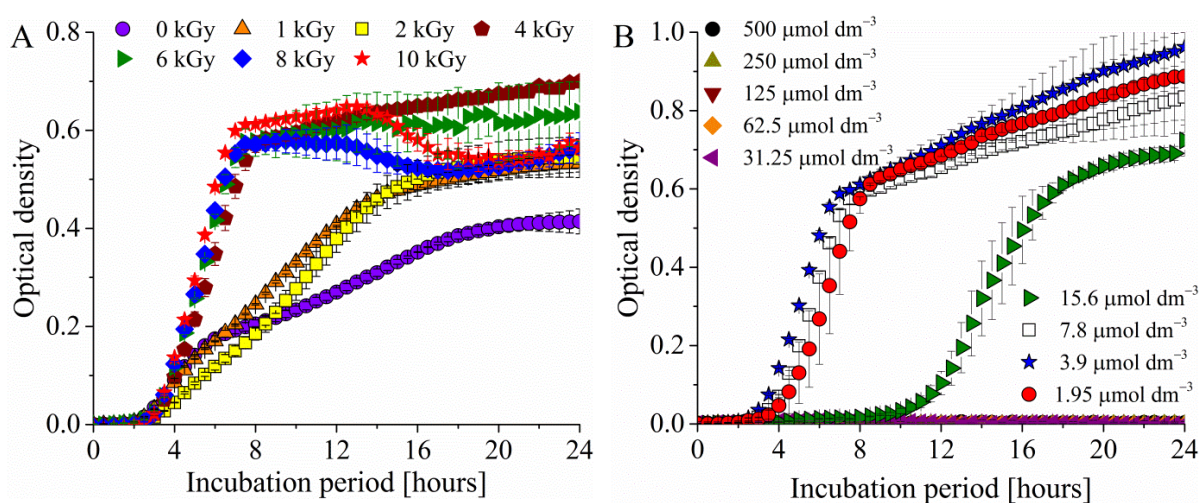


**Fig. 38.** Broth microdilution assays carried out for testing the antibacterial activity of irradiated  $5 \times 10^{-4} \text{ mol dm}^{-3}$  SMX solutions (A) and SMX dilution series (B) against *Staphylococcus aureus*.

Both analytical techniques used for antibacterial activity testing evidenced the well-known synergistic effects of SMX and TMP in SMX+TMP and SUM solutions. Growth of bacterial strains was seen only at 10 kGy absorbed doses (Fig. 39). Results presented on the example of *S. aureus* bacteria are well illustrating the changes in antibacterial activity seen in case of *P. aeruginosa* and *E. coli* exposed to SUM or SMX+TMP.

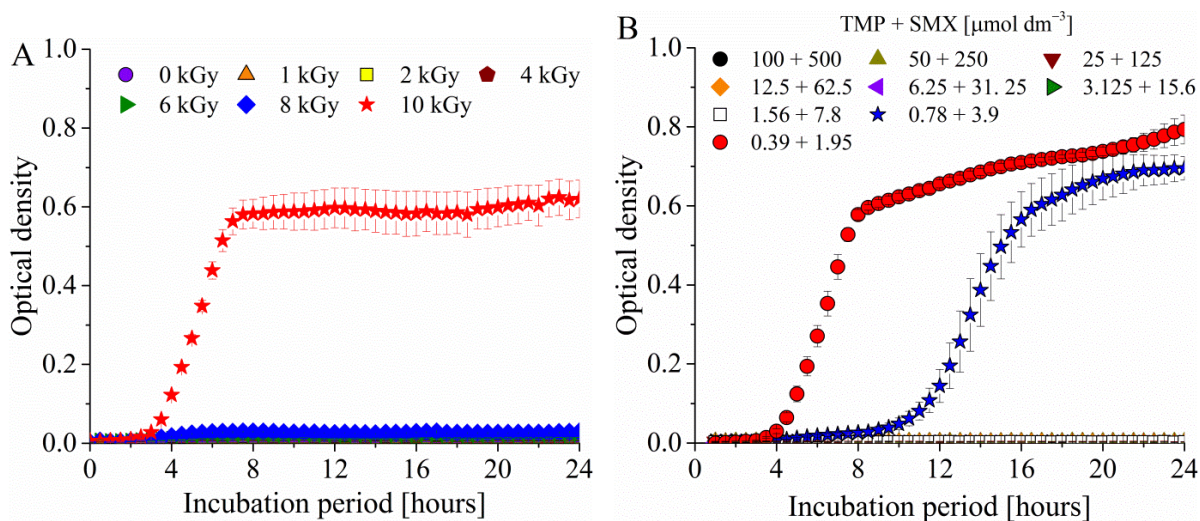


**Fig. 39.** Broth microdilution assay carried out for testing antibacterial activity of SMX+TMP against *Staphylococcus aureus* at different stages of radiolytic decomposition (A) and in dilution series of the initial sample (B).

Generally, ionizing radiation treatment induced reduction of antibacterial activities against all test organisms. However, practically complete elimination of initial antibiotics (> 98%) was required to terminate the biological activity. Results suggest that radiolytic products do not possess antibacterial activity, as the inhibitory effects were removed parallel with the initial molecules. It should be noted that antibiotics showing biological activity below the limit of detection may also pose environmental threat, if synergistically acting pharmaceutical agents are also present. All these suggest necessity of complete antibiotic removal from wastewater in order to reduce the risk of antibacterial resistance development to the background level.

## 7 Summary

---

The variety of analytical techniques employed enabled a comprehensive insight into the radiation-induced degradation mechanism of aerated dilute aqueous solutions of sulfonamide antibiotics.

The initial steps of the degradation were investigated through transient intermediate kinetics, using pulse radiolysis technique. Absorption spectra of transient intermediates detected at 10  $\mu$ s following the pulse in  $N_2O$ -saturated sulfonamide solutions – when OH radicals are the main reactive species – peaked in the 365 – 410 nm wavelength range. The measured values are consistent with the ones published. When the  $\cdot OH$  was removed from the solution by *t*-BuOH radical scavenger, the absorbance belonging to the OH adduct disappeared from the spectra. The similarities in the absorption spectra and their intensities suggest that the preferred target of the  $\cdot OH$  in case of all molecules is the benzene ring. The result of  $\cdot OH$  addition to the aromatic ring is formation of hydroxy-cyclohexadienyl radicals. When the irradiation was performed under aerated conditions, hydroxy-cyclohexadienyl radicals transformed to peroxy radicals in reactions with dissolved  $O_2$ . Peroxy radicals may transform to hydroxylated molecules by  $HO_2\cdot$  elimination or they undergo ring opening to aliphatic compounds. The reaction rate constants of  $\cdot OH$  reactions with sulfonamides ( $k_{OH}$ ) were evaluated by the time dependence of the absorbance build-up, measuring the pseudo-first-order rate constants in the  $2 \times 10^{-5} - 1 \times 10^{-4} \text{ mol dm}^{-3}$  concentration range. The slope of the pseudo-first-order rate constant values plotted in the function of sulfonamide concentration provides the second-order rate constant. These were generally in the  $4.5 - 9.5 \times 10^9 \text{ mol}^{-1} \text{ dm}^3 \text{ s}^{-1}$  range that is consistent with the literature values. The  $k_{OH}$  observed in sulfonamide solutions are close to the theoretical maximum, the diffusion controlled rate constant ( $1.1 \times 10^{10} \text{ mol}^{-1} \text{ dm}^3 \text{ s}^{-1}$ ). Such high  $k_{OH}$  values are typical for benzene type molecules. The rate constants with the free pyrimidine ( $1.6 \times 10^8 \text{ mol}^{-1} \text{ dm}^3 \text{ s}^{-1}$ ) and the isoxazole rings ( $3.5 \times 10^9 \text{ mol}^{-1} \text{ dm}^3 \text{ s}^{-1}$ ) are lower. The reaction rate constants determined – and the ones found in the literature – support the mechanism suggested by the absorption spectra, in which the  $\cdot OH$  attack mainly occurs on the benzene ring.

Stable organic products formed, in course of irradiation of  $1 \times 10^{-4} \text{ mol dm}^{-3}$  concentration solutions, were identified by LC-MS/MS. At the early stages of the decomposition process,



all products detected in high concentrations were hydroxylated derivatives, as foreshadowed by the results of pulse radiolysis experiments. In addition to formation of monohydroxylated products, double hydroxylation also took place in most cases, albeit with low yields. Products other than hydroxylated ones appeared in remarkably lower relative abundance, in approximately 5–10 times lower amounts. Concentration of hydroxylated products peaked at around 0.6 kGy, but these products quickly disappeared by increasing the absorbed dose to 1 kGy. Since the product – dose curve was just slightly shifted to higher dose, as compared to that of the starting molecule – decay curves, it is suggested that  $\cdot\text{OH}$  shows similar reactivity with the products as with the starting molecules. The final products of hydroxyl radical reactions with organic compounds are substances like aldehydes, alcohols, ketones and carboxylic acids. These compounds with low molecular mass are usually the last step prior to complete mineralization. Identification of these products was not possible by LC-MS/MS. However, the strong decrease of the initial 4.9–5.9 pH seen in all sulfonamide solutions refers to appearance of acids in high concentration. The slope of the pH – dose dependence was very steep up to 1.5 kGy, in the phase where the ring disintegration was the most intense. Following the disappearance of the initial molecules at around 2.5 kGy, the pH levelled off at constant values in the range of pH = 3.6–3.8. Formation of oxamic-, maleic-, acetic-, formic-, pyruvic- and oxalic acids toward the end of mineralization was reported in the literature.

Ion chromatography evidenced that generally 5–20% of the initial nitrogen content transforms to  $\text{NO}_3^-$ . Steeper slopes of  $\text{NO}_3^-$  formation curves above 1 kGy suggest that  $\text{NO}_3^-$  formation mainly occurs after the aromatic rings have been destructed to smaller fragments. The kinetics of  $\text{NH}_4^+$  formation was completely different from the  $\text{NO}_3^-$  production. The  $\text{NH}_4^+$  concentration increased in the function of absorbed dose and leveled off at 2.5 kGy. However, the increase of the  $\text{NH}_4^+$  formation rate was slower than that of the degradation of the starting sulfonamide molecules. This implies a complex  $\text{NH}_4^+$  formation process taking place through several internal steps.  $\text{NO}_2^-$  was not detected. Following the quantification of  $\text{NH}_4^+$ ,  $\text{NO}_3^-$  and  $\text{NO}_2^-$  ion concentrations, a mass balance for nitrogen was made. The loss of nitrogen, estimated from the decrease of TN upon irradiation, was also taken into account. By considering these constituents, a perfect mass-balance was obtained only for sulfanilamide, while all other compounds showed 10–30% deficit. These results refer to incomplete mineralization of inter-chain nitrogen. The residue is probably in form of simple nitrogen containing organic acids. Formation of  $\text{SO}_4^{2-}$  and

$\text{SO}_3^{2-}$  were monitored, as well. Linear dose dependence of  $\text{SO}_4^{2-}$  formation was measured up to 2.5 kGy absorbed dose. In most solutions,  $\text{SO}_4^{2-}$  concentration ranged from 6.2 to 8.8  $\text{mg dm}^{-3}$  at this dose. Higher amount (11.8  $\text{mg dm}^{-3}$ ) was detected only in sulfathiazole sample that is due to the two sulfur atoms in its chemical structure. By prolonged irradiation, no notable  $\text{SO}_4^{2-}$  formation was observed, the curves generally levelled off at constant values. These amounts are in a good agreement with the theoretical amounts of sulfur present in the solutions. Correspondingly,  $\text{SO}_3^{2-}$  was not present in measurable quantities. The changes in total sulfur content were followed up by ICP-MS measurements. These measurements demonstrated that the sulfur content is practically not changing during irradiation. Similar results were reported in case of SMZ and SDZ solutions.

Possible general pathways of radiolytic degradation were proposed on the basis of the results presented and also using some literature data (Fig. 40). Degradation of sulfonamide antibiotics, starting from the hydroxylation of the intact molecules and going through many intermediate products, finally ends up with inorganic species. The number of O atoms building into products ( $\sim 1.5$ ) upon single  $\cdot\text{OH}$  attack, strong decrease of pH and appearance of fragmented low molecular mass organic acids at low doses ( $< 1$  kGy) show that phenol formation, ring opening and fragmentation occur simultaneously. Due to the aromatic structure, the rate constants in  $\cdot\text{OH}$  reaction with mono- and double hydroxylated products are similar to the rate constants of  $\cdot\text{OH}$  reactions with initial molecules. Nevertheless, all rings undergo oxidative degradation up to  $\sim 1$  kGy absorbed dose. Phenols disappeared from the solution not much after the decay of the starting sulfonamide molecules. Based on COD, TOC, TN and pH measurements, mineralization is a multistep processes. The molecules are first step-by-step oxidized and ultimately mineralized. The idea of first hydroxylation and then gradual degradation to smaller fragments is in agreement with the faster decrease of COD than TOC up to 2.5 kGy. Although, qualitatively many details are understood, much work is still needed on the quantification, qualitative determination of the intermediate products with low yields and on improving the material balances.

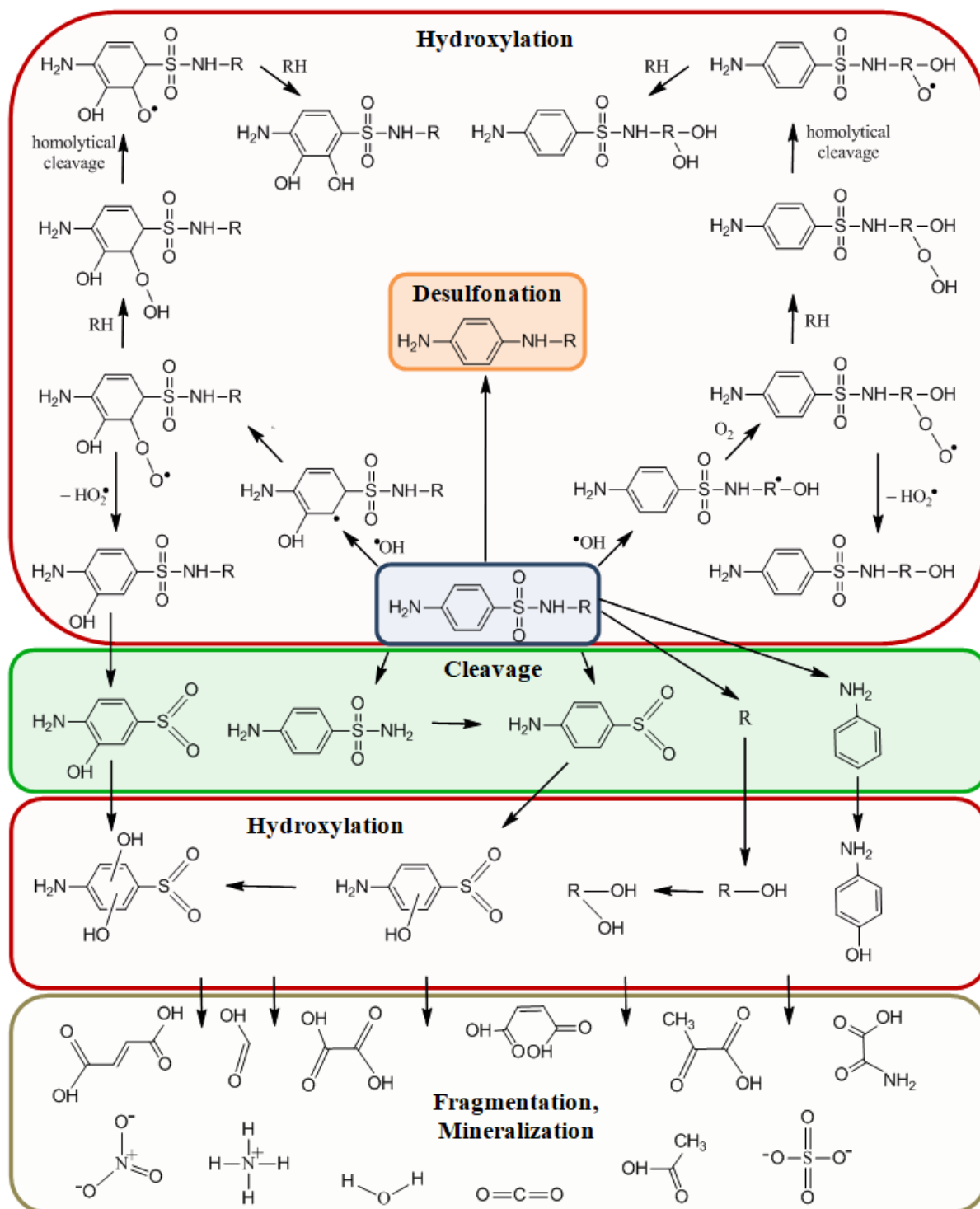


**Fig. 40.** Possible degradation pathways of sulfonamide antibiotics in course of ionizing radiation treatment.

To investigate the biodegradability of sulfonamide transformation products in natural water bodies and in the biological step of wastewater purification,  $BOD_5$  was determined by inoculation with both river water and activated sludge, respectively. The biodegradability was expressed in form of  $BOD_5 COD^{-1}$  ratio. Toxicity was investigated on most commonly applied test organisms (*Vibrio fischeri*, *Pseudokirchneriella subcapitata* and *Daphnia*

*magna*). Factors strongly influencing the BOD<sub>5</sub> or toxicity experiments were evaluated before measuring and discussing the biodegradation of target molecules. These factors are the pollutant concentration dilution – taking place along the treatment process due to mineralization – and the presence of H<sub>2</sub>O<sub>2</sub> formed in radical reactions.

Results evidenced that pollutant dilution caused by mineralization and the effects of H<sub>2</sub>O<sub>2</sub> have to be considered in evaluation and comparison of products, product groups and the starting molecules in biological experiments. To obtain reliable data in ecotoxicity assay, the H<sub>2</sub>O<sub>2</sub> concentrations should be reduced to at least  $0.5 \times 10^{-4} \text{ mol dm}^{-3}$  in *V. fischeri* and *P. subcapitata* experiments, while, practically complete removal is needed in case of *D. magna*. In BOD measurements performed by manometric techniques, reducing the H<sub>2</sub>O<sub>2</sub> concentration to at least  $0.5 \times 10^{-4} \text{ mol dm}^{-3}$  is needed. In both studies, using equal pollutant loads is also recommended to obtain comparable results. Anyway, ionizing radiation treatment resulted in transformation of non-biodegradable sulfonamides (BOD<sub>5</sub> COD<sup>-1</sup> < 0.2) to substances biodegradable by both river water and activated sludge (BOD<sub>5</sub> COD<sup>-1</sup> = 0.6 – 0.8). Ready biodegradability takes place only when both hydroxylated derivatives and initial molecules are removed. Toxicity assay was conducted on a battery of experiments using test organisms from three trophic levels. Toxicity tests on individual organisms showed a diverse picture. In some cases, toxicity reduced with increasing the absorbed dose, but temporary increase in toxic potential as a function of absorbed dose was also measured.

Broth microdilution and agar diffusion antibacterial susceptibility assays showed that strong synergism of sulfamethoxazole and trimethoprim effects occurred even when the antibacterial activities of both molecules were below the limit of detection. In this way, trace amounts of sulfamethoxazole or trimethoprim exert selective pressure on environmental bacterial species particularly in case of their joint presence. Practically complete elimination of initial antibiotics (>98%) was required to terminate the antibacterial activity. Strong correlation of antibacterial activity removal and the parent compound decomposition suggests formation of radiolytic products with no antibacterial potency.

## 8 Theses

---

1. The presence of dissolved O<sub>2</sub> increases the degradation efficiency of sulfonamide antibiotics during ionizing radiation treatment in dilute aqueous solution. The reaction between the substrate and the <sup>•</sup>OH has the highest contribution to this degradation.

*(Publications 3 and 4)*

2. The preferred target of the <sup>•</sup>OH attack on sulfonamides is the benzene ring. Addition of <sup>•</sup>OH to the aromatic ring leads to formation of hydroxy-cyclohexadienyl type radicals. The reaction rate constants were found to be in the  $4.5 \times 10^9 - 9.5 \times 10^9 \text{ mol}^{-1} \text{ dm}^3 \text{ s}^{-1}$  range.

*(Publication 3)*

3. The main radiolytic degradation processes are hydroxylation, desulfonation and ring cleavage. At early stages of oxidation, formation of hydroxylated products is predominant (< 0.8 kGy), while formation of acidic organic molecules and inorganic species are suggested following the ring cleavage (>1 kGy).

*(Publications 3 and 4)*

4. Gamma irradiation of persistent sulfonamide antibiotics results in transformation to substances readily biodegradable by both river water and activated sludge. Higher level of oxidation is needed to reach the same biodegradability in river water, as in activated sludge.

*(Publication 2)*

5. Increasing the absorbed dose during the irradiation of sulfonamide solutions generally leads to gradual disappearance of toxicity. However, some of the early products were more harmful to test organisms than the initial molecules.

*(Publications 2, 3 and 4)*

6. Trace amounts of sulfamethoxazole pose environmental threat regarding antibiotic resistance development by exerting selective pressure on environmental bacterial species particularly in case of their joint presence with trimethoprim. Ionizing radiation treatment is suitable for removal of this antibacterial activity and it leads to formation of products with no antibacterial activity.

7. Concentrations of toxic  $\text{H}_2\text{O}_2$  forming during ionizing radiation treatment should be reduced to at least  $0.5 \times 10^{-4} \text{ mol dm}^{-3}$  in *V. fischeri*, *P. subcapitata* and BOD experiments to minimize its effects. *D. magna* is more susceptible and requires practically complete elimination of  $\text{H}_2\text{O}_2$ .

*(Publication 1)*

8. Setting the pollutant concentration to equal values is necessary in biological studies targeting comparison of different products or product groups. Mineralization reduces pollutant concentration as a function of the absorbed dose and results in „dilution series”. Otherwise, the properties of product groups formed at different absorbed doses are not accurately comparable because the test organisms are exposed to decreasing pollutant concentration as the irradiation proceeds.

*(Publication 1)*

## 9 List of publications related to PhD thesis

---

1. Sági, G., Bezsényi, A., Kovács, K., Klátyik, S., Darvas, B., Székács, A., Wojnárovits, L., Takács, E., 2017. The impact of H<sub>2</sub>O<sub>2</sub> and the role of mineralization in biodegradation or ecotoxicity assessment of advanced oxidation processes. *Radiation Physics and Chemistry*, In Press. <https://doi.org/10.1016/j.radphyschem.2017.09.023>  
Impact factor: 1.315 (2016), Citations: 0
2. Sági, G., Kovács, K., Bezsényi, A., Csay, T., Takács, E., Wojnárovits, L., 2016. Enhancing the biological degradability of sulfamethoxazole by ionizing radiation treatment in aqueous solution. *Radiation Physics and Chemistry* 124, 179–183.  
Impact factor: 1.315, Citations: 9
3. Sági, G., Csay, T., Pátzay, G., Csonka, E., Takács, E., Wojnárovits, L., 2015. Analytical approaches to the OH radical induced degradation of sulfonamide antibiotics in dilute aqueous solutions. *Journal of Pharmaceutical and Biomedical Analysis* 106, 52–60.  
Impact factor: 3.169, Citations: 17
4. Sági, G., Csay, T., Pátzay, G., Csonka, E., Wojnárovits, L., Takács, E., 2014. Oxidative and reductive degradation of sulfamethoxazole in aqueous solutions: decomposition efficiency and toxicity assessment. *Journal of Radioanalytical and Nuclear Chemistry* 301, 475–482.  
Impact factor: 1.034, Citations: 14

## 10 List of other publications

---

1. Kovács, K., Sági, G., Takács, E., Wojnárovits, L., 2017. Use of bovine catalase and manganese dioxide for elimination of hydrogen peroxide from partly oxidized aqueous solutions of aromatic molecules – Unexpected complications. *Radiation Physics and Chemistry* 139, 147–151.  
Impact factor: 1.315 (2016), Citations: 0
2. Illés, E., Tegze, A., Kovács, K., Sági, G., Pap, Z., Takács, E., Wojnárovits, L., 2017. Hydrogen peroxide formation during radiolysis of aerated aqueous solutions of organic molecules. *Radiation Physics and Chemistry* 134, 8–13.  
Impact factor: 1.315 (2016), Citations: 0
3. Szabados, E., Sági, G., Somodi, F., Maróti, B., Srankó, D., Tungler, A., 2017. Wet air oxidation of paracetamol over precious metal/Ti mesh monolith catalyst. *Journal of Industrial and Engineering Chemistry* 46, 364–372.  
Impact factor: 4.421 (2016), Citations: 0
4. Szabados, E., Sági, G., Kovács, A., Takács, E., Wojnárovits, L., Tungler, A., 2015. Comparison of catalysis and high energy irradiation for the intensification of wet oxidation as process wastewater pretreatment. *Reaction Kinetics, Mechanisms and Catalysis* 116, 95–103.  
Impact factor: 1.265, Citations: 1

## 11 Acknowledgement

---

At first and foremost, I would like to express a deep sense of gratitude to my supervisors Prof. Erzsébet Takács and Prof. Zoltán Homonnay for guidance and support that helped me in carrying out the present work. The same tribute is entitled to Prof. László Wojnárovits and Dr. Tamás Csay for the helpful and constructive discussions and lectures.

My special thanks go to the members of the Radiation Chemistry Department I have worked with: Dr. Krisztina Kovács, Dr. László Szabó, Gergely Rácz, Dr. Renáta Homlok, Katalin Gonter and Éva Koczog. They contributed greatly to solving problems and tasks, which I was facing. I owe particular thanks to Zoltán Papp (Institute of Isotopes Co. Ltd, Budapest, Hungary), who was always a flexible and reliable partner in performing  $\gamma$ -irradiation.

I also owe thanks to Prof. Csilla Mohácsi-Farkas and Károly Szabacsi (Department of Microbiology and Biotechnology, Szent István University of Budapest, Hungary) for introducing me into the practice of microbiological assays. I am grateful to Éva Kovács Széles, Kornél Fél (Nuclear Security Department of the Hungarian Academy of Sciences Centre for Energy Research, Budapest, Hungary), György Pátzay and Emil Csonka (Department of Chemical and Environmental Process, Budapest University of Technology and Economics, Budapest, Hungary) for the opportunity to get an insight into ICP-MS and ion chromatography. I would also like to thank Szandra Klátyik, Béla Darvas and András Székács (Agro-Environmental Research Institute, National Research and Innovation Centre, Budapest, Hungary) for introducing me into the practice of ecotoxicity screening.

I owe a special debt of gratitude to Anikó Bezsenyi (Budapest Sewage Works Pte Ltd., South-Pest Wastewater Treatment Plant, Budapest, Hungary) for her kind help in experiments involving activated sludge and for the fruitful discussions regarding biological wastewater treatment technology.

Last but not least, my greatest debt is owed to my parents, my sister and my wife. I am grateful for their devotion and sacrifices.



## 12 References

---

- [1] Brunton, L., Chabner, B., Knollman, B., 2011. Goodman & Gilman's the pharmacological basis of therapeutics, 12<sup>th</sup> edition. McGraw-Hill Inc.
- [2] Baran, W., Adamek, E., Ziemanska, J., Sobczak, A., 2011. *J. Hazard. Mater.* 196, 1–15.
- [3] Bendz, D., Paxéus, N. A., Ginn, T. R., Loge, F. J., 2005. *J. Hazard. Mater.* 122, 195–204.
- [4] Göbel, A., Thomsen, A., McArdell, C. S., Joss, A., Giger, W., 2005. *Environ. Sci. Technol.* 39, 3981–3989.
- [5] Spongberg, A. L., Witter, J. D., 2008. *Sci. Total Environ.* 397, 148–157.
- [6] Porter, R. S., 2011. The Merck manual of diagnosis and therapy. Merck Sharp & Dohme Corp., Whitehouse Station.
- [7] Finberg, R. W., Guharoy R., 2012. Clinical use of anti-infective agents: A guide on how to prescribe drugs used to treat infections. Springer, New York.
- [8] The state of world fisheries and aquaculture: Opportunities and challenges, 2014. Food and Agriculture Organization of the United Nations, Rome.
- [9] Animal Health Institute industry statistics, 2014. URL: <http://www.ahi.org/about-animal-medicines/industry-statistics/>. Last accessed: 03.07.2017.
- [10] The use of drugs in food animals: Benefits and risks, 1999. National Research Council Committee on Drug Use in Food Animals. National Academy Press, Washington, D. C.
- [11] Evaluation of the EU Legislative Framework in the Field of Medicated Feed, Final Report, 2010. European Commission, Brussels.
- [12] Monitoring antimicrobial usage in food animals for the protection of human health, 2002. World Health Organization, Oslo.
- [13] Sarmah, A. K., Meyer, M. T., Boxall, A. B., 2006. *Chemosphere* 65, 725–759.
- [14] Choi, K.-J., Kim, S.-G., Kim, C.-W., Kim, S. H., 2007. *Chemosphere* 66, 977–984.
- [15] Zou, S., Xu, W., Zhang, R., Tang, J., Chen, Y., Zhang, G., 2011. *Environ. Pollut.* 159, 2913–2920.
- [16] Luo, Y., Xu, L., Rysz, M., Wang, Y., Zhang, H., Alvarez, P. J. J., 2011. *Environ. Sci. Technol.* 45, 1827–1833.
- [17] Wei, R., Ge, F., Huang, S., Chen, M., Wang, R., 2011. *Chemosphere* 82, 1408–1414.
- [18] Burkholder, J., Libra, B., Weyer, P., Heathcote, S., Kolpin, D., Thorne, P. S., Wichman, M., 2007. *Environ. Health Perspect.* 115, 308–312.
- [19] Watanabe, N., Bergamaschi, B. A., Loftin, K. A., Meyer, M. T., Harter, T., 2010. *Environ. Sci. Technol.* 44, 6591–6600.
- [20] Batt, A. L., Snow, D. D., Aga, D. S., 2006. *Chemosphere* 64, 1963–1971.
- [21] Barnes, K. K., Kolpin, D. W., Furlong, E. T., Zaugg, S. D., Meyer, M. T., Barber, L. B., 2008. *Sci. Total Environ.* 402, 192–200.
- [22] Teijon, G., Candela, L., Tamoh, K., Molina-Díaz, A., Fernández-Alba, A. R., 2010. *Sci. Total Environ.* 408, 3584–3595.
- [23] Fram, M. S., Belitz, K., 2011. *Sci. Total Environ.* 409, 3409–3417.
- [24] Schaidler, L. A., Rudel, R. A., Ackerman, J. M., Dunagan, S. C., Green Brody, J., 2014. *Sci. Total Environ.* 468–469, 384–393.

- [25] Zhang, R., Tang, J., Li, J., Cheng, Z., Chaemfa, C., Liu, D., Zheng, Q., Song, M., Luo, C., Zhang, G., 2013. *Sci. Total Environ.* 450–451, 197–204.
- [26] Zhang, R., Tang, J., Li, J., Zheng, Q., Liu, D., Chen, Y., Zou, Y., Chen, X., Luo, C., Zhang, G., 2013. *Environ. Pollut.* 174, 71–77.
- [27] D'Costa, V. M., King, C. E., Kalan, L., Morar, M., Sung, W. W. L., Schwarz, C., Froese, D., Zazula, G., Calmels, F., Debruyne, R., Golding, G. B., Poinar, H. N., Wright, G. D., 2011. *Nature* 477, 457–461.
- [28] Davies, J., Davies, D., 2010. *Microbiol. Mol. Biol. Rev.* 74, 417–433.
- [29] Gagné, F., Blaise, C., André, C., 2006. *Ecotoxicol. Environ. Saf.* 64, 329–336.
- [30] Crouse, B. A., Ghoshdastidar, A. J., Tong, A. Z., 2012. *Environ. Res.* 112, 92–99.
- [31] Tello, A., Austin, B., Telfer, T. C., 2012. *Environ. Health Perspect.* 120, 1100–1106.
- [32] Szczepanowski, R., Linke, B., Krahn, I., Gartemann, K.-H., Gützkow, T., Eichler, W., Pühler, A., Schlüter, A., 2009. *Microbiology* 155, 2306–2319.
- [33] Hagy, J. D., Boynton, W. R., Keefe, C. W., Wood, K. V., 2004. *Estuaries* 27, 634–658.
- [34] Tait, S., Clarke, W. P., Keller, J., Batstone, D. J., 2009. *Water Res.* 43, 762–772.
- [35] Kümmerer, K., 2008. Pharmaceuticals in the environment. Sources, fate, effects and risks. Springer, Heidelberg.
- [36] Souza, F. S., Féris, L. A., 2016. *Water Environ. Res.* 88, 871–877.
- [37] Brown, K. D., Kulis, J., Thomson, B., Chapman, T. H., Mawhinney, D. B., 2006. *Sci. Total Environ.* 366, 772–783.
- [38] Karthikeyan, K. G., Meyer, M. T., 2006. *Sci. Total Environ.* 361, 196–207.
- [39] Gao, L., Shi, Y., Li, W., Niu, H., Liu, J., Cai, Y., 2012. *Chemosphere* 86, 665–671.
- [40] Gracia-Lor, E., Sancho, J. V., Serrano, R., Hernández, F., 2012. *Chemosphere* 87, 453–462.
- [41] Guerra, P., Kim, M., Shah, A., Alaei, M., Smyth, S. A., 2014. *Sci. Total Environ.* 473–474, 235–243.
- [42] Alidina, M., Hoppe-Jones, C., Yoon, M., Hamadeh, A. F., Li, D., Drewes, J. E., 2014. *Sci. Total Environ.* 478, 152–162.
- [43] Kosma, C. I., Lambropoulou, D. A., Albanis, T. A., 2014. *Sci. Total Environ.* 466–467, 421–438.
- [44] Karigar, C. S., Rao, S. S., 2011. *Enzyme Res.* 2011, 1–11.
- [45] Guasch, H., Ginebreda, A., Geiszinger, A., 2012. The handbook of environmental chemistry. Emerging and priority pollutants in rivers. Springer, New York.
- [46] Lin, A. Y.-C., Yu, T.-H., Lateef, S. K., 2009. *J. Hazard. Mater.* 167, 1163–1169.
- [47] Sim, W.-J., Lee, J.-W., Oh, J.-E., 2010. *Environ. Pollut.* 158, 1938–1947.
- [48] Joss, A., Zabczynski, S., Göbel, A., Hoffmann, B., Löffler, D., McArdell, C. S., Ternes, T. A., Thomsen, A., Siegrist, H., 2006. *Water Res.* 40, 1686–1696.
- [49] Doelle, H. W., Rokem, S., Berovic, M., 2009. Biotechnology, Volume X. Eolss Publishers Co. Ltd., Oxford.
- [50] Hirsch, R., Ternes, T., Haberer, K., Kratz, K. L., 1999. *Sci. Total Environ.* 225, 109–118.
- [51] Batt, A. L., Bruce, I. B., Aga, D. S., 2006. *Environ. Pollut.* 142, 295–302.
- [52] Dickenson, E. R. V., Snyder, S. A., Sedlak, D. L., Drewes, J. E., 2011. *Water Res.* 45, 1199–1212.

- [53] Jelic, A., Gros, M., Ginebreda, A., Cespedes-Sánchez, R., Ventura, F., Petrovic, M., Barcelo, D., 2011. *Water Res.* 45, 1165–1176.
- [54] Heberer, T., 2002. *J. Hydrol.* 266, 175–189.
- [55] Benotti, M. J., Brownawel, B. J., 2007. *Environ. Sci. Technol.* 41, 5795–5802.
- [56] García-Galán, M. J., Díaz-Cruz, M. S., Barceló, D., 2010. *Talanta* 81, 355–366.
- [57] Blair, B. D., Crago, J. P., Hedman, C. J., Klaper, R. D., 2013. *Chemosphere* 93, 2116–2123.
- [58] Klosterhaus, S. L., Grace, R., Hamilton, M. C., Yee, D., 2013. *Environ. Int.* 54, 92–99.
- [59] Tewari, S., Jindal, R., Kho, Y. L., Eo, S., Choi, K., 2013. *Chemosphere* 91, 697–704.
- [60] Aydin, E., Talinli, I., 2013. *Chemosphere* 90, 2004–2012.
- [61] Andreozzi, R., Caprio, V., Insola, A., Marotta, R., 1999. *Catal. Today* 53, 51–59.
- [62] Ribeiro, A. R., Nunes, O. C., Pereira, M. F. R., Silva, A. M. T., 2015. *Environ. Int.* 75, 33–51.
- [63] Cesaro, A., Naddeo, V., Belgiorno V., 2013. *J. Bioremed. Biodeg.* 4.
- [64] Oller, I., Malato, S., Sánchez-Pérez, J. A., 2011. *Sci. Total Environ.* 409, 4141–4166.
- [65] Pérez-Moya, M., Graells, M., Castells, G., Amigó, J., Ortega, E., Buhigas, G., Pérez, L. M., Mansilla, H. D., 2010. *Water Res.* 44, 2533–2540.
- [66] Neafsey, K., Zeng, X., Lemley, A. T., 2010. *J. Agric. Food Chem.* 58, 1068–1076.
- [67] Huber, M. M., Canonica, S., Park, G.-Y., von Gunten, U., 2003. *Environ. Sci. Technol.* 37, 1016–1024.
- [68] Moreira, F. C., Soler, J., Alpendurada, M. F., Boaventura, R. A. R., Brillas, E. Vilar, V. J. P., 2016. *Water Res.* 105, 251–263.
- [69] Tokumura, M., Sugawara, A., Raknuzzaman, M., Habibullah-Al-Mamun, M., Masunaga, S., 2016. *Chemosphere* 159, 317–325.
- [70] Zhang, S., Gitungo, S., Axe, L., Dyksen, J. E., Raczko, R. F., 2016. *Water Res.* 105, 85–96.
- [71] Umar, M., Aziz, H. A., Yusoff, M. S., 2010. *Waste Manag.* 30, 2113–2121.
- [72] Deng, Y., Englehardt, J. D., 2006. *Water Res.* 40, 3683–3694.
- [73] Gonzalez, O., Sans, C., Esplugas, S., 2007. *J. Hazard. Mater.* 146, 459–464.
- [74] Trovó, A. G., Nogueira, R. F. P., Agüera, A., Fernandez-Alba, A. R., Sirtori, C., Malato, S., 2009. *Water Res.* 43, 3922–3931.
- [75] Batista, A. P. S., Nogueira, R. F. P., 2012. *J. Photoch. Photobio. A* 232, 8–13.
- [76] Barhoumi, N., Oturan, N., Olvera-Vargas, H., Brillas, E., Gadri, A., Ammar, S., Oturan, M. A., 2016. *Water Res.* 94, 52–61.
- [77] Wan, Z., Hu, J., Wang, J., 2016. *J. Environ. Manage.* 182, 284–291.
- [78] Kabra, K., Chaudhary, R., Sawhney, R. L., 2004. *Ind. Eng. Chem. Res.* 43, 7683–7696.
- [79] Baran, W., Adamek, E., Sobczak, A., Makowski, A., 2009. *Appl. Catal. B-Environ.* 90, 516–525.
- [80] Kaniou, S., Pitarakis, K., Barlagianni, I., Poullos, I., 2005. *Chemosphere* 60, 372–380.
- [81] Hu, L., Flanders, P. M., Miller, P. L., Strathmann, T. J., 2007. *Water Res.* 41, 2612–2626.
- [82] Abellán, M. N., Bayarri, B., Giménez, J., Costa, J., 2007. *Appl. Catal. B-Environ.* 74, 233–241.
- [83] Calza, P., Medana, C., Pazzi, M., Baiocchi, C., Pelizzetti, E., 2004. *Appl. Catal. B-Environ.* 53, 63–69.
- [84] Cai, Q., Hu, J., 2017. *J. Hazard. Mater.* 323, 527–536.

- [85] Huang, X., Feng, Y., Hu, C., Xiao, X., Yu, D., Zou, X., 2015. *Chemosphere* 138, 183–189.
- [86] Baran, W., Sochacka, J. Wardas, W., 2006. *Chemosphere* 65, 1295–1299.
- [87] Glaze, W. H., Kang, J.-W., 1989. *Ind. Eng. Chem. Res.* 28, 1573–1580.
- [88] Umar, M., Roddick, F., Fan, L., Aziz, H. A., 2013. *Chemosphere* 90, 2197–2207.
- [89] Duguet, J. P., Brodard, E., Dussert, B., Mallevialle, J., 1985. *Ozone-Sci. Eng.* 7, 241–258.
- [90] Esplugas, S., Giménez, J., Contreras, S., Pascual, E., Rodríguez, M., 2002. *Water Res.* 36, 1034–1042.
- [91] Legrini, O., Oliveros, E., Braun, A. M., 1993. *Chem. Rev.* 93, 671–698.
- [92] Munter, R., 2001. *Proc. Estonian Acad. Sci. Chem.* 50, 59–80.
- [93] Gottschalk, C., Libra, J. A., Saupe, A., 2000. *Ozonation of water and waste water* Wiley-VCH, Weinheim.
- [94] Adams, C., Wang, Y., Loftin, K., Meyer, M., 2002. *J. Environ. Eng.* 128, 253–260.
- [95] Ternes, T. A., Stüber, J., Hermann, N., McDowell, D., Ried, A., Kampmann, M., Teiser, B., 2003. *Water Res.* 37, 1976–1982.
- [96] Huber, M. M., Göbel, A., Joss, A., Hermann, N., Löffler, D., McArdell, C. S., Ried, A., Siegrist, H., Ternes, T. A., von Gunten, U., 2005. *Environ. Sci. Technol.* 39, 4290–4299.
- [97] Dantas, R. F., Contreras, S., Sans, C., Esplugas, S., 2008. *J. Hazard. Mater.* 150, 790–794.
- [98] Lin, A. Y.-C., Lin, C.-F., Chiou, J.-M., Hong, P. K. A., 2009. *J. Hazard. Mater.* 171, 452–458.
- [99] Garoma, T., Umamaheshwar, S. K., Mumper, A., 2010. *Chemosphere* 79, 814–820.
- [100] del Mar Gómez-Ramos, M., Mezcua, M., Agüera, A., Fernández-Alba, A. R., Gonzalo, S., Rodríguez, A., Rosal, R., 2011. *J. Hazard. Mater.* 192, 18–25.
- [101] Kim, T.-H., Kim, S. D., Kim, H. Y., Kim, S. J., Lee, M., Yu, S., 2012. *J. Hazard. Mater.* 227–228, 237–242.
- [102] von Sonntag, C., 2008. *Water Sci Technol.* 58, 1015–1021.
- [103] Swallow, A. J., 1973. *Radiation chemistry*. Longman Group Limited, London.
- [104] Pimblott, S. M., LaVerne, J. A., Mozumder, A., Green, N. J. B., 1990. *J. Phys. Chem.* 94, 488–495.
- [105] Choppin, G., Rydberg, J., Liljenzin, J.-O., 1995. *Radiochemistry and nuclear chemistry*, 2<sup>nd</sup> edition. Butterworth-Heinemann Ltd., Oxford.
- [106] Baxendale, J. H., Busi, F., 1982. *The study of fast processes and transient species by electron pulse radiolysis*. D. Reidel Publishing Company, Dordrecht.
- [107] Green, N. J. B., Harris, R., 1992. *Chem. Phys. Lett.* 198, 81–88.
- [108] Agarwal, A., 2014. *Simulation studies of recombination kinetics and spin dynamics in radiation chemistry*. Springer, Heidelberg.
- [109] Woods, R. J., Pikaev, A. K., 1994. *Applied radiation chemistry: Radiation processing*. Wiley & Sons, New York.
- [110] Yamaguchi, H., Uchihori, Y., Yasuda, N., Takada, M., Kitamura, H., 2005. *J. Radiat. Res.* 46, 333–341.
- [111] Illés, E., Tegze, A., Kovács, K., Sági, G., Papp, Z., Takács, E., Wojnárovits, L., 2017. *Radiat. Phys. Chem.* 134, 8–13.
- [112] Watts, M. J., Hofmann, R., Rosenfeldt, E. J., 2012. *J. Am. Water. Works Ass.* 104, 47–48.
- [113] Barazesh, J. M., Hennebel, T., Jasper, J. T., Sedlak, D. L., 2015. *Environ. Sci. Technol.* 49, 7391–7399.

- [114] Saritha, P., Aparna, C. Himabindu, V. Anjaneyulu, Y., 2007. *J. Hazard. Mater.* 149, 609–614.
- [115] Goi, A., Trapido, M., 2002. *Chemosphere* 46, 913–922.
- [116] Lin, S. H., Lin, C. M., Leu, H. G., 1999. *Water Res.* 33, 1735–1741.
- [117] Scully, N. M., McQueen, D. J., Lean, D. R. S., 1996. *Limnol. Oceanogr.* 41, 540–548.
- [118] Mostofa, K. M. G., Yoshioka, T., Mottaleb, M. A., 2012. Photobiogeochemistry of organic matter, principles and practices in water environments. Springer, London.
- [119] Luukkonen, T., Teeriniemi, J., Prokkola, H., Rämö, J., Lassi, U., 2014. *Water SA* 40, 73–80.
- [120] Talinli, I., Anderson, G. K., 1992. *Water Res.* 26, 107–110.
- [121] Lee, E., Lee, H., Kim, Y. K., Sohn, K., Lee, K., 2011. *Int. J. Environ. Sci. Technol.* 8, 381–388.
- [122] Wu, T., Englehardt, J. D., 2012. *Environ. Sci. Technol.* 46, 2291–2298.
- [123] Keen, O. S., Linden, K. G., 2013. *Environ. Sci. Technol.* 47, 13020–13030.
- [124] Szabó, L., Tóth, T., Rácz, G., Takács, E., Wojnárovits, L., 2016. *Radiat. Phys. Chem.* 124, 84–90.
- [125] Şolpan, D., Güven, O., 2002. *Radiat. Phys. Chem.* 65, 549–558.
- [126] Pillai, S. D., Shayanfar, S., 2014. Electron beam pasteurization and complementary food processing technologies. Woodhead Publishing, Amsterdam.
- [127] Illés, E., Takács, E., Dombi, A., Gajda-Schranz, K., Gonter, K., Wojnárovits, L., 2012. *Radiat. Phys. Chem.* 81, 1479–1483.
- [128] Szabó, L., Tóth, T., Homlok, R., Takács, E., Wojnárovits, L., 2012. *Radiat. Phys. Chem.* 81, 1503–1507.
- [129] Kovács, K., He, S., Míle, V., Földes, T., Pápai, I., Takács, E., Wojnárovits, L., 2016. *Radiat. Phys. Chem.* 124, 191–197.
- [130] Bonin, J., Janik, I., Janik, D., Bartels, D. M., 2007. *J. Phys. Chem. A* 111, 1869–1878.
- [131] Helz, G. R., Zepp, R. G., Crosby, D. G., 1993. Aquatic and Surface Photochemistry. CRC Press, Boca Raton.
- [132] Gligorovski, S., Strekowski, R., Barbati, S., Vione, D., 2015. *Chem. Rev.* 115, 13051–13092.
- [133] Pirro, D. M., Wessol, A. A., 2001 Lubrication Fundamentals, 2<sup>nd</sup> edition. Marcel Dekker Inc., New York.
- [134] Ivanov, V. S., 1992. Radiation chemistry of polymers. VSP, Utrecht.
- [135] Pálfi, T., Földvári, C., Takács, E., Wojnárovits, L., 2009. *Magy. Kem. Foly.* 3–4, 114–117.
- [136] Chmielewski, A. G., 2005. *Nukleonika* 50, S17–S24.
- [137] Han, B., Ko, J., Kim, J., Kim, Y., Chung, W., Makarov, I. E., Ponomarev, A. V., Pikaev, A. K., 2002. *Radiat. Phys. Chem.* 64, 53–59.
- [138] Pikaev, A. K., 2000. *High Energy Chem.* 34, 1–12.
- [139] Cooper, W. J., Curry, R. D., O’Shea, K. E., 1998. Environmental applications of ionizing radiation. John Wiley & Sons Inc., New York.
- [140] Han, B., Kim, J., Kim, Y., Choi, J. S., Makarov, I. E., Ponomarev, A. V., 2005. *Water Sci. Technol.* 52, 317–324.
- [141] Liu, Y., Hu, J., Wang, J., 2014. *Environ. Technol.* 35, 2028–2034.

- [142] Guo, Z., Zhou, F., Zhao, Y., Zhang, C., Liu, F., Bao, C., Lin, M., 2012. *Chem. Eng. J.* 191, 256–262.
- [143] Chu, L. B., Wang, J., Liu, Y., 2015. *Radiat. Phys. Chem.* 108, 102–105.
- [144] Wan, Z., Wang, J.-L., 2016. *Nucl. Sci. Tech.* 27.
- [145] Liu, Y., Hu, J., Wang, J., 2014. *Radiat. Phys. Chem.* 96, 81–87.
- [146] Liu, Y., Wang, J., 2013. *J. Hazard. Mater.* 250–251, 99–105.
- [147] Kim, H. Y., Yu, S. H., Lee, M. J., Kim, T. H., Kim, S. D., 2009. *Radiat. Phys. Chem.* 78, 267–272.
- [148] Kim, H. Y., Jeon, J., Yu, S., Lee, M., Kim, T.-H., Kim, S. D., 2013. *Chemosphere* 93, 2480–2487.
- [149] Kim, H. Y., Lee, O. M., Kim, T. H., Yu, S., 2015. *Water Environ. Res.* 87, 321–325.
- [150] Liu, Z., Zhang, H., Shao, B., Zhao, R., 2006. *Nucl. Instrum. Meth. B* 252, 285–289.
- [151] Kim, H. Y., Kim, T.-H., Cha, S. M., Yu, S., 2017. *Chem. Eng. J.* 313, 556–566.
- [152] Schieffer, H. B., Irvine, D. G., Buzik, S. C., 1997. *Understanding toxicology: Chemicals, their benefits and risks.* CRC Press, New York.
- [153] Ingerslev, F., Halling-Sørensen, B., 2000. *Environ. Toxicol. Chem.* 19, 2467–2473.
- [154] Pandard, P., Devillers, J., Charissou, A.-M., Poulsen, V., Jourdain, M.-J., Férard, J.-F., Grand, C., Bispo, A., 2006. *Sci. Total Environ.* 363, 114–125.
- [155] Kungolos, A., Emmanouil, C., Tsiridis, V., Tsiropoulos, N., 2009. *Sci. Total Environ.* 407, 4610–4615.
- [156] ISO/ASTM 51538, 2009. Practice for use of the ethanol-chlorobenzene dosimetry system.
- [157] Buxton, G. V., Greenstock, C. L., Helman, W. P., Ross, A. B., 1988. *J. Phys. Chem. Ref. Data* 17, 513–886.
- [158] Vértes, A., Nagy, S., Klencsár, Z., 2003. *Handbook of nuclear chemistry: Chemical applications of nuclear reactions and radiations.* 2003. Kluwer Academic Publishers, Dordrecht.
- [159] Buxton, G. V., Stuart, C. R., 1995. *J. Chem. Soc. Faraday Trans.* 91, 279–281.
- [160] Meyers, R. A., 2000. *Encyclopedia of analytical chemistry.* John Wiley & Sons Ltd., Chichester.
- [161] Michalski, R., Kurzyca, I., 2006. *Pol. J. Environ. Stud.* 15, 5–18.
- [162] Kosaka, K., Yamada, H., Matsui, S., Echigo, S., Shishida, K., 1998. *Environ. Sci. Technol.* 32, 3821–3824.
- [163] ISO 6060:1989, 1989. Water quality – Determination of the chemical oxygen demand.
- [164] Kubota, S., Tsuchiya, Y., 2009. *Water quality and standards volume I.* EOLSS Publishers Co. Ltd., Oxford.
- [165] Mays, L. W., 1996. *Water resources handbook.* McGraw-Hill, New York.
- [166] Kovács, K., Sági, G., Takács, E., Wojnárovits, L., 2017. *Radiat. Phys. Chem.* 139, 147–151.
- [167] DIN EN 1899-1, 1998. Water quality – Determination of biochemical oxygen demand after n days (BOD<sub>n</sub>).
- [168] OECD Test No. 301, 1992. OECD Guidelines for the Testing of Chemicals, Section 3, Degradation and Accumulation. Test No. 301: Ready Biodegradability.

- [169] Suess, M. J., 1982. Examination of water for pollution control. A reference handbook, volume 3. Biological, bacteriological and virological examination. Pergamon Press, Oxford.
- [170] Barinova, S., Tavassi, M., Nevo, E., 2010. Microscopic algae in monitoring of the Yarqon River (Central Israel). Lambert Academic Publishing, Saarbrücken.
- [171] DIN EN ISO 11348-2, 1999. Water quality - Determination of the inhibitory effect of water samples on the light emission of *Vibrio fischeri* (Luminescent bacteria test) - Part 2: Method using liquid-dried bacteria.
- [172] OECD Test No. 201, 2011. OECD guidelines for the testing of chemicals, section 2, effects on biotic systems. Test No. 201: Freshwater alga and cyanobacteria, growth inhibition test.
- [173] Scandinavian Culture Collection for Algae & Protozoa, 2017. URL: <http://www.sccap.dk/>. Last accessed: 10.07.2017.
- [174] OECD Test No. 202, 2004. OECD guidelines for the testing of chemicals, section 2, effects on biotic systems. Test No. 202: Daphnia sp. acute immobilisation test.
- [175] ISO 8192:1986. 1986. Water quality - Test for inhibition of oxygen consumption by activated sludge.
- [176] Chambers, H. F., DeLeo, F. R., 2009. *Nat. Rev. Microbiol.* 7, 629–641.
- [177] Lister, P. D., Wolter, D. J., Hanson, N. D., 2009. *Clin. Microbiol. Rev.* 22, 2009: 582–610.
- [178] Kronvall, G., 2010. *Acta Pathol. Microbiol. Immunol. Scand.* 118, 621–639.
- [179] Tadesse, D. A., Zhao, S., Tong, E., Ayers, S., Singh, A., Bartholomew, M. J., McDermott, P. F., 2012. *Emerg. Infect. Dis.* 18, 741–749.
- [180] Iglewicz, B., Hoaglin, D. C., 1993. How to detect and handle outliers. ASQC
- [181] Boreen, A. L., Arnold, W. A., McNeill, K., 2004. *Environ. Sci. Technol.* 38, 3933–3940.
- [182] Boreen, A. L., Arnold, W. A., McNeill, K., 2005. *Environ. Sci. Technol.* 39, 3630–3638.
- [183] Babić, S., Horvat, A. J. M., Pavlović, D. M., Kaštelan-Macan, M., 2007. *TrAC-Trend. Anal. Chem.* 26, 1043–1061.
- [184] Mezyk, S. P., Neubauer, T. J., Cooper, W. J., Peller, J. R., 2007. *J. Phys. Chem. A* 111, 9019–9024.
- [185] Alfassi, Z. B., 1997. Peroxy-radicals. Wiley, New York.
- [186] von Sonntag, C., 2006. Free-radical-induced DNA damage and its repair. Springer, Heidelberg.
- [187] Behar, D., Behar, B., 1991. *J. Phys. Chem.* 95, 7552–7556.
- [188] Wojnárovits, L., Takács, E., 2013. *Radiat. Phys. Chem.* 87, 82–87.
- [189] Masuda, T., Shinohara, H., Kondo, M., 1975. *J. Radiat. Res.* 16, 153–161.
- [190] Dogan, I., Steenken, S., Schulte-Frohlinde, D., Icli, S., 1990. *J. Phys. Chem.* 94, 1887–1894.
- [191] Lindsey, M. E., Meyer, M., Thurman, E. M., 2001. *Anal. Chem.* 73, 4640–4646.
- [192] Rong, S.-P., Sun, Y.-B., Zhao, Z.-H., 2014. *Chinese Chem. Lett.* 25, 187–192.
- [193] Byers, W., Lindgren, G., Noling, C., Peters, D., 2002. Industrial water management: A systems approach. 2nd edition. CH2M HILL Inc., Corvallis.
- [194] Gonçalves, A. G., Órfão, J. J. M., Pereira, M. F. R., 2012. *J. Hazard Mater.* 239–240, 167–174.
- [195] Shende, R. V., Mahajani, V. V., 1994. *Ind. Eng. Chem. Res.* 33, 3125–3130.

- [196] Homlok, R., Takács, E., Wojnárovits, L., 2013. *Chemosphere* 91, 383–389.
- [197] Yang, C.-W., Hsiao, W.-C., Chang, B.-V., 2016. *Chemosphere* 150, 559–565.
- [198] Gaffney, P. E., Heukelekian, H., 1958. *Sewage Ind. Wastes* 30, 673–679.
- [199] Lambropoulou, D., Evgenidou, E., Saliverou, V., Kosma, C., Konstantinou, I., 2017. *J. Hazard. Mater.* 323, 513–526.
- [200] Schlüter-Vorberg, L., Prasse, C., Ternes, T. A., Mückter, H., Coors, A., 2015. *Environ. Sci. Technol. Lett.* 2, 342–346.
- [201] Pintar, A., Besson, M., Gallezot, P., Gibert, J. Martin, D., 2004. *Water Res.* 38, 289–300.
- [202] Dalton, H., Stirling, D. I., Quayle, J. R., 1982. *Philos. Trans. R. Soc. Lond. B Biol. Sci.* 297, 481–496.
- [203] Adamek, E., Baran, W., Ziemiańska, J., Sobczak, A., 2012. *Appl. Catal. B-Environ.* 126, 29–38.



## ADATLAP

### a doktori értekezés nyilvánosságra hozatalához\*

#### I. A doktori értekezés adatai

A szerző neve: Sági Gyuri

MTMT-azonosító: 10045953

A doktori értekezés címe: Degradation of sulfonamides in aqueous solution by ionizing radiation

DOI-azonosító46: 10.15476/ELTE.2017.178

A doktori iskola neve: Környezettudományi Doktori Iskola

A doktori iskolán belüli doktori program neve: Környezetfizika Doktori Program

A témavezető neve és tudományos fokozata:

- Takács Erzsébet, MTA doktora, MTA Energiatudományi Kutatóközpont.
- Homonnay Zoltán, MTA doktora, ELTE Kémiai Intézet.

#### II. Nyilatkozatok

##### 1. A doktori értekezés szerzőjeként

- a) hozzájárulok, hogy a doktori fokozat megszerzését követően a doktori értekezésem és a tézisek nyilvánosságra kerüljenek az ELTE Digitális Intézményi Tudástárban. Felhatalmazom a Természettudományi kar Dékáni Hivatal Doktori, Habilitációs és Nemzetközi Ügyek Csoportjának ügyintézőjét, hogy az értekezést és a téziseket feltöltse az ELTE Digitális Intézményi Tudástárba, és ennek során kitöltse a feltöltéshez szükséges nyilatkozatokat.
- b) kérem, hogy a mellékelt kérelemben részletezett szabadalmi, illetőleg oltalmi bejelentés közzétételéig a doktori értekezést ne bocsássák nyilvánosságra az Egyetemi Könyvtárban és az ELTE Digitális Intézményi Tudástárban;
- c) kérem, hogy a nemzetbiztonsági okból minősített adatot tartalmazó doktori értekezést a minősítés (dátum)-ig tartó időtartama alatt ne bocsássák nyilvánosságra az Egyetemi Könyvtárban és az ELTE Digitális Intézményi Tudástárban;
- d) kérem, hogy a mű kiadására vonatkozó mellékelt kiadó szerződésre tekintettel a doktori értekezést a könyv megjelenéséig ne bocsássák nyilvánosságra az Egyetemi Könyvtárban, és az ELTE Digitális Intézményi Tudástárban csak a könyv bibliográfiai adatait tegyék közzé. Ha a könyv a fokozatszerzést követően egy évig nem jelenik meg, hozzájárulok, hogy a doktori értekezésem és a tézisek nyilvánosságra kerüljenek az Egyetemi Könyvtárban és az ELTE Digitális Intézményi Tudástárban.

##### 2. A doktori értekezés szerzőjeként kijelentem, hogy

- a) az ELTE Digitális Intézményi Tudástárba feltöltendő doktori értekezés és a tézisek saját eredeti, önálló szellemi munkám és legjobb tudomásom szerint nem sértem vele senki szerzői jogait;
- b) a doktori értekezés és a tézisek nyomtatott változatai és az elektronikus adathordozón benyújtott tartalmak (szöveg és ábrák) mindenben megegyeznek.

##### 3. A doktori értekezés szerzőjeként hozzájárulok a doktori értekezés és a tézisek szövegének plágiumkereső adatbázisba helyezéséhez és plágiumellenőrző vizsgálatok lefuttatásához.

Kelt: 2017. november 14.

  
a doktori értekezés szerzőjének aláírása

\*ELTE SZMSZ SZMR 12. sz. melléklet